Dissertations, Master's Theses and Master's Reports

2020

Mechanisms of Pathogen Inactivation in Wastewater and Pharmaceutical Applications

Christa L. Meingast
Michigan Technological University, clmeinga@mtu.edu

MECHANISMS OF PATHOGEN INACTIVATION IN WASTEWATER AND
PHARMACEUTICAL APPLICATIONS

By

Christa Louise Meingast

A DISSERTATION

Submitted in partial fulfillment of the requirements for the degree of

DOCTOR OF PHILOSOPHY

In Environmental Engineering

MICHIGAN TECHNOLOGICAL UNIVERSITY

2020

This dissertation has been approved in partial fulfillment of the requirements for the Degree of DOCTOR OF PHILOSOPHY in Environmental Engineering.

Department of Civil and Environmental Engineering

Dissertation Co-Advisor: *Dr. Caryn Heldt*

Dissertation Co-Advisor: *Dr. Veronica Webster*

Committee Member: *Dr. Paul Doskey*

Committee Member: *Dr. Sharon Long*

Department Chair: *Dr. Audra Morse*

Table of Contents

List of Figures

ix

List of Tables

Preface

The work completed in this dissertation was part of several collaborative research projects. Chapter 2 was completed in the environmental engineering department as part of a biosolids research team. Chapter 3, 4, and 5 were completed in the chemical engineering department as part of Heldt's Bioseparations Laboratory.

Chapter 2: Low-Cost, Low-Tech Biosolids Treatment. The dissertation author completed the literature review. The dissertation author was assisted with data collection by Karina Eyre (MS), Tanner Keyzers (MS), Rebecca Green (MS), Julianna Mickle (BS), George Austin (BS), Rachel Eikenberry (BS), and Kaitlyn Sterling (BS). The dissertation author was assisted with data analysis by Karina Eyre, Tanner Keyzers, Rebecca Green, Dr. Eric Seagren (PI), and Dr. Jennifer Becker (PI). Drs. Seagren and Becker have not revised this chapter for accuracy and are not responsible for any errors or misstatements. The pilot-scale data presented in this chapter are not representative of the final results of the study overseen by Drs. Seagren and Becker. Data from this chapter has been published in the following peer reviewed conference proceedings.

> [4] Meingast, C., J.G. Becker, and E.A. Seagren (2015). "Effects of biosolids moisture content on indicator organism reduction via freezing and thawing." Poster presentation and *Proceedings of the WEF/IWA Residuals and Biosolids 2015 Conference*, June 7-10, 2015, Washington, D.C.
>
> [3] Meingast, C.L., J.G. Becker and E.A. Seagren. (2015). "The reduction of pathogen indicator organisms during biosolids storage: The role of moisture content and freeze-thaw cycles." Poster presentation at the *2015 Research and Education Conference, Association of Environmental Engineering and Science Professors (AEESP)*, New Haven, CT, June 13-16, 2015.

[2] Meingast, C., J.G. Becker, and E.A. Seagren. (2015). "Effects of biosolids moisture content on indicator organism reduction via freezing and thawing." Podium presentation at the *2015 Michigan Water Environment Association Annual Conference*, Boyne Falls, MI, June 21-24, 2015.

[1] Meingast, C., M. Bowman, J. G. Becker, and E. A. Seagren. (2013). "Development of a sustainable process for Class A biosolids production at Gogebic-Iron Wastewater Authority." Podium presentation at the 59th *Annual Upper Peninsula Wastewater Operators Conference, Michigan Water Environment Association (MWEA) Local Section 21*, Harris, MI, May 14-15, 2013.

Chapter 3: Arginine Enveloped Virus Inactivation and Potential Mechanisms. The dissertation author completed the literature review and was assisted with analysis by Dr. Caryn L. Heldt. This chapter is published in Biotechnology Progress.

[1] Meingast, C.L., and Heldt, C.L.* (2019) Arginine Enveloped Virus Inactivation and Potential Mechanisms. *Biotechnology Progress*. e2931.

Chapter 4: Physiochemical Properties of Enveloped Viruses and Arginine Dictate Inactivation. Data collection was performed by the dissertation author with assistance from Pratik Joshi (PhD candidate), Dylan Turpeinen (PhD candidate), and Jacob LeBarre (BS). Data analysis was performed by the dissertation author with assistance from Pratik Joshi, and Dr. Caryn L. Heldt (PI). Xuankuo Xu (Bristol Myers Squibb), Melissa Holstein (Bristol Myers Squibb), Hasin Feroz (Bristol Myers Squibb), Swarnim Ranjan (Bristol Myers Squibb), Sanchayita Ghose (Bristol Myers Squibb) helped with discussion. This chapter will be prepared as a manuscript for publishing.

Chapter 5: Influence of Buffer Type and Concentration on Virus Inactivation during Low pH Treatment. The dissertation author completed the literature review. The dissertation author was assisted by Pratik Joshi (PhD candidate) in data collection and analysis. The dissertation author was assisted by Pratik Joshi, Xuankuo Xu (Bristol Myers Squibb), Melissa Holstein (Bristol Myers Squibb), Hasin Feroz (Bristol Myers Squibb), Swarnim Ranjan (Bristol Myers Squibb), Sanchayita Ghose (Bristol Myers Squibb), Dr. Caryn L. Heldt (PI) in discussion. This chapter will be prepared in conjunction with additional results as a manuscript for publication.

Acknowledgements

The support and generosity from many people and groups was required for the success of this project.

I am extremely grateful to my research co-advisor Dr. Caryn Heldt for always believing in me and providing invaluable direction. I not only improved as a writer and researcher with her guidance, but also learned to be a better mentor and colleague from her kindness, patience and understanding. I would like to express my appreciation for my co-advisor Dr. Veronica Webster for her generous support. She was always there for me when I needed a strong mentor to lean on. Her honesty and compassion gave me the peace of mind I required to make it through my degree.

Thank you to my committee members Dr. Sharon Long and Dr. Paul Doskey. Dr. Long taught me the importance of record keeping and minimizing contamination in biological laboratories. Dr. Doskey helped advance my research with compelling questions while also being attentive to my well-being as a student.

I'd like to acknowledge the assistance of Xuankuo Xu, Melissa Holstein, Hasin Feroz, Swarnim Ranjan, and Sanchayita Ghose from Bristol Myers Squibb for the thought-provoking discussions on the arginine data. Thank you to Dr. Ebenezer Tumban for a thorough review of my arginine literature review. Thank you to Dr. John Blaho from The City College of New York for his guidance with propagating and quantifying viruses.

Thank you to the Heldt's Bioseparations Team for their friendship and support. I could not have advanced my research without their help with laboratory techniques and

in-depth research discussions. I appreciate all of the edits and comments from the team on my writing and presentations.

Thank you to the Becker-Seagren Biosolids Team. We had memorable moments together digging through biosolids at local wastewater treatment plants. Thank you also to the wastewater treatment plant managers Zane MacKenzie and Mark Bowman for their positive attitudes and assistance with the biosolids pilot scale studies.

I am extremely grateful to my family and friends for their unconditional support and encouragement throughout my studies. They gave me the confidence and strength I needed to persevere in my research.

List of abbreviations

Chapter 2:

GIWA: Gogebic-Iron Wastewater Authority

LCLT: low-cost, low-tech

MGD: million gallons per day

NH_3: ammonia

PLWSA: Portage Lake Water and Sewage Authority

TS: total solids

U.S. EPA: United States Environmental Protection Agency

UV: ultraviolet

VFA: volatile fatty acids

VS: volatile solids

WWTPs: wastewater treatment plants

Chapter 3:

APP: antimicrobial peptides

BVDV: bovine viral diarrhea virus

CHA: cleaved hemagglutinin

CPP: cell penetrating peptides

DNA: deoxyribose nucleic acid

F: fusion protein

FDA: Food and Drug Administration

HA: hemagglutinin

HIV: human immunodeficiency virus

HN: hemagglutinin neuraminidase protein

HSV-1: herpes simplex virus 1

HSV-2: herpes simplex virus 2

LRV: $\log_{10}$ reduction value

NA: neuraminidase

NaCl: sodium chloride

NDV: newcastle disease virus

M1: matrix-1 protein

M2: matrix-2 protein

MMV: mouse minute virus

PCR: polymerase chain reactions

RNA: ribonucleic acid

SuHV-1: pseudorabies virus

UCHA: uncleaved hemagglutinin protein

XMuLV: xenotropic murine leukemia virus

Chapter 4

ACS: American Chemical Society

ATCC: American Type Culture Collection

BT-1: bovine turbinate cells

CO_2: carbon dioxide

CPE: cytopathic effect

DLS: dynamic light scattering

DMEM: Dulbecco's Modified Eagle Medium

DMSO: dimethyl sulfoxide

DNA: deoxyribose nucleic acid

EMEM: Eagles Medium Essential Media

HCL: hydrochloric acid

LRV: $\log_{10}$ reduction value

MβCD: methyl-β-cyclodextrin

NaOH: sodium hydroxide

PBS: phosphate buffered saline

PYB: pyrenebutyric acid

RK-13: rabbit kidney cells

SDS: sodium dodecyl sulfate

TEM: transmission electron microscopy

TFA: trifluoroacetic acid

Chapter 5

ATCC: American Type Culture Collection

CO_2: carbon dioxide

CPE: cytopathic effect

DMEM: Dulbecco's Modified Eagle Medium

DNA: deoxyribose nucleic acid

EMEM: Eagles Medium Essential Media

HCL: hydrochloric acid

LRV: $\log_{10}$ reduction value

NaOH: sodium hydroxide

PBS: phosphate buffered saline

PK-13: porcine kidney cells

PPV: porcine parvovirus

PYB: pyrenebutyric acid

RK-13: rabbit kidney cells

SDS: sodium dodecyl sulfate

X-MLV: xenotropic murine leukemia virus

Abstract

Infectious diseases are a significant threat to public health. Though society enacts practices to prevent the spread of these dangerous diseases, challenges remain. Therefore, continual advancements in treatment and prevention are required. Wastewater treatment and viral clearance in pharmaceutical applications are two key health measures that prevent the spread of infections.

A low-cost, low-technology biosolids treatment process was developed to improve wastewater treatment by collecting key information on storage temperature, ammonia, volatile solids, moisture content, pH, and pathogen inactivation in biosolids over long-term storage at two wastewater treatment plants located in northern climates of the United States. Inactivation of pathogens in the biosolids was enhanced by freeze-thaw cycles, intermediate moisture contents (16% total solids), and time. Biosolids required over a year of long-term storage to reach standard pathogen limits for treatment in northern climates.

To improve viral clearance in therapeutic protein manufacturing, the use of arginine and buffers was studied at pH $\geq$ 4 to retain the stability of the final protein product. A stabilized virus membrane structure, resulting from lipid packing density or membrane proteins, hindered the inactivation efficacy of arginine and buffers. The influence of membrane properties on arginine and buffer interactions supports the inactivation mechanisms of viral membrane deformation. Increased hydrophobicity and clustering enhanced the inactivation of enveloped viruses by arginine at pH 4 and 7.

Electrostatic interactions increased the inactivation of enveloped viruses by buffers at pH 4.

Overall, the mechanisms for pathogen inactivation were further understood for the improvement of biosolids treatment and therapeutic protein manufacturing to facilitate the prevention of infectious diseases.

1   Introduction and Chapter Summaries

1.1   Introduction

Infectious diseases affect billions of people annually, significantly impacting world health[1]. Infectious diseases are caused by microorganisms and are spread from one person to another[2]. These highly dangerous diseases resulted in 3 million mortalities in 2016 through lower respiratory infections alone, ranking as the fourth top cause of death[1]. Recent coronavirus outbreaks that produce severe respiratory infections include the Middle East Respiratory coronavirus (MERS-CoV), severe acute respiratory syndrome coronavirus (SARS-CoV), and the novel coronavirus (SARS-CoV-2)[3]. Additional infections including diarrheal diseases (1.4 million deaths) and tuberculosis (1.3 million deaths) were also classified in the top ten causes of death worldwide[1]. For this reason, considerable safety measures must be taken to minimize the threat of infectious diseases.

In order to prevent infectious diseases, society has enacted practices to protect itself through immunization, health measures, surveillance, and treatment[4] . Though many barriers exist that impede infectious diseases from causing harm to public health, humans still remain vulnerable to these microorganisms. For this reason, advancements need to continually be implemented to fight current obstacles in treatment and prevention of infectious diseases[4].

Wastewater treatment and viral clearance during pharmaceutical applications are two examples of health measures that society enacts to minimize the spread of infectious diseases. Wastewater is liquid or water-transported wastes originating from residential, business, industry, or natural sources[5]. Wastewater processes remove and treat infectious

materials from residential areas to prevent the spread of disease. Viral clearance in pharmaceutical applications prevents infections by removing or inactivating viruses from biological medical products[6]. Examples of biological medical products include recombinant therapeutic proteins, monoclonal antibodies, glycoproteins, and tissue/ blood products[6]. This dissertation investigates various processes that improve wastewater treatment and viral clearance in therapeutic protein manufacturing to protect the public from infectious diseases.

1.2   Chapter Summaries

The chapters of this dissertation describe different projects focused around the removal of infectious pathogens that can cause human disease.

Chapter 2 focuses on the improvement of wastewater treatment through a low-cost, low-technology biosolids treatment method. Many wastewater treatment plants are looking to upgrade their biosolids treatment systems to open additional avenues for land application and distribution of biosolids[7]. However, a large majority of wastewater treatment plants lack the resources to implement the high-tech and high-costs processes required to upgrade their biosolids treatment. Therefore, there is a growing need for low-cost, low-tech treatment options. One example of low-cost, low-tech treatment is the inactivation of pathogens in biosolids through long-term storage. However, long-term storage is not widely used since universal conditions required to meet treatment standards are not known. To further understand the conditions required to meet pathogen inactivation standards during long-term storage, a year-long pilot-scale study was undertaken at Gogebic Iron Wastewater Authority (GIWA) and Portage Lake Water and

Sewer Authority (PLWSA). Fundamental information was collected on the impact of key parameters including storage temperature, organic matter content, ammonia, pH, and moisture on the rate of inactivation of pathogens. The data collected provided insight into the conditions required for low-cost, low-technology biosolids treatment processes.

Chapter 3 is a literature review on the mechanisms of enveloped virus inactivation by the amino acid arginine. Arginine inactivates enveloped viruses at conditions that retain protein stability, making it a desired viral clearance process during therapeutic protein manufacturing. Conditions for optimal inactivation include arginine concentrations of 0.7-1 M, an incubation time of 60 minutes, and a synergistic factor of either $\geq 40°C$, $\leq pH 4$, or Tris buffer [8-16]. However, not all enveloped viruses are fully inactivated by arginine at these optimal conditions. Viruses that are resistant to arginine have increased protein stability or increased membrane stability[17]. Arginine interacts with both proteins and lipids, and therefore, either interaction may be key to understanding the mechanisms of inactivation. Three hypotheses are drawn to explain the mechanisms of inactivation by arginine. Hypothesis 1 describes inactivation through inhibition of viral protein function. Hypothesis 2 describes inactivation through membrane destabilization. Hypothesis 3 describes inactivation by membrane pore formation. Understanding the mechanisms of arginine may elucidate the use of functional groups, charges, or additives to enhance inactivation.

Chapter 4 dives into the mechanisms and improvement of enveloped virus inactivation by arginine. First, the effect of virus structure on inactivation by arginine was explored. Enveloped viruses with highly stable membranes were less affected by arginine than enveloped viruses with less stable membranes. Additionally, the sensitivity of

viruses to membrane cholesterol depletion correlated to arginine sensitivity. The influence of membrane properties on inactivation supported the mechanism of membrane deformation by arginine. To enhance the inactivation of viruses with stabilized membranes, arginine-derivatives, arginine clustering, hydrophobicity, and buffer type were examined. Overall, higher hydrophobicity and arginine-clustering increased inactivation by arginine. Dynamic light scattering (DLS) and transmission electron microscopy (TEM) were used to determine structural changes to viruses after arginine exposure. Increasing virus size after arginine exposure was observed, supporting lipid expansion or arginine binding as the mechanism for inactivation. Overall, the data supports membrane deformation as the mechanisms of arginine inactivation. Inactivation can be enhanced through added hydrophobicity or increased arginine clustering.

Chapter 5 explores the influence of virus properties, buffer properties, and time on the inactivation of viruses at pH 4. Enveloped viruses including pseudorabies virus (SuHV-1), herpes simplex virus 1 (HSV-1), and equine arteritis virus (EAV), and the non-enveloped porcine parvovirus (PPV) were tested with glycine, acetate, and citrate buffers at concentrations ranging from 20-500 mM. Inactivation levels were dependent on all properties tested. The stabilized membrane of small EAV protected the virus against inactivation at pH 4. Similarly, the non-enveloped PPV was also unaffected by pH 4, likely resulting from the absence of a lipid bilayer. EAV and PPV may require harsher conditions for inactivation, such as lower pH or higher temperatures. Larger viruses with less stabilized membranes (HSV-1 and SuHV-1) were inactivated to the highest levels by citrate and the lowest levels by glycine. Higher buffer concentrations either increased or had no effect on inactivation. Buffers with opposite charges to the

4

virus produced higher inactivation. It is hypothesized that electrostatic interactions between the virus and the buffer promote inactivation. Overall, inactivation by buffers at pH 4 is virus-specific, however, solution conditions can be optimized to increase inactivation.

2 Low-Cost, Low-Tech Biosolids Treatment

2.1 Introduction

Clean water and sanitation are essential for life. Wastewater processes support life by treating and removing contaminated water from populated areas to prevent the accumulation of infectious materials. Wastewater contains liquid or water-transported wastes originating from residential, business, industry, or natural sources (groundwater, surface water, or stormwater)[18]. In the absence of wastewater treatment, infectious waste would accumulate in populated areas, leading to poor sanitation and disease.

Treatment of wastewater in the United States commonly includes preliminary, primary, secondary, and tertiary processes, illustrated in **Figure 2-1**[18]. Treatment processes remove solids, nutrients, pathogens, organic compounds, and odors to convert wastewater into an effluent that is safe for human and environmental health[18]. Preliminary treatment applies bar screens and grit chambers to separate large materials such as rags or grit. A portion of suspended solids and organic matter are removed via primary sedimentation. Secondary treatment uses biological treatment to remove additional suspended solids and biodegradable organics. Tertiary treatment employs final disinfection for safe discharge. Examples of final disinfection practices include chemicals or ultraviolet light (UV). After treatment is completed, the final effluent is discharged into a surface water body.
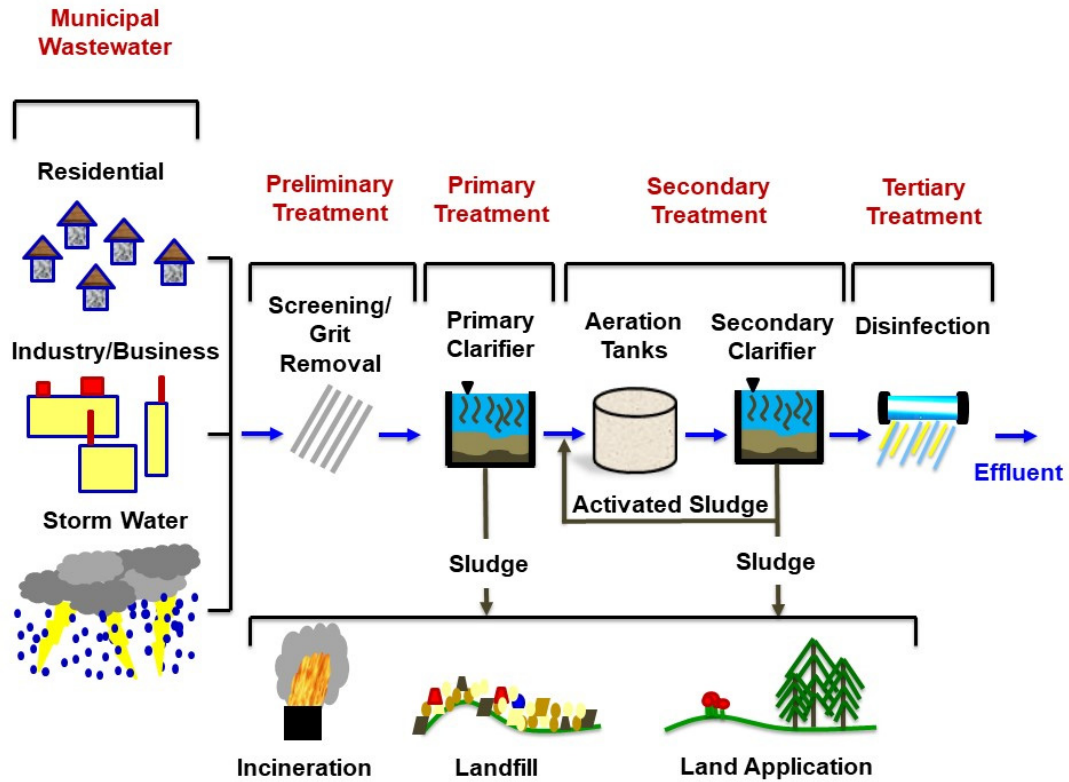
Figure 2-1. Wastewater originates from residential industry/business or stormwater sources. Treatment includes preliminary, primary, secondary, and tertiary processes. Solids can be disposed of by incineration, landfill, or land application.

Wastewater solids contain pathogens and use an oxygen demand, and therefore, solids must be removed before safe discharge. Solids are typically removed from wastewater during primary and secondary treatment through clarifiers. Though termed solids, this wastewater constituent is a semisolid liquid between 0.25-12% solids[18]. Solids disposal options include incineration, surface landfills, or reuse by land application after treatment[18]. Treated wastewater solids contain high nutrient and organic matter content, and, therefore reuse through land application is a sustainable and cost-effective means of disposal.

Because of the presence of pathogens and the potential to attract vectors (e.g.

7

rodents, insects, and birds), treatment of wastewater solids is required to protect human and environmental health before reuse. Treated residual wastewater solids are termed biosolids (**Figure 2-2**). The United States Environmental Protection Agency (U.S. EPA) regulates biosolids treatment, quality, use, and disposal under the Code of Federal Regulations, Title 40, Part 503 rule[19]. Under the EPA regulations, biosolids products are classified into two distinct levels: Class A and Class B. Class A biosolids undergo an advanced sludge process train, reducing pathogens below detectable limits, while Class B biosolids receive a less aggressive treatment and contain low but detectable levels of pathogens. As a consequence of advanced treatment, Class A biosolids can be re-used with limited regulations.

Figure 2-2. Treated sewage solids are termed biosolids. Biosolids can be land applied as a fertilizer or soil amendment.

Wastewater Treatment Plants (WWTPs) throughout the U.S. are pursuing Class A biosolids treatment systems to open additional avenues for land application and distribution of biosolids[7]. Public scrutiny, lack of resources and high energy costs are only a fraction of challenges that WWTPs face[20]. To adequately treat wastewater, plants utilize 2-4% of the total energy generated in the U.S. in a given year, producing high operation costs[21]. Rural WWTPs pay ~$0.16 per cubic meter of wastewater treated or about $700,000 per year[22]. By producing Class A biosolids, WWTPs can land apply biosolids without the extra costs associated with lower quality biosolids, while gaining revenue for the final product to supplement energy costs. However, the majority of Class A biosolids treatment processes are high-tech and high-cost, leaving many WWTPs without the resources to implement the design. Consequently, there is an increasing demand for low-cost, low-tech (LCLT) treatment options to produce Class A biosolids.

2.2   Literature Review

2.2.1   Pathogens in Biosolids

Numerous pathogenic organisms exist in wastewater solids including bacteria, viruses, protozoa, helminths, and fungi (**Table 2-1**)[23], and therefore, solids must be treated to reduce pathogens before reuse. If solids are improperly treated, pathogens can spread to agricultural soil during land application. Therefore, it is important to understand the quantity and type of microorganism present in the solid waste for effective treatment and safe re-use.

Table 2-1. Pathogens commonly found in biosolids include bacteria, viruses, and parasites.

Pathogen	Size Range	Common in Biosolids
Bacteria	~1-3 μm	*Salmonellae* *Escherichia coli* *M. tuberculosis* *Clostridium perfringens*
Virus	~20-200 nm	Adenovirus Enterovirus Hepatitis A virus Rotavirus
Parasite	~1 μm-30 m	*Ascaris lumbricoides* *Ascaris suum* *Taenia* *Anclostoma duodenale*

High concentrations of bacteria exist in wastewater treatment solids. The most prevalent bacteria include species that infect the human gut. Typical conditions for gut bacteria survival are high organic content in mesophilic temperatures of around 37 °C[23].

Over 140 different types of viruses have been found in biosolids[23]. These viruses commonly cause respiratory illness, acute gastroenteritis, conjunctivas, and diarrhea. Feces of infected individuals contain very high levels of virus. The infectious dose of enteric viruses, ranging from 10-100 infectious units, is very low, making proper treatment necessary for human safety[23].

The majority of parasites found in biosolids are classified under helminth ova, which include *Ascaris* ova, or protozoa. These parasites are prevalent around the world causing many illnesses. Parasite infectivity can range from 1-10 cysts egg per person[24]. With low infectivity dose, it is crucial to properly treat for parasites. Parasites are the most resilient pathogen in biosolids due to their protective outer shell, and therefore, are

commonly used as indicator organisms. Indicator organisms are organisms whose abundance suggests the presence of various pathogenic species. Whether it be bacteria, viruses, or parasites, it is important to properly treat sewage solids to reduce pathogens.

2.2.2   Biosolids Treatment

In 1984, the U.S. EPA created a policy that endorsed the beneficial reuse of biosolids as a fertilizer or soil amendment. The EPA defines biosolids as "a primarily organic solid product produced by wastewater treatment processes that can be beneficially recycled[19]." For this reason, biosolids are seen as an item for re-use. Biosolids refer to sewage solids that have undergone treatment to reduce pathogens and the potential for vector attractions. Class A biosolids can be applied to agricultural land, disturbed areas, forests, recreation areas, cemeteries, and residential gardens[19]. The U.S. EPA regulates biosolids monitoring, testing, treatment, and pathogen levels.

Class A and Class B biosolids are two distinct levels of treated sewage solids. Class A biosolids undergo an advanced process train to reduce pathogens below detectable limits. Class A biosolids can be disposed of with limited EPA regulations due to undetectable pathogen levels. Class B biosolids receive less aggressive treatment and contain detectable, but low, levels of pathogens. Class B biosolids are more restricted than Class A when it comes to reuse as a result of pathogen levels as well as metals content and vector attraction criteria. Required pathogen limits for Class A and B biosolids are included in **Table 2-2**[19].

Table 2-2. Class A and B Pathogen Limits. Class A has stricter pathogen limits but a wider range of land application options compared to Class B Biosolids.

Pathogen	Class A Limit	Class B Limit
Fecal coliforms	< 1000 MPN/g dry solids	< 2 million MPN/g dry solids
Enteric viruses	< 1 plaque with a 3-$\log_{10}$ reduction	N/A
Helminth ova	< 1 viable ovum/4 g dry solids with a 2-$\log_{10}$ reduction shown	N/A

2.2.2.1 Alternatives to Meet Class A Pathogen Requirements

Both Class A and B biosolids have several treatment options to meet EPA standards. As discussed further below, six alternatives exist for producing Class A biosolids under the EPA part 503 regulations[19]:

Alternative 1*: Thermally Treated Biosolids*

Specific time and temperature regimes must be met.

Alternative 2*: Sewage Sludge Treated in a High pH-High Temperature Process*

Specific pH, temperature, time and air-drying methods must be met.

Alternative 3*: Sewage Sludge Treated in Other Processes*

Fecal coliform or Salmonella, the density of enteric viruses, and the density of helminth ova are all at or below the EPA pathogen limits through a specific treatment process. Once this has been met, the plant may maintain operating conditions for pathogen reduction.

Alternative 4*: Sewage Sludge Treated in Unknown Processes*

EPA regulatory limits for Salmonella or fecal coliform bacteria, enteric viruses, and viable helminth ova at the time of biosolids disposal are met. Monitoring for pathogens must occur before all biosolids disposal applications.

Alternative 5: *Biosolids Treated in a Process to Further Reduce Pathogens (PFRP)*

Solids must be treated in one of the PFRPs listed in Appendix B of the EPA 503 regulations. The PFRP's include:

- *Composting*: aerobic decomposition of solids using a within-vessel or static aerated pile method. Temperatures must remain at 55°C (131°F) or higher for 3 consecutive days.

- *Heat Drying*: sewage solids are dried to 10% total solids or lower by hot gases. Temperatures of the solids must exceed 80°C (176°F) or the wet bulb temperature exposed to the solids must exceed 80°C (176°F).

- *Heat Treatment*: solids reach a temperature of ≥180°C (356°F) over 30 minutes.

- *Thermophilic Aerobic Digestion*: solids maintain aerobic conditions for 10 consecutive days at 55°C to 60°C (131°F to 140°F).

- *Beta Ray and Gamma Ray Radiation*: solids are treated with beta rays or gamma rays at doses of at least 1.0 megarad at room temperature.

- *Pasteurization*: solids temperature is maintained at 70°C (158°F) or higher for 30 minutes or longer.

Alternative 6: *Use of a Process Equivalent to PFRP*

Solids are treated with a process equivalent to a PFRP that meets EPA pathogen regulations. The permitting authority determines the equivalency of the process.

2.2.2.2 Vector Attraction Reduction

Vectors are organisms that are attracted to biosolids and could contribute to the spread of pathogens[19]. Insects, birds, and rodents are examples of vectors. To prevent the spread of pathogens, vector attraction is reduced through the breakdown of volatile solids, inhibition of microbial activity, or enacting a physical barrier. The 503 regulations state that pathogen and vector attraction reduction (VAR) can occur simultaneously with other biosolids treatments. A total of 12 options exist to satisfy vector attraction reduction requirements:

VAR Option 1: 38% volatile suspended solids reduction.

VAR Option 2: anaerobic digestion.

VAR Option 3: aerobic digestion.

VAR Option 4: anaerobic digestion system meets specific oxygen uptake rates.

VAR Option 5: aerobic processes greater than 40°C.

VAR Option 6: pH raised to 12 and maintained at pH 11.5 for 24 hours.

VAR Option 7: solids content exceeds 75% and the product contains stabilized solids.

VAR Option 8: unstabilized solids must be over 90% total solids before it can be added and mixed with other materials.

VAR Option 9: injected into the earth's surface to create a barrier between the vectors and biosolids.

VAR Option 10: incorporated into the soil within eight hours from discharge.

VAR Option 11: covered on-site with soil or other material.

VAR Option 12: pH of domestic septage must be raised to 12 and held for 30 minutes.

2.2.3   Low-Cost, Low-Tech Treatment

From the above alternatives and VAR options, it is clear that there are several ways to treat biosolids. However, what alternatives can be used to meet low-cost, low-tech demands for producing Class A biosolids? Alternative 6 for Class A biosolids treatment can be used to produce an equivalent process to a PFRP, allowing for the creation of a low-cost, low-tech certified process. Under Alternative 6, a Pathogen Equivalency Committee (PEC) provides guidance and expertise to create an equivalent process to a PFRP. The guidance includes a three-$\log_{10}$ reduction of enterovirus and a two-$\log_{10}$ reduction of helminth ova. Though a specific log-reduction must be met, pathogen limits must also be satisfied (**Table 2-2**).

Sustainable LCLT treatment alternatives for producing Class A biosolids do exist and have been successfully implemented. Options for LCLT treatment include long term storage, air drying, and cake storage[25]. Many large WWTPs currently implement LCLT treatments, including Chicago, Illinois and San Jose, California[25,26]. The Stickney Water Reclamation Plant (Metropolitan Water Reclamation District of Greater Chicago) combines long-term storage, air drying, and cake storage to treat their biosolids to a Class A level[27]. Biosolids are first treated in Chicago with the use of anaerobic digestion (35° C for 20 days), followed by two solid process trains to obtain a final product that is Class A

certified and yields 60% total solids. The two sludge process trains include a high solids sludge process train (HSSPT) and a low solids sludge process train (LSSPT). The HSSPT and LSSPT produce equal amounts of treated biosolids throughout the year. During the HSSPT, solids are conditioned with a cationic polymer followed by dewatering with centrifuges to 25% total solids. This material is transported to a storage lagoon throughout the year, except when the temperature is below -4°C. In the LSSPT, solids are pumped straight from the anaerobic digesters into a separate set of lagoons. Both the LSSPT and HSSPT lagoons are filled for a period of 1 to 3 years. Solids settle to the bottom, while supernatant is recycled back to the WWTP. Lastly, the solids are air-dried to achieve a final product of 60% total solids.

Though many WWTPs are beginning to enact LCLT practices, widespread adoption and regulatory approval of these methods have been hindered by a lack of information on the impacts of environmental factors and biosolids properties on pathogen inactivation. Most determinations of equivalency for LCLT treatment are based on environmental conditions at each individual site. However, if similar conditions exist and pathogens requirements are met across various sites, the process could qualify for national equivalency. Reduced testing, increased public confidence, and a sustainable and safe process are benefits for national equivalency. However, the application for equivalency can be time-consuming and expensive. The best way to obtain this certification is to provide the EPA with a full record of pathogen inactivation related to environmental conditions at various sites. If mechanisms for pathogen reduction are well enough understood, new low-cost, low-tech processes could be realized on a national basis.

One of the most effective LCLT treatment options is long-term storage. Long-term storage (lagoon storage) is defined as a process where biosolids are stored and left unfed for a specific period of time, allowing for pathogen inactivation and organic matter decomposition[25]. To initiate long-term storage, lagoons are filled with biosolids continuously or intermittently, which can take several months to a year to accomplish. Biosolids are typically aerobically or anaerobically digested prior to this process. During the filling of the lagoon, solids settle and the supernatant is collected and returned to the beginning of the wastewater treatment process. This system is then left unfed to allow for pathogen destruction and organic matter breakdown. Once pathogens in the lagoon have dropped to levels certified by the EPA, biosolids can be used as a fertilizer or soil amendment. **Figure 2-3** shows a schematic of the lagoon storage process. Inactivation of pathogens during long-term storage occurs through a variety of mechanisms including chemical action, storage time, temperature, and freeze-thaw cycles.
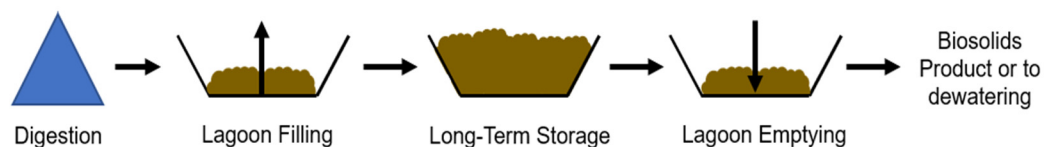
Figure 2-3. Long-Term Lagoon Storage/Treatment[18]. During long-term storage, lagoons are filled and left to sit for a period of time to allow for pathogen inactivation and organic matter breakdown.

Chemical Action

        Chemical action refers to any process of inactivation that involves the composition or structure of active chemical substances. Specific properties of the solids that aid in pathogen die-off during chemical action include unionized ammonia (NH_3) content, pH, total solids, volatile solids, and volatile fatty acid content. Biosolids that undergo anaerobic digestion contain large amounts of ammonia[28]. The fraction of toxic ammonia, NH_3, is minor at normal operating conditions (pH 5.0-7.0), because the dominant species is NH_4^+, ammonium ion. Even at low levels, NH_3 produces toxic effects against pathogens, including enteric viruses[29-31], pathogenic bacteria[32,33], and *Ascaris* ova[32,34,35]. Ammonia in urea concentrations of 0.4% inactivates *Ascaris* eggs and Salmonella to Class A limits after short treatment times at 28°C[32]. Poliovirus and F2 bacteriophage are undetectable after treatment with 800 mg of NH_3/L within hours at 20°C[29]. Overall, the levels of toxic ammonia in biosolids can inactivate pathogens.

        Total solids (TS) and volatile solids (VS) are principle factors affecting pathogen reduction in lagoon storage. It is widely accepted that increasing total solids reduces pathogens through desiccation and autolysis of cells[27,36-41]. For example, fecal coliforms were reduced to Class A levels at 90% total solids at 38°C in less than 10 days[37]. Inversely, high moisture content increases the decay rate for pathogenic bacteria as a result of the increased non-pathogenic bacterial competition[42]. Volatile solids also affect pathogen growth and decay in biosolids. Volatile solids are organic matter that act as a food source for bacteria in biosolids. At low ratios of volatile solids, the food source is low, decreasing bacteria growth[43]. However, at a high ratio of volatile solids, increased

growth of non-pathogenic bacteria can occur, inhibiting pathogenic bacterial growth. Both total solids and volatile solids affect pathogen inactivation at high and low levels.

Volatile fatty acids (VFAs) are fatty acids containing two to six carbon atoms and are naturally occurring in wastewater solids[44]. VFAs reduce bacteria growth[45-53] and produce toxic effects on *Ascaris* ova[54,55]. Inactivation of Salmonella occurs within 12 days during anaerobic digestion at a VFA concentration of 5000 mg/L at pH 6.0 [46]. VFAs have been more effective in pathogen inactivation at lower pH values where the acids exist primarily in the uncharged form. Because of the hydrophobic nature of the uncharged form, the acid can readily cross the lipid bilayer to distress the pathogen and cause inactivation[54]. Overall, unionized ammonia (NH_3) content, pH, total solids, volatile solids, and volatile fatty acid content all affect pathogenic growth and decay in biosolids treatment (**Table 2-3**).

Table 2-3. Literature Review on the Inactivation of Pathogens by Chemical Action

Chemical Action	Concentration	Conditions	Pathogen Reduction
NH3	0.4 % Urea	28°C, days	Class A limits of *Ascaris* eggs and salmonella[32]
	800 mg NH3/L	20°C, Hours	Poliovirus and F2 bacteriophage to undetectable limits[29]
TS	90% TS	38°C, 10 days	FC to Class A levels[37]
VFAs	5000 mg/L	pH 6.0, 12 days	Salmonella to undetectable limits[46]

Storage Time and Temperature

Information exists at different temperature ranges (elevated and ambient) about the time of exposure in inactivating pathogens during long-term storage[34]. Microbial activity in biosolids can produce high temperatures of up to 60°C that aid in the reduction of pathogens[56]. In biosolids at 55°C, *E. coli* and Salmonella were reduced by 8-$\log_{10}$ in 60 min and 10 min, respectively[57]. At 49.5°C in anaerobically digested, vacuum filtered, and air-dried biosolids, an 8-$\log_{10}$ reduction in Salmonella, poliovirus, and *Ascaris suum* eggs occurred in 7, 10, and 40 days, respectively[58]. Natural ambient temperatures can also inactivate pathogens in biosolids to Class A levels. In the southern hemisphere, where ambient temperatures remain around 13.3°C with little variability, Class A

pathogen inactivation in biosolids occurs within 1-3 years[59-64]. In northern climates that have greater temperature variability and can reach below freezing, pathogen inactivation can take longer[62,65,66]; however, Class A biosolids can still be produced in these climates. The amount of time needed to meet EPA standards is primarily based on the degradation of *Ascaris* ova, which are the most resilient pathogen because of their protective outer shell. Time and temperature can be varied in diverse climates to meet Class A regulations for biosolids (**Table 2-4**).

Table 2-4. Literature Review on the Inactivation of Pathogens by Storage Time and Temperature.

Temperature	Time	Pathogen Inactivation
55°C	60 min	8-log reduction E. *Coli*[57]
	10 min	8-log reduction salmonella[57]
49.5°C	7 days	Salmonella[58]
	10 days	Poliovirus[58]
	40 days	*Ascaris* Ova[58]
Southern Hemisphere-temps around 13.3°C with little variability	1-3 years	Class A Levels[59-61,64]
Norther Hemispheres-greater temp variability	> 3 years	Class A Levels[62,65]

Freeze-Thaw Cycles

Freeze-thaw cycles are widely known to increase dewaterability (or ability to lose water) in biosolids through structure modifications[67-70]. Recent investigations have demonstrated that freeze-thaw cycles can inactivate bacterial pathogens[71-73] in dewatered sanitary wastewater (blackwater)[74], stabilization ponds[75], activated sludge[76,77], reed beds[66], untreated wastewater treatment solids[77] and biosolids slurries treated via aerobic or anaerobic digestion[78].

The ideal conditions (i.e. temperature, freezing rate, # of cycles, and moisture content) for freeze-thaw cycles to reduce pathogens are not well understood. The rate of freezing and thawing is thought to be the key component of inactivation[77]. At slow rates of freezing (~1°C/min), liquid water molecules diffuse out of cells through the membrane in response to the chemical potential gradient and contribute to the formation of extracellular ice crystals[79,80]. Cellular damage under these conditions may result from cell desiccation and/or the stress exerted by extracellular ice crystals as they grow and squeeze cells in diminishing unfrozen channels containing high concentrations of rejected solutes[71,79]. In contrast, at high rates of freezing (~100°C/min), ice crystals form at rates faster than liquid water molecules can diffuse through the cell membrane. If sufficiently large, the resulting intracellular ice crystals disrupt the cell membrane and inactivate cells. For example, freezing to -65°C in yeast cells at a cooling rate of 1°C/min leaves a cell density of 30% of the initial concentration, while a cooling rate of 200°C/min leaves a cell density of 21% the original concentration[80]. Cellular damage and/or inactivation can also occur during thawing, e.g., resulting from osmotic shock.

Summary

From the literature, it is apparent that chemical action, temperature, storage time, and freeze-thaw cycles have a large impact on pathogen reduction during long-term storage. The mechanisms needed to inactivate pathogens are known to change across differing climates, operating parameters, and biosolids properties. However, the correlation between these essential mechanisms in pathogen die-off is not well understood. Fundamental information on how key environmental parameters affect pathogen inactivation is needed so that conditions necessary to achieve Class A pathogen inactivation requirements in LCLT biosolids treatment systems can be accurately and reliably predicted.

2.3 Objectives

The overall goal of this multi-phase project is to develop a universal approach for a long-term storage process to serve as a Class A treatment alternative. First, a preliminary study was performed to determine the relationship between total solid content and pathogen reduction in biosolids subjected to freeze-thaw cycles. After the preliminary study was completed, a broad research effort was initiated to determine the impact of key process parameters on the inactivation of pathogens during long-term storage. Pilot-scale studies for long-term storage were performed in conjunction with two collaborating WWTPs; the Portage Lake Water and Sewage Authority (PLWSA) in Houghton, MI, and the Gogebic-Iron Wastewater Authority (GIWA) in Ironwood, MI.

This overall goal was investigated through the following specific research objectives:

Objective 1: Determine the relationship between total solids and pathogen reduction in biosolids subjected to freeze-thaw cycles.

We hypothesize the total solids content of the biosolids sample will affect the rate of biosolids freezing, which affects pathogen inactivation.

Pathogen inactivation may occur during biosolids storage under ambient conditions; however, the mechanisms and rates of pathogen inactivation under these conditions are not well understood. **Objective 1** used a combination of field and laboratory experiments to quantify the effects of freeze-thaw cycles on the inactivation of fecal coliforms in biosolids with varying moisture levels. This information is needed because WWTPs can use natural freeze-thaw cycles in cold regions to predict and optimize pathogen inactivation in biosolids.

Objective 2: Evaluate the pathogen inactivation under long-term storage as a function of environmental conditions.

We hypothesize that the mechanisms inactivating pathogens during lagoon storage can be understood by ambient environmental conditions, storage temperature, moisture, organic matter, ammonia (NH₃), volatile fatty acids (VFAs), alkalinity, and pH.

To further understand the mechanisms of pathogen inactivation during long-term storage, a year-long pilot-scale study was conducted at GIWA and PLWSA to meet **objective 2**. Fundamental information was collected on the impact of key parameters, e.g., storage temperature, organic matter content (measured as volatile solids (VS)), NH₃ content, pH, and TS on the rate of pathogen inactivation. This data can be used to

develop a rational and universal approach for the design of a LCLT Class A biosolids treatment process.

Completing the above research objectives will improve our understanding of pathogen inactivation under a broad range of conditions, enabling rational design of LCLT treatment systems for high-quality biosolids production. This will contribute to the greater implementation and EPA approval of LCLT treatment processes under alternative 6 for Class A biosolids treatment, thus allowing more wastewater treatment plants to sustainably and economically produce high-quality biosolids.

2.4   Materials and Methods

2.4.1   Study Sites

Study sites for **objectives 1** and **2** included Gogebic Iron Wastewater Authority (GIWA, Ironwood, Michigan, USA) and Portage Lake Water and Sewage Authority (PLWSA, Houghton, Michigan, USA) (**Figure 2-4**). The two WWTPs are similar in size and have comparable treatment processes. GIWA treats an average wastewater flow of 3.4 million gallons per day (mgd) and PLWSA treats an average flow of 3.1 mgd. **Table 2-5** provides information for wastewater treatment schemes. The key differences in biosolids treatments are seen during secondary treatment where GIWA undergoes oxidation ditch activated sludge, while PLWSA uses a conventional activated sludge process.
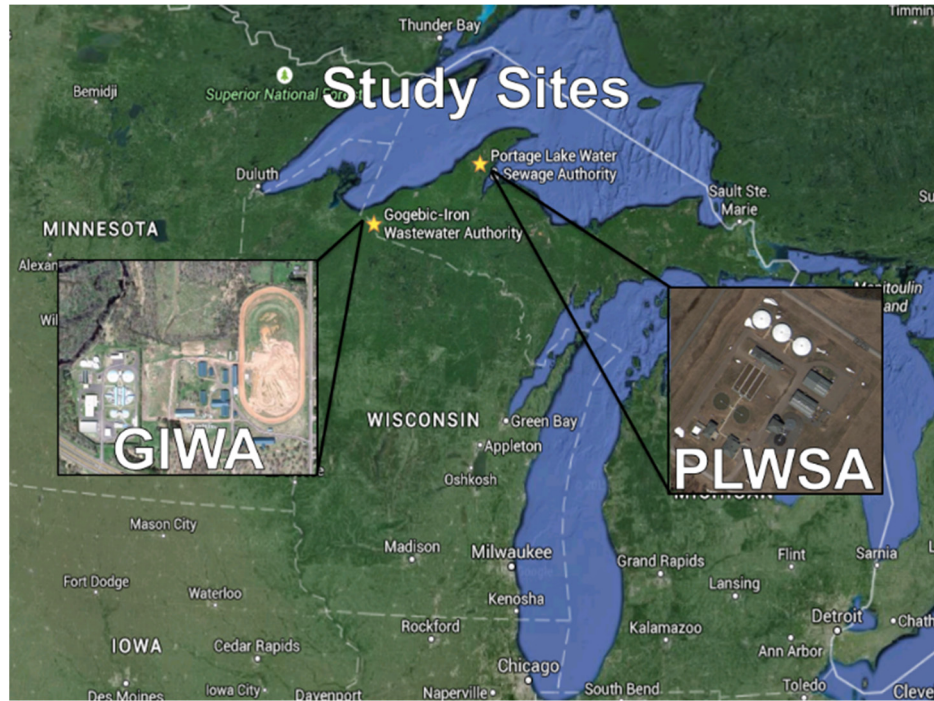
Figure 2-4. Location of GIWA and PLWSA Study Sites. GIWA is located in Ironwood, Michigan while PLWSA is located in Houghton, MI.

Treatment Process	GIWA	PLWSA
Pretreatment	Screening and grit removal	Screening and grit removal
Primary Treatment	Primary clarification	Primary clarification
Secondary Treatment	Oxidation ditch activated sludge	Conventional activated sludge
Tertiary Treatment	Phosphorus removal via chemical addition, chlorination, dechlorination and effluent aeration	Phosphorus removal via chemical addition and UV disinfection

Table 2-5. Comparison of GIWA and PLWSA Wastewater Treatment Processes. Differences in biosolids treatments are seen during secondary treatment where GIWA undergoes oxidation ditch activated sludge, while PLWSA uses a conventional activated sludge process.

GIWA and PLWSA perform mesophilic anaerobic digestion for vector attraction reduction, followed by dewatering via belt-filter press during the solids process train. Both plants produce materials that are classified as Class B biosolids. Large uninsulated storage sheds are currently used for winter biosolids storage at PLWSA and GIWA.

2.4.2 Objective 1: Effect of Freeze-Thaw Cycles on Biosolids

2.4.2.1 Field Study

A 3 ft high biosolids pile was constructed with freshly dewatered biosolids in the un-insulated biosolids storage shed at PLWSA in May of 2013. Temperature profiles were monitored at 3 locations within the pile. For each temperature profile, four Thermochron iButton temperature data loggers (Embedded Data Systems; Lawrenceburg, KY), with temperature ranges of -5 to 26 ˚C, were waterproofed with a silicone sealant, secured to a wooden stake at 0, 5, 10, 20, and 50 cm depths (measured from the top of the pile) and programmed to record the temperature at 4 h intervals for one year. When the biosolids were not frozen, samples were collected monthly at each depth for analysis of total solids and fecal coliforms. Total solids and fecal coliform levels were quantified in each sample using the EPA Method 1684[81], and the Most Probable Number Method EPA Method 1681[82], respectively.

2.4.2.2 Freeze-Thaw Cycle Pathogen Inactivation

A 200 g biosolids sample, collected from GIWA or PLWSA, was diluted with sterile deionized water to achieve desired total solids concentrations, which ranged from 5 to 25% total solids. Initial total solids and fecal coliform levels were quantified in each

27

sample using the EPA Method 1684[81], and the Most Probable Number Method EPA Method 1681[82], respectively. The sample was then divided into 100 g subsamples, placed in Erlenmeyer flasks, and covered tightly with Parafilm. One subsample served as the control and was incubated at 4 °C for 48 hr. The other subsample was incubated at -20 °C for 48 hr and then thawed for 24 hr at 4 °C. After 72 hr, the subsample subjected to the freeze-thaw cycle and control were analyzed for fecal coliforms.

2.4.2.3   Freezing Rate

Tests were performed to relate percent total solids to the freezing rate of biosolids. **Figure 2-5** illustrates the basic approach of the freezing rate experiments. Insulated biosolids were placed on top of a water bath at 5 ˚C and in a freezer at -5 ˚C. A below-freezing temperature on top and an above-freezing temperature on the bottom of the biosolids created a temperature gradient. The temperature gradient caused the cooling front in the biosolids to move from top to bottom to simulate conditions in natural lagoon storage freezing[83]. The system was operated in this manner for 24 hr. Temperature profiles in the biosolids were obtained every 100 s (1.67 min) in all of the freezing rate experiments.
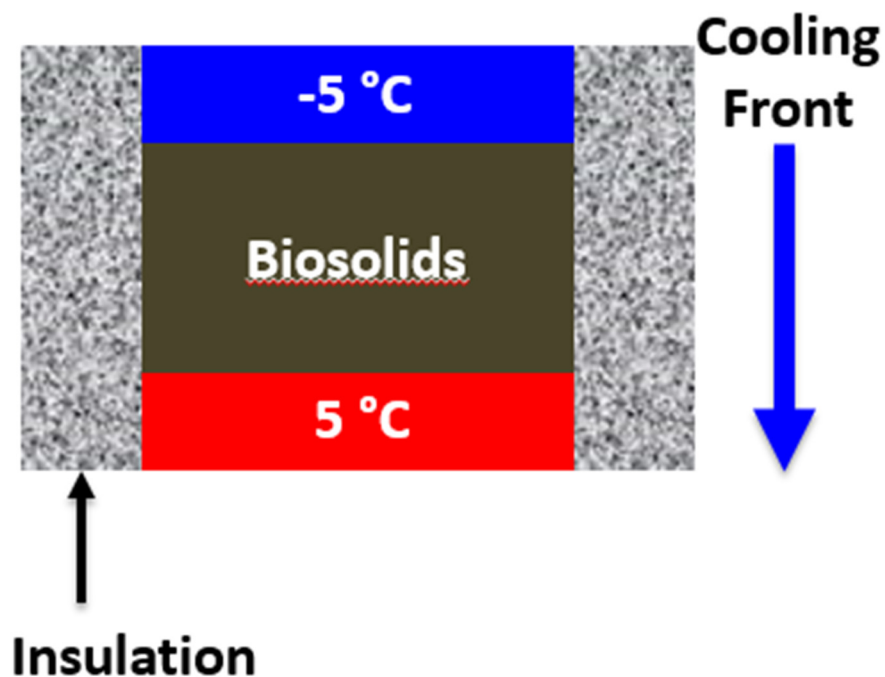
Figure 2-5. Schematic of the biosolids freezing rate experiments. Biosolids were placed between insulation with a water bath at 5°C beneath, and air at -5°C to ensure the cooling front moved top to bottom.

2.4.2.4   Scanning Electron Microscopy

Prior to analysis with a FEI Philips XL 40 Environmental Scanning Electron Microscope, biosolids were oven-dried at 40°C for 1.5 days, directly mounted onto a sample button using carbon tape, and coated with a 10 μm-thick platinum-palladium alloy. Images of biosolids were taken from 10-100 μm in diameter at a resolution of 15.0 kV.

2.4.3 Objective 2: Pilot-Scale Studies

2.4.3.1 Pilot-Scale Test Boxes

Whether biosolids are stored indoors or outdoors affects solar radiation, temperature, and moisture content. Therefore, two pilot-scale tests were assembled in triplicate at each site, with pilot test boxes located inside and outside the storage shed. The pilot-scale boxes were designed to meet four main specifications. First, the boxes had to maintain structural integrity while holding ~two tons of solids, plus precipitation throughout the year, and undergoing freeze/thaw cycles of the biosolids. Next, the boxes had to remain watertight for up to two years, not allowing leachate to leak from the structure. Thirdly, the boxes had to allow drainage water from the biosolids to be collected and disposed of properly. Lastly, the boxes had to withstand ambient temperatures (~20°F to 95°F). To simulate average dimensions of a biosolids pile, boxes were built 4' high, 4' wide, and 8' long, using exterior-grade plywood, 2-in x 4-in braces, and additional reinforcements (**Figure 2-6**),
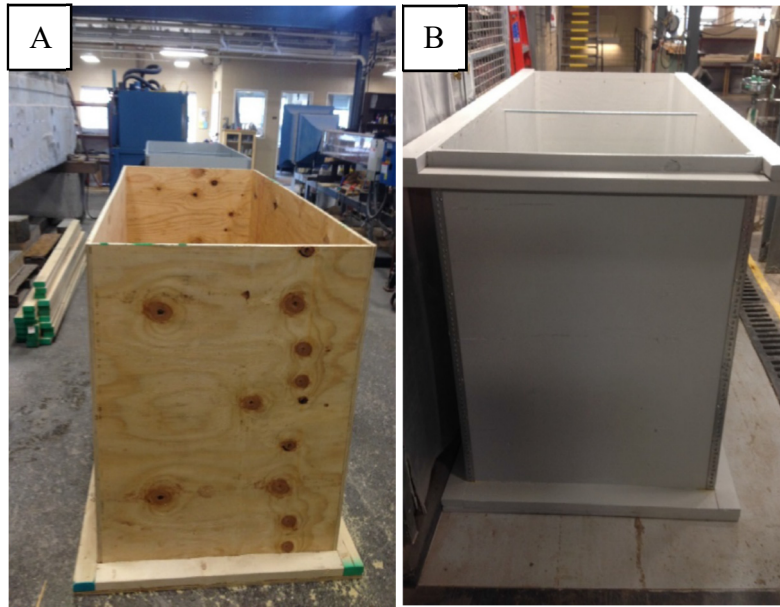
Figure 2-6. Wooden box construction **A)** during assembly and **B)** after completing assembly and painting.

Liners, a drainage system, and temperature sensor stacks were installed in the pilot boxes to meet design criteria. First, a sand layer was added to the bottom of the boxes to protect the liner from the wood (**Figure 2-7A**). Custom-made, potable water grade vinyl liners (Tri-City Vinyl, Saginaw, MI) were placed inside the interior of the box and attached to the outside by wood cleats (**Figure 2-7B**). Next, a hole was cut in the liner and the box to fit a polyvinyl chloride (PVC) drainage pipe (ASTM No. D2729 specifications) at the bottom of the box (**Figure 2-7C**). Small gravel was added to the box below the drainage pipe (**Figure 2-7D**) followed by size 6A gravel to a depth of ~ 2" to ensure proper drainage and prevent clogging (**Figure 2-7E**). Over the gravel, filter fabric was laid down to allow leachate to drain while holding solids in place (**Figure 2-7F**).

Figure 2-7. Boxes showing **A)** 1.5-2'' base sand layer, **B)** vinyl liner, **C)** drainage pipe, **D)** small gravel layer, **E)** 6A gravel to a level of ~2" and, **F)** cross braces, sensor stacks, and filter fabric on bottom.

To begin filling the boxes, biosolids were carefully placed around the filter paper to prevent exposure to any of the sand or gravel. Boxes were filled by shoveling biosolids from a front-end loader to attain even packing consistency across all boxes to a level of 3 feet (**Figure 2-8**).

Figure 2-8. Final construction of pilot scale boxes. A front-end loader was used to evenly fill boxes with biosolids.

2.4.3.2   *Enumeration of Microorganisms*

To meet the requirements for alternative 6 of Class A biosolids production, or a "Process Equivalent to a PFRP", pathogen limits of $\geq$ 3-$\log_{10}$ reduction of total enteric viruses, $\geq$ 2-$\log_{10}$ reduction of viable *Ascaris ova*, and $\geq$ 1-$\log_{10}$ reduction of fecal coliforms had to be met[19]. However, biosolids in the U.S. do not contain high enough

levels of *Ascaris ova* or enteric viruses to demonstrate adequate pathogen reduction. For this reason, *Ascaris ova* and enteric viruses were seeded into the pilot-scale boxes to levels of 10^4 *Ascaris ova*/g total solids and 10^5-10^6 plaque-forming units (PFU) enteric virus/g total solids. The vaccine-grade type 1 human poliovirus (ATCC) was used as the enteric virus and is an attenuated virus that is noninfectious.

Sentinel Chamber Design

Chambers were designed for spiking pathogens into the biosolids. Separate chamber designs for *Ascaris ova* (~35 to 50 µm diameter)[84] and poliovirus (~28 nm diameter)[85] were created based on pathogen size. Chambers included a membrane system that prevented the release of pathogens while allowing for an exchange of gas and liquid with the biosolids. Therefore, conditions inside and outside the chambers in the biosolids boxes were essentially the same.

The *ova* chambers followed the design from Gould et al[86]. ANKOM F57 filter bags (ANKOM Technology, Macedon NY) were used because their pore size (25 µm) was small enough to contain the *ova*. Additionally, the filter bags were chemically resistant and capable of being heat-sealed. A complete *ova* sentinel bag is shown in **Figure 2-9**.
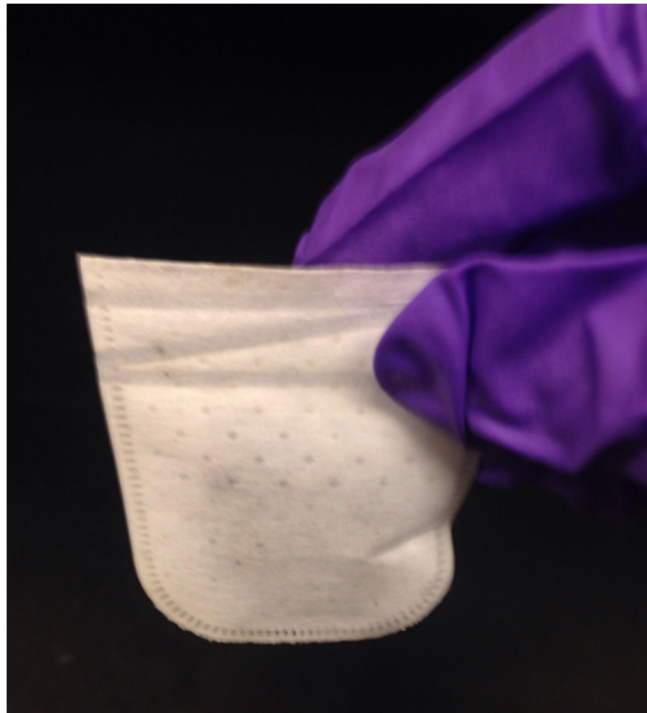
Figure 2-9. Complete *Ascaris* ova chamber with a pore size of 25 µm to contain the ova.

Sentinel chambers for poliovirus followed the design of Sidhu and Toze[87]. The sentinel chambers were composed of a Teflon tube that was open on both ends. The tube was secured at each end by a membrane (25 mm-diameter, 0.025-µm pore size, Millipore). The membrane was protected by a marine-grade stainless steel mesh (0.5 mm). An O-ring secured the membrane and mesh within a groove at the end of the chamber. Brass pressure plates, screws, and nuts held the full assembly together.

The Teflon chambers were fabricated by the Michigan Tech College of Engineering Machine Shop. **Figure 2-10A** illustrates the brass pressure plates that are on the top and bottom of the Teflon chamber. **Figure 2-10B** shows the side view of the chamber. The screws and nuts were made from stainless steel to prevent corrosion and rust. **Figure 2-10C** illustrates the top view of the chamber. The area between the first and second

circles were notched so that an O-ring and membrane could sit on the grove in the chamber. **Figure 2-10D** shows the final view of a complete sentinel chamber.
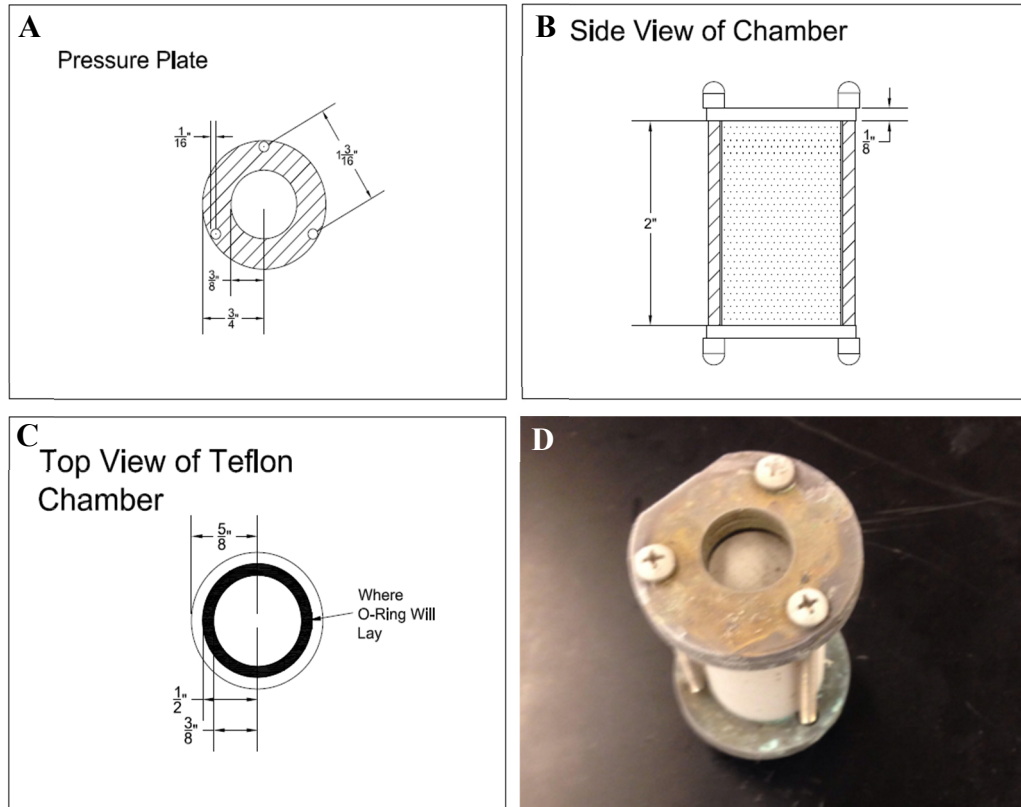
Figure 2-10. Sentinel chamber design for poliovirus. **A)** pressure plate, **B)** side view of sentinel chamber, **C)** top view of Teflon chamber, **D)** complete poliovirus sentinel chamber.

Sentinel Chamber Seeding and Safety

Sentinel chambers were seeded through the use of biological safety procedures to prevent environmental release or worker exposure. Before the release of sentinel chambers into the environment, precautions were taken to ensure accurate quantity and safety of pathogens.

The *Ascaris* eggs sentinel chambers were filled in a designated biosafety area. Three grams of biosolids were placed at the bottom of each bag, ensuring the top of the

bags were free of biosolids. After, ova were added and mixed into the biosolids to a final concentration of 10^4 ova/gram. The bags were sealed three times with a heat sealer (ANKOM HS). Any bags that could not be sealed properly (biosolids inhibiting sealing of bags) were properly disposed of by autoclaving for 60 min at 121°C. The integrity of all *ova* bags was tested before use by placing two ova spiked bags into a biosolids pile for seven days. The bags were then stirred in a beaker of deionized water for 24 hours. Double centrifugation was used with water and then magnesium chloride to retrieve any helminth ova that could have escaped from the bag into the water. Looking under the microscope, no eggs were found from this test, ensuring the safety of the sealed bags.

A biological safety cabinet (BSC) was used to assemble and spike the poliovirus sentinel chambers. The Teflon chamber, bottom membrane, mesh, O-ring, and two brass plates were assembled. Five grams of biosolids were then weighed and added to the semi-completed chamber. The chamber was placed inside the BSC, and the virus was added and mixed into the biosolids to a concentration of 10^5 MTT$_{50}$/ gram. The top membrane, mesh, O-ring, and two brass plates were assembled to the structure. The top and bottom brass plates were fastened tightly to secure the O-rings in place. To ensure that the virus would not escape the chamber, ample time and attention were taken to guarantee the membranes and mesh were correctly positioned in the Teflon chamber. The complete chambers were wiped down with 10% bleach followed by deionized water. To test the structural integrity and safety of the chambers, one chamber underwent 5 freeze/thaw cycles over the course of a week. The chamber was disassembled to check the membrane and mesh for any damage. No damage was observed.

Sentinel Chamber Installation and Retrieval

Ascaris ova chambers were placed in a nylon monofilament drawstring bag with a 25-µm mesh size (filterbag.com) and hung from a pipe for biosolids installation. The drawstring bag hung in a "low" position, a "middle" position, and a "high" position to represent different heights within the biosolids. Each pipe was placed inside an outer PVC pipe that was placed in the bulk biosolids and packed with biosolids to surround the chambers. To sample the ova, the inner pipe was lifted out, and a chamber was randomly chosen for analysis.

The poliovirus sentinel chambers were installed in the pilot-scale test boxes using a similar design as the *Ascaris* ova chambers. (**Figure 2-11**). The chambers were inserted through holes on each side of a square pipe and secured with a zip tie (**Figure 2-11B**). The square pipe was then inserted in an outer PVC pipe (**Figure 2-11A**) placed in the bulk biosolids and packed with biosolids to surround the chambers. As a control, chambers with pathogen-spiked biosolids were stored in plastic bags at 4°C. Controls were measured at each sampling event.

Figure 2-11. Installation of poliovirus sentinel chambers in pilot-scale boxes. **A)** Pipe in pipe design and **B)** poliovirus sentinel chamber installation.

Environmental Conditions

Biosolids temperature was measured in triplicate at 0.5', 1.5' and 2.5' from the top of the 3' high bulk biosolids using Thermochron iButton sensors (Embedded Data Systems). The iButton sensors have an accuracy of $\pm$ 1°C and an operating range of -40 to + 85°C. These devices measure and store temperature data every 2 hours for up to 2 years. The first two stacks, made from PVC, had iButton cables running from the iButtons to the top of the biosolids. These cables were connected to a computer with the use of an iButton Adaptor (Embedded Data Systems) to download the temperature data. The third iButton stack was not connected to cables, therefore, data could not be downloaded unless the iButtons were taken out of the test box and connected to an iButton probe cable reader (Embedded Data Systems, Cat. No. DS1402-RP3+). The third stack was a safety measure in case the main iButtons failed. All iButtons were waterproofed with Marine Adhesive Goop (Eclectic Products, Inc.) and mounted with the use of a clip holder (Embedded Data Systems)

Physical/Chemical Parameters

Pilot-scale test boxes were sampled monthly at each WWTP while the biosolids were unfrozen. Samples were analyzed for total solids, volatile solids, pH, VFAs, and ammonia. Sampling was performed based on the guidance for sampling dewatered sludge drying beds under the USEPA (1989)[88]. Sampling practices included compositing four samples from separate quarters of each box, and preserving samples for analysis.

Total and volatile solids were measured by the EPA method 1684[89]. EPA Method 9045D[90] was used to measure the pH of the biosolids. Volatile fatty acids, bicarbonate

alkalinity, and total alkalinity were determined through the use of the Anderson and Yang titration method[91]. The HACH company TNTplus 832 (range 2 to 47 mg/L NH$_3$-N) Ammonia Method 10205 colorimetry procedure, equivalent to the USEPA Method 350.1[92], was used to measure the content of ammonia-nitrogen in the biosolids.

Microbial Assays

Levels of fecal coliforms, infectious enteric viruses, and *Ascaris* ova were monitored throughout the study for compliance with Class A pathogen requirements[19]. Coliphage levels were measured for comparison to enteric viruses.

Fecal coliforms were measured by the most probable number (MPN) EPA Method 1681[93]. Briefly, a sample of 30 grams of collected biosolids was homogenized in a blender with 270 mL of water. After, the sample was diluted several times in phosphate-buffered water. Samples from four separate serial dilutions were then placed in glass tubes with 2 mL of sterile A-1 Media and an inverted gas collection tube. There were 5 tubes per dilution, with 4 dilutions tested, making a total of 20 tubes per sample. These tubes were incubated at 35°C ± 5°C for 2 hours, and then at 44.5°C ± 5°C for 22 hours. A most probable number program was used to calculate the fecal coliform concentration based on the number of positive gas bubbles found in the inverted collection tubes. Quality control included on-going precision and recovery samples, spiked samples, and duplicated analyses.

Enteric virus levels were measured based on a two-step process. First, poliovirus was recovered from the biosolids using the methods of ASTM D4994-89[94]. After, the virus was quantified using either the 1) plaque assay from Appendix H in Control of Pathogens and Vector Attraction in Sewage Sludge[95] or the 2) quantal assay from

Chapter 15 of the USEPA Manual of Methods for Virology[96]. The plaque assay was used at the beginning of the study to measure high levels of poliovirus, whereas the quantal assay was used at the end of the study to measure low levels of poliovirus.

Ascaris ova were measured following the method of Bowman et al.[97]. First, biosolids were collected from the sentinel bags, broken up, homogenized and sieved (20, 60, 80, and 100 mesh) to remove large particles. The remaining particles were allowed to settle overnight in a solution containing an anionic detergent (7x) to release eggs adhered to particles. Eggs were then separated from particles with the use of settlement, flotation, and sieving. After, eggs were suspended in formalin and incubated at 22-28°C for a minimum of 28 days. Eggs were centrifuged after the incubation period, treated with 10% sodium hypochlorite (bleach) to decolorize the outer shell of the eggs, centrifuged, and suspended in water. A 100 µL of the sample was placed on a slide, and 1st stage, 2nd stage, and 3rd stage viable ova were counted. The sub-sample results were multiplied for a representative sample.

Levels of coliphage reduction are not required to meet PFRP equivalency. However, coliphages were measured because of their similar size, morphology, and structure to enteric viruses. Coliphages are abundant in wastewater and measured with a simple and rapid culture-based assay. The single agar layer EPA Method 1602[98] was used to measure coliphages. Both the male-specific coliphage (MS2, ATCC #15597-B1) and host (E. *coli* HS (pFamp) R, ATCC #700891), and the somatic coliphage (phi-X 174, ATCC #13706-B1) and host (E. *coli* CN-13, ATCC #700609) were used for the study. Coliphages were propagated in their host, filtered through a 0.22 µm syringe filter, and mixed with 40% glycerol to allow for frozen storage. These phages were used as a positive control for the

study. To begin the single agar layer procedure, 12 grams of biosolids were mixed with 100 mL of water in a sterile container. Dilutions were made using phosphate-buffered dilution water. The log-phase host was added to each dilution and mixed with tryptic soy agar, warmed to 49°C ± 5°C, and appropriate antibiotics were added. Agar at 11 mL and the phage solution were poured into five 150-mm Petri dishes. After the agar hardened, the Petri dishes were sealed with parafilm to hold in moisture and placed in an incubator for 16-24 hours at 36°C ± 5°C. After, the plate was counted in plaque-forming units to determine a coliphage quantity.

2.5   Results and Discussion

2.5.1   Objective 1: Effects of Freeze-Thaw Cycles on Biosolids

Freeze-thaw cycles naturally occur in biosolids over winter storage in northern climates. Freeze-thaw cycles increase dewaterability (or ability to lose water) of biosolids[67-70] and can inactivate pathogens in biosolids. However, little is known about the effect of pathogen inactivation in anaerobically digested biosolids. Here we study the influence of freeze-thaw cycles on pathogen inactivation in anaerobically digested biosolids as a function of moisture content. Understanding the correlation of freeze-thaw cycles to pathogen inactivation in sewage solids will allow WWTPs to utilize a natural process to treat biosolids.

2.5.1.1   Visual Analysis of Physical Changes

Biosolids properties after winter storage were evaluated. Based on a visual assessment of the biosolids, it was obvious that the physical characteristics of the

biosolids had changed after over-winter storage. **Figure 2-12A** shows the biosolids pile in the GIWA storage shed after winter storage. **Figure 2-12B** shows a close-up of the top layer of biosolids that experienced freeze-thaw cycles over the winter. Biosolids were very dry with a light texture. This is quite different from the physical appearance of the fresh biosolids as demonstrated in **Figure 2-13B**. **Figure 2-13** provides a comparison of the freeze-dried and non-frozen biosolids. The biosolids that experienced freeze-thaw cycles have a smaller particle diameter, and reduced pore size between particles, while the non-frozen biosolids particles clump together, and contain large pore spaces between the flocs. The nature of the biosolids subjected to freeze-thaw cycles at the particle scale is illustrated in **Figure 2-14** by the environmental scanning electron microscopy images of biosolids particles from GIWA. A biosolids particle is comprised of a complex array of structures of various shapes and sizes. Overall, biosolids properties change after exposure to freeze-thaw cycles to a lighter and drier texture.
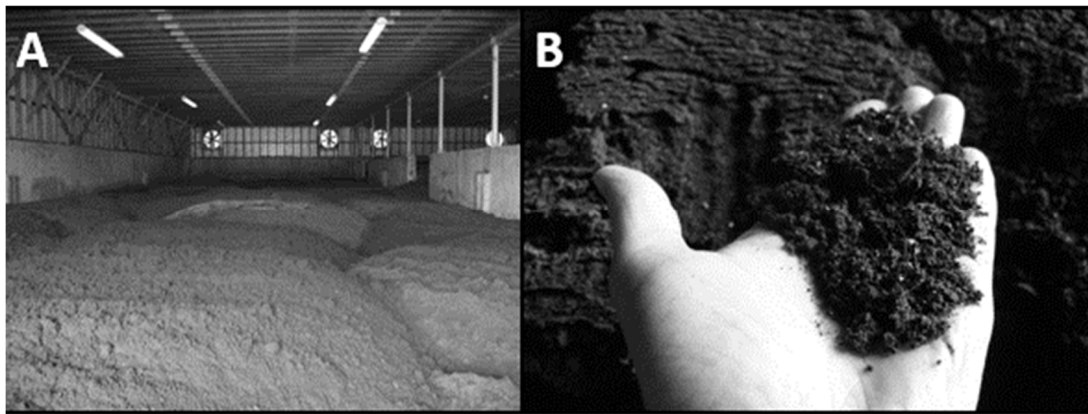
Figure 2-12. Freeze-dried biosolids **A)** in the GIWA storage shed after winter storage, and **B)** in a close-up view.
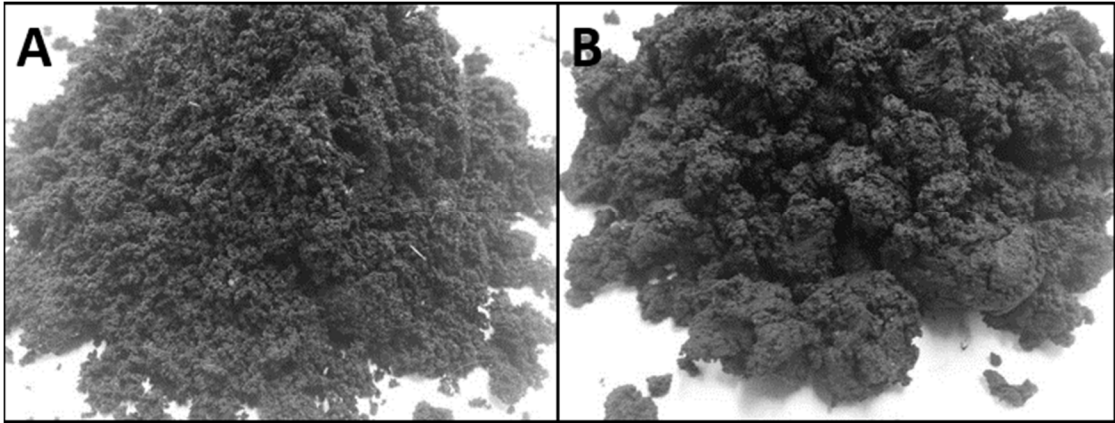
Figure 2-13. Comparison of **A)** freeze-dried biosolids to **B)** non-frozen biosolids from GIWA. Structural changes occur after freezing which includes a less dense texture.
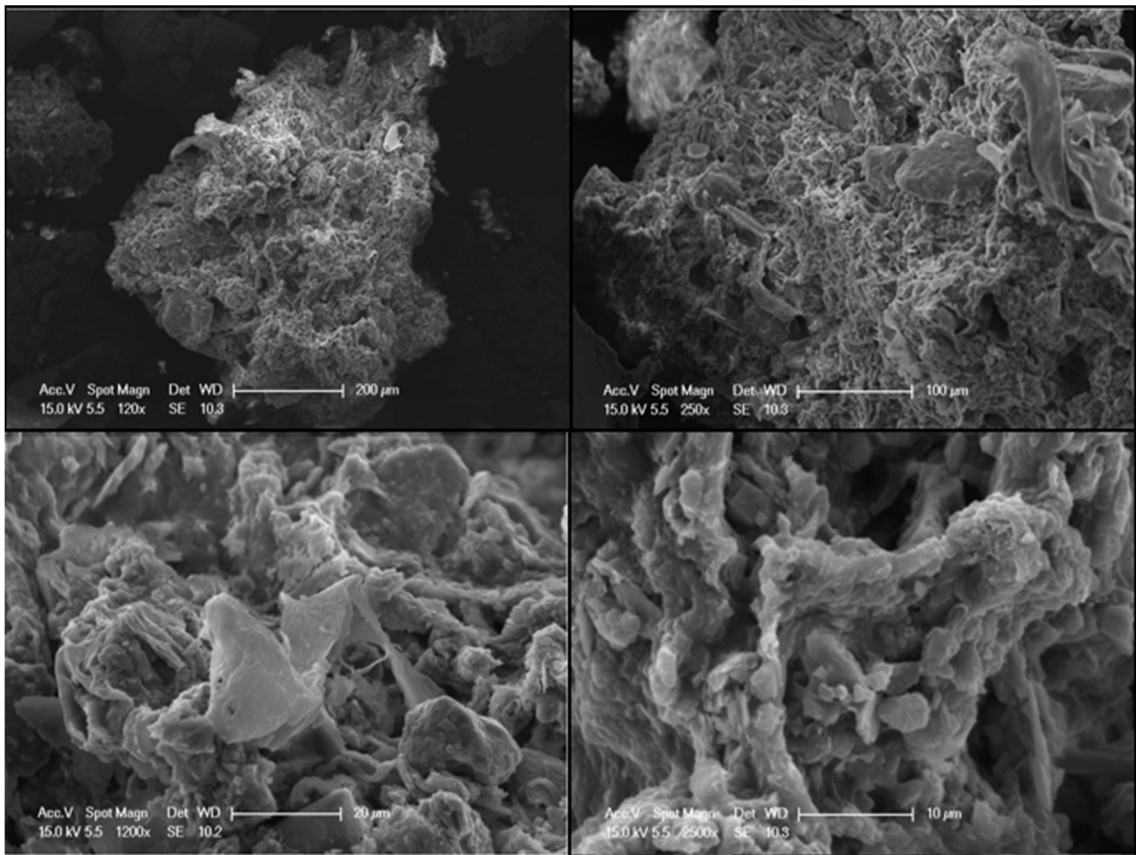
Figure 2-14. SEM Images of freeze-dried biosolids from GIWA. A biosolids particle clearly is comprised of a complex array of structures of various shapes and sizes.

2.5.1.2 Field Study

During the field study, fecal coliforms and total solids were measured at five depths in a pile located in the enclosed biosolids storage shed at PLWSA from May 2013 to June 2014. Similar patterns were observed at all depths for temperature, total solids, and fecal coliforms (**Figure 2-15**). The temperature in the biosolids followed an overall trend of increasing from May through August, decreasing from August through November, and increasing again from March through June. It is important to note that the iButtons had a lower temperature limit of -5°C. Ambient temperatures below this level occurred frequently between November 2013 and March 2014[99], thus it is likely that temperatures below -5°C occurred in the pile. Overall, biosolids temperature followed temporal patterns and variation in temperature decreased with increasing depth.
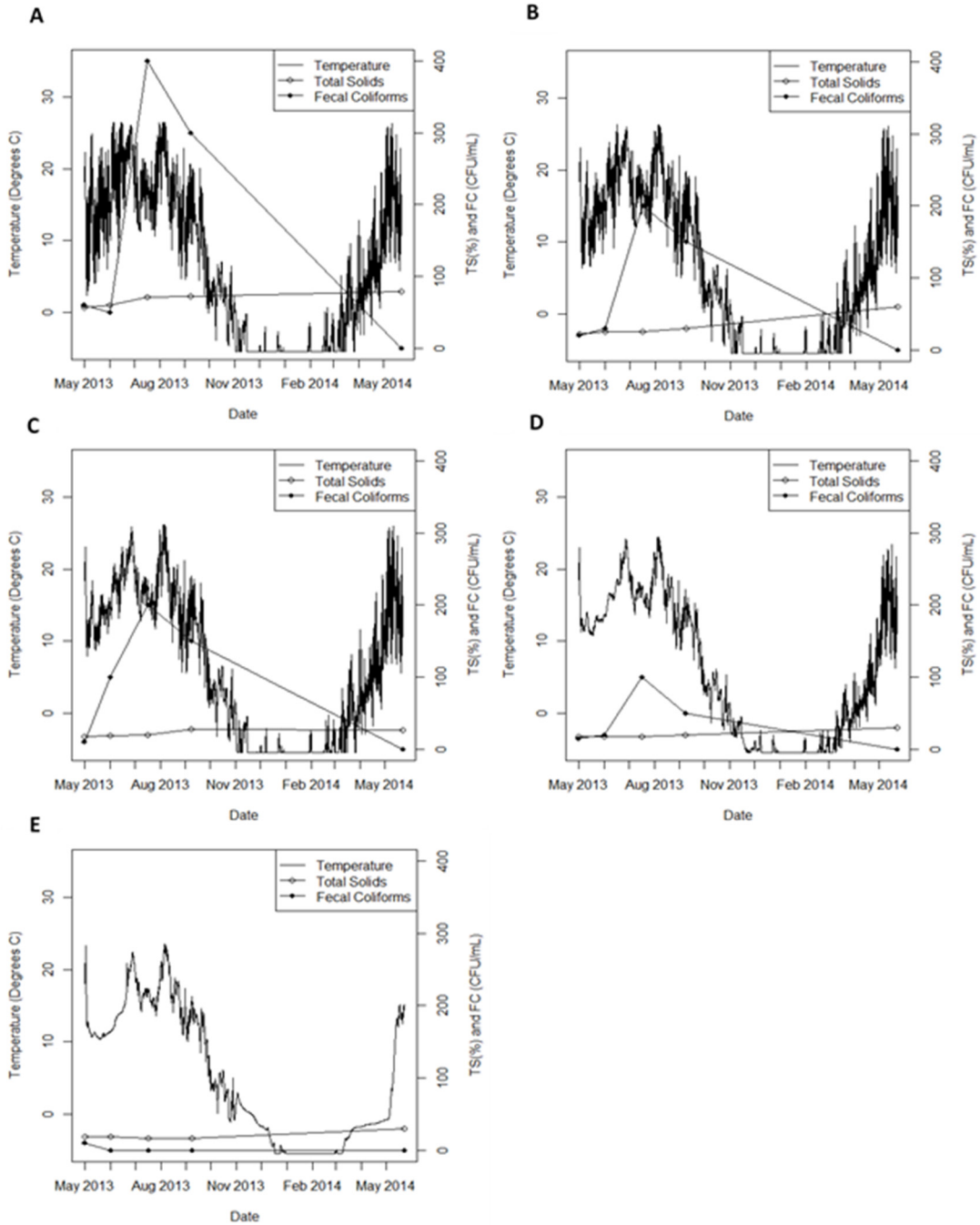
Figure 2-15. Temperature, total solids (TS), and fecal coliforms (FC) measured at depths of **A)** 0 cm, **B)** 5 cm, **C)** 10 cm, **D)** 20 cm, and **E)** 50 cm, as measured from the surface of biosolids stored in an enclosed storage shed at PLWSA. Note that the minimum temperature that could be measured was -5˚C, but lower ambient temperatures were frequently observed between November 2013 and March 2014.

46

From May through October, when temperatures remained above 5°C and below 27°C, regrowth of fecal coliforms occurred at all depths except 50 cm (**Figure 2-15**). However, after October when freeze-thaw cycles occurred in the biosolids, fecal coliform numbers decreased to non-detectable levels at all depths. At the 50 cm depth, regrowth was never observed and fecal coliforms decreased to non-detectable levels by September.

Total solids steadily increased for all depths (other than 50 cm), presumably resulting from a combination of evaporation and freeze-drying (**Figure 2-15**). The largest increase in total solids occurred at the 0 and 5 cm depths after September 2013, suggesting that freeze-drying was especially important at the top of piles. Total solids were highest at the 0 cm depth and eventually reached 79%. At the 50 cm depth, a small decrease in total solids was initially observed, presumably resulting from the input of drainage from the upper layers. Thus, the 50 cm depth behaved differently than the above layers. The total solids increased at the 50 cm depth from 17% in November 2013 to 30% in June 2014.

2.5.1.3 *Freeze-Thaw Cycles Pathogen Inactivation*

The relationship between freeze-thaw cycles, total solids, and fecal coliform reduction are presented in **Figure 2-16** with samples from both GIWA and PLWSA. Despite the different biosolids sources, the data suggest a similar trend in fecal coliform reduction as a function of total solids for samples frozen at -20°C. Lower percent fecal coliform reductions were observed at low total solids (< 10% TS), and high total solids (≈ 25% TS). At intermediate solids contents (10-20% TS), the percent reduction in fecal coliforms plateaued with reductions ranging from 60-95% with many data points around 80-90%. The maximum reduction (93.5%) in fecal coliforms was observed at 16% total

solids. These results suggest that there may be an optimum range of total solids for maximizing fecal coliform inactivation during freeze-thaw cycles; however, additional data points at the upper and lower total solids regions are required to confirm these trends.
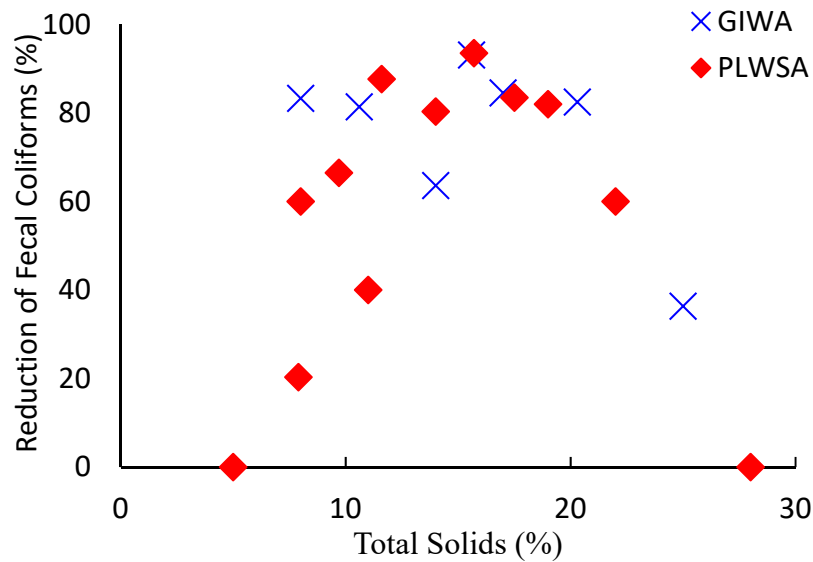
Figure 2-16. Percent fecal coliform (FC) reduction after one freeze-thaw cycle in relation to total solids (TS). There is an ideal total solids content that produces the highest reduction of fecal coliforms.

2.5.1.4   Freezing Rate

Implicit in the analysis of the field- and laboratory-scale data is the assumption that the biosolids freezing rate increases with increasing total solids content. To evaluate the effect of total solids content on the biosolids freezing rate, the rate at which a one-dimensional freezing front migrated through biosolids was determined with thermocouples at various depths within biosolids samples. Total solids values of 8, 13, 16, and 18% were tested.

The initial rates of temperature changes were compared for each total solid condition and thermocouple location. As expected, the initial rate of temperature change was slowest in the 8% total solids sample and fastest in the 18% total solids sample (**Figure 2-17**). The initial rates of temperature change in the 13% and 16% total solids samples were similar and in between those measured in the 8 and 18% total solids. These results are consistent with our hypothesis that the freezing rate for biosolids decreases with increasing moisture content. In addition, the similar freezing rates (between 5-10ºF/hour) measured at the intermediate total solids levels (13 and 16%) are consistent with the similar levels of fecal coliform reduction at those total solids levels.
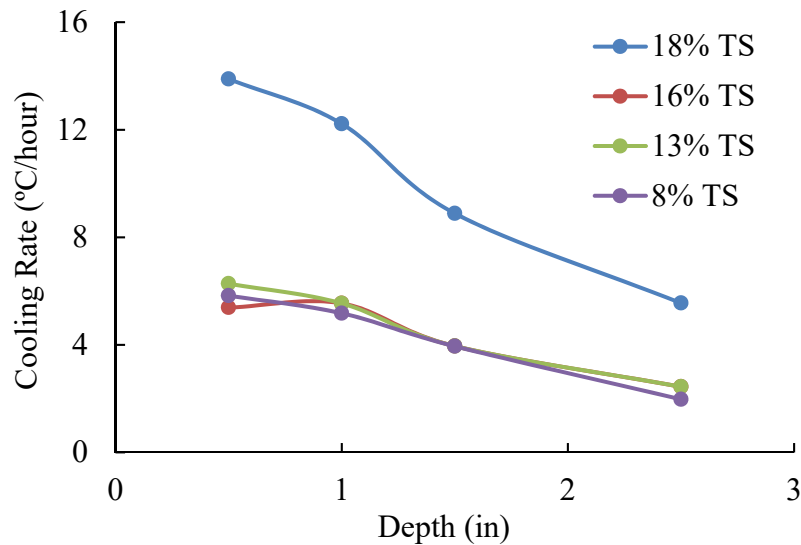
Figure 2-17. Initial cooling rate at various depths in biosolids. The largest rate of cooling occurred at the highest total solids content.

2.5.1.5   Discussion

The field study provided anecdotal evidence that freeze-thaw cycles contribute to the inactivation of fecal coliforms during biosolids storage. While fecal coliform die-off

was observed at all depths during storage, the greatest reduction in fecal coliform levels occurred in the top and driest layers (**Figure 2-15**). These observations suggest that the biosolids moisture content affects the degree of fecal coliform inactivation during freeze-thaw cycles. Therefore, a laboratory study designed specifically to quantify the fecal coliform reduction in biosolids during freezing at different total solids was undertaken using samples collected at PLWSA and GIWA.

This laboratory evaluation was needed because little is known about the effects of freeze-thaw on pathogen inactivation in wastewater solids. Sanin et al. (1994) studied the correlation between temperature, freezing rate, and freezing time on pathogen reduction in activated sludge (rather than digested and dewatered biosolids), and observed pathogen inactivation after freezing and thawing[77]. Likewise, freezing and thawing have been used as a pretreatment technique to improve the dewaterability of sludge through the formation of compact aggregates that enhance sludge thickening and filtration[100]. However, the effects of several important variables, such as moisture content, on the efficacy of freeze-thaw cycles for pathogen reduction in stored biosolids has not been studied.

The laboratory data showed that inactivation of fecal coliforms appears to be less effective at lower (below 10% total solids) and higher total solids concentrations (above 20% total solids) compared to intermediate total solids concentrations (between 12% and 20%). To understand these results, it is important to understand that freezing temperatures alone do not cause cell death. In fact, cells have several strategies for preserving viability in freezing temperatures, including increasing cell membrane fluidity, producing polyols (i.e., alcohols with multiple hydroxyl groups) and antifreeze

proteins, and creating cold-shock proteins and cold-active enzymes[101]. The interactions between ice crystals and cells produce inactivation during freeze-thaw cycles.

The rate at which freezing occurs determines the size and location (intra- or extracellular) of ice crystals inside/outside the pathogenic microorganism[79]. At the lowest total solids, pathogens cool slowly enough that water can move across the membrane via exostosis before freezing[79]. Thus, the ice crystals that form are primarily outside the pathogenic membrane, where they cause less damage than intramembrane ice crystals, which can disturb coat proteins and nucleic acids[74] and rupture pathogens if sufficiently large. The formation of ice crystals outside of the membrane at slow freezing rates could explain why fecal coliform inactivation is lower at the lower total solids levels. Note that some inactivation is still expected because ice formation causes differences in the extramembrane and intramembrane solute concentrations that can cause dehydration and other cell damage during freezing and thawing[102]. When cells cool more rapidly (i.e., higher total solids), water may freeze (crystallize) before passing through the membrane. The size of these intramembrane ice crystals also depends on the rate of freezing[79,103]. When the rate of cooling is very fast, the rate of ice nucleation (initiation of ice crystal structures) is faster than the rate of ice crystal growth, resulting in large numbers of small crystals, which are less damaging than the large crystals that are expected to form at somewhat lower cooling rates. **Figure 2-18** shows a schematic of the freezing concepts.
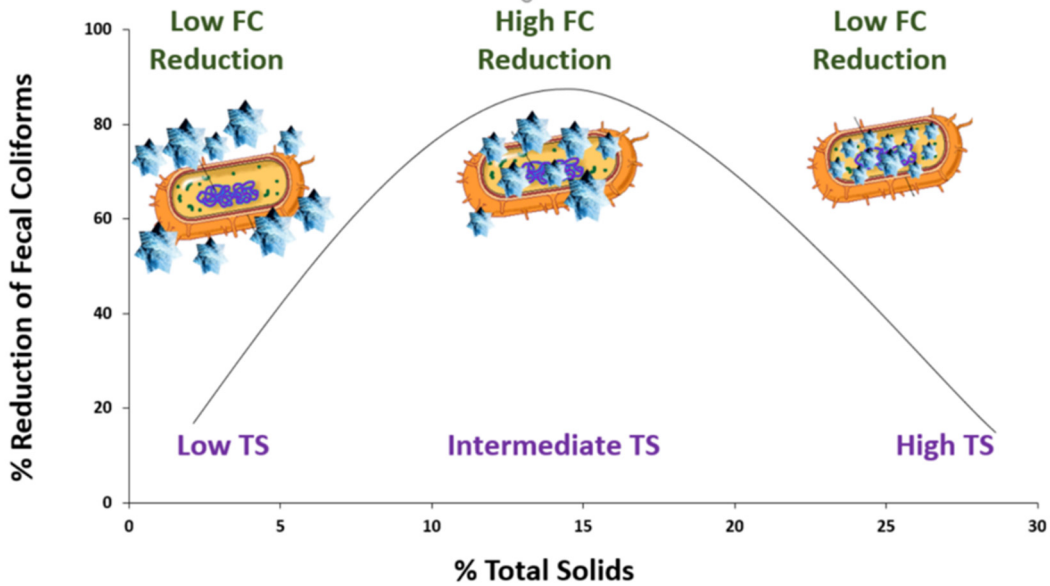
Figure 2-18. Conceptual model for inactivation of fecal coliforms (FC) at different total solids (TS). At low total solids and high total solids, the fecal coliform reduction is low. At intermediate total solids, the fecal coliform reduction is high.

2.5.2 Objective 2: Pilot-Scale Studies

Pilot-scale studies were initiated at PLWSA in July and GIWA in August of 2016. Environmental conditions and key physical/chemical properties were monitored throughout the study. Though poliovirus sentinel chambers were set up during this study, the data had not yet been collected for these enteric viruses and are not included in this dissertation. Data collection occurred from August 2016- August 2017 to demonstrate emerging trends, though the long-term storage study continued for up to a year after 2017 and was followed by air drying.

2.5.2.1 Environmental Conditions

Biosolids temperatures in the test boxes at PLWSA and GIWA are presented in **Figure 2-19**. As expected based on ambient temperatures, biosolids temperature decreases from August through December and increases from March through August. Multiple freeze/thaw cycles were observed at both plants.
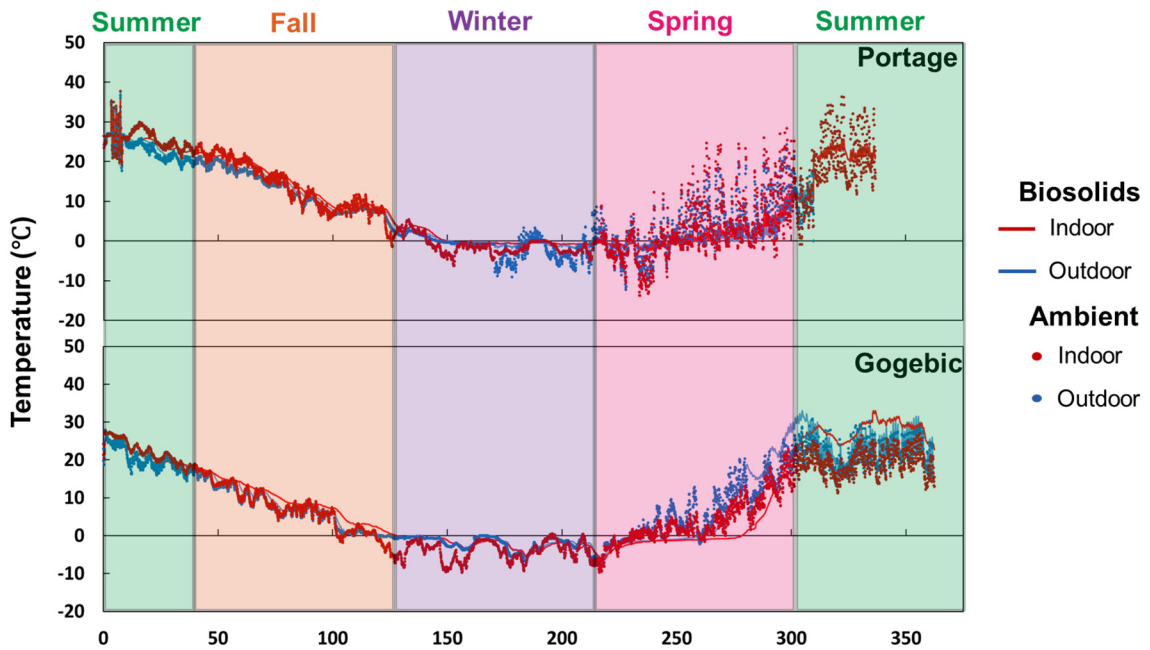
Figure 2-19. Ambient and Biosolids Temperatures during long-term storage at **A)** PLWSA and **B)** GIWA. Biosolids temperatures closely followed the trends for ambient temperatures.

2.5.2.2 Physical/Chemical Parameters

Total and volatile solids at GIWA and PLWSA contain some similarities and differences (**Figure 2-20**). The total solids at both plants stayed relatively constant until December and increased after the winter thaw. At both plants, biosolids stored indoors dried out to a greater extent than those stored outdoors. The volatile solids at PLWSA and

GIWA decreased indoors and outdoors. However, the volatile solids at PLWSA experienced a large decrease (60% to 20%) between day 28 and 59 followed by an increase to 60% VS, while the volatile solids at GIWA gradually dropped from 50% to 30%.
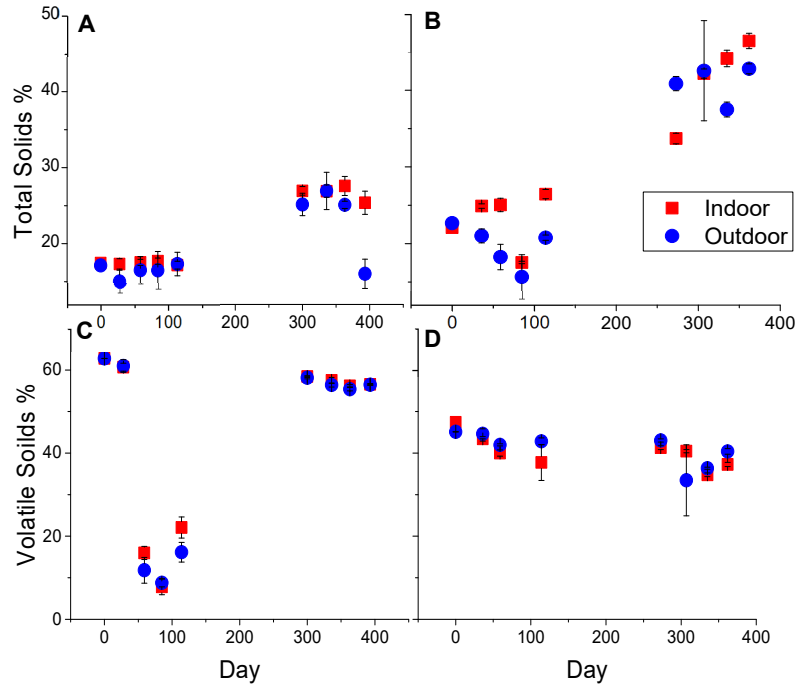
Figure 2-20. Total Solids at **A)** PLWSA and **B)** GIWA, and Volatile Solids at **C)** PLWSA and **D)** GIWA.

The pH levels observed in the test boxes are shown in **Figure 2-21**. Initial pH levels at both plants started above pH 8 and dropped throughout the study. The pH at PLWSA steadily dropped to 6.5 while the pH at GIWA drastically dropped to below 5. The pH differences in the indoor and outdoor boxes at GIWA started to increase after winter thaw where pH levels in the indoor boxes dropped to 6.0 while pH levels in the outdoor boxes dropped to 4.5.
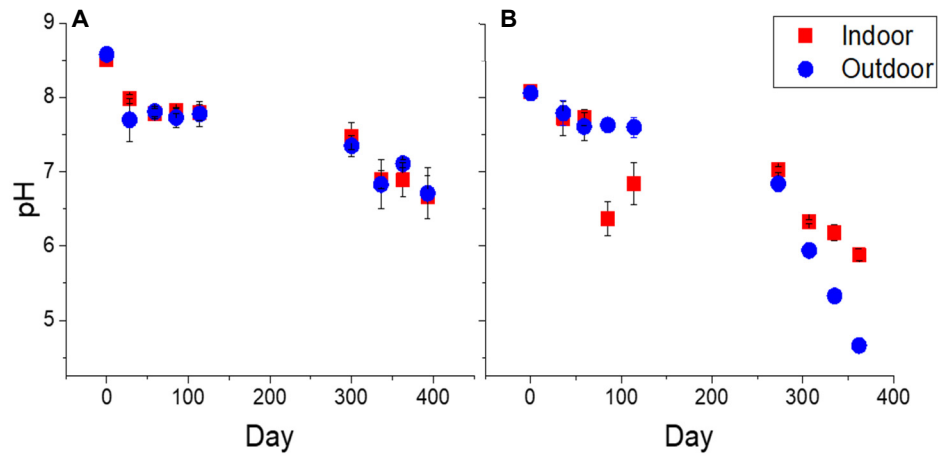
Figure 2-21. pH at **A)** PLWSA and **B)** GIWA. pH decreased at both plants, but decreased more drastically at GIWA.

There were no distinct trends in the bicarbonate and volatile fatty acid levels (**Figure 2-22**). At both WWTPs, the volatile fatty acid levels remained below 40,000 mg/kg. At low pH values, these levels of volatile fatty acids have been shown to inactivate pathogens[46].
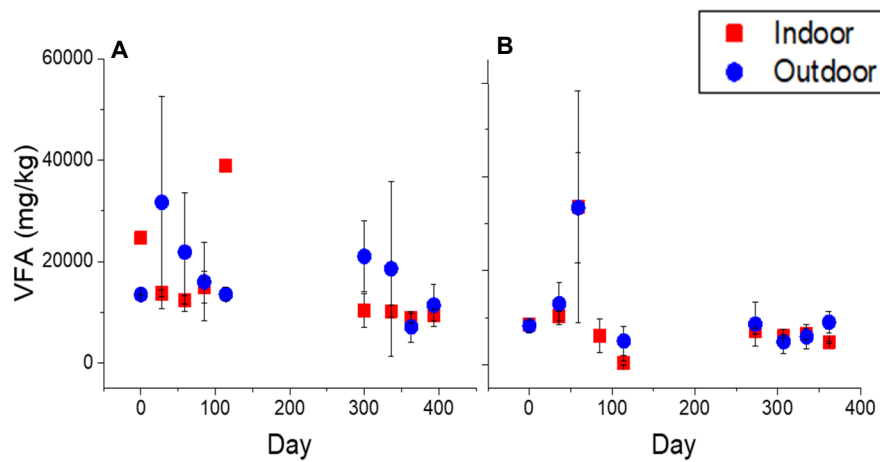
Figure 2-22. Volatile Fatty Acid (VFA) concentrations at **A)** PLWSA and **B)** GIWA. VFAs decreased in both plants.

The ammonia concentrations at PLWSA increased before winter and decreased after winter (data not shown). There is no clear trend in ammonia at GIWA. However, after winter, ammonia concentration increased in the indoor boxes and decreased in the outdoor boxes at GIWA. The main trends for physical/chemical parameters included an increase in total solids and a decrease in pH.

2.5.2.3   Pathogen Inactivation

The data from both plants followed similar trends, providing evidence into the reproducibility of long-term storage treatment. Comparable pathogen inactivation was observed at GIWA and PLWSA. Pathogen indicator organisms including fecal coliforms, *Ascaris ova*, and coliphages were measured. Though the enteric poliovirus was spiked into the biosolids, inactivation data for this specific pathogen is not included. Enteric virus inactivation was measured after the completion of this report. Fecal coliforms decreased steadily at both locations, and after winter reached Class A levels as shown in **Figure 2-23**.
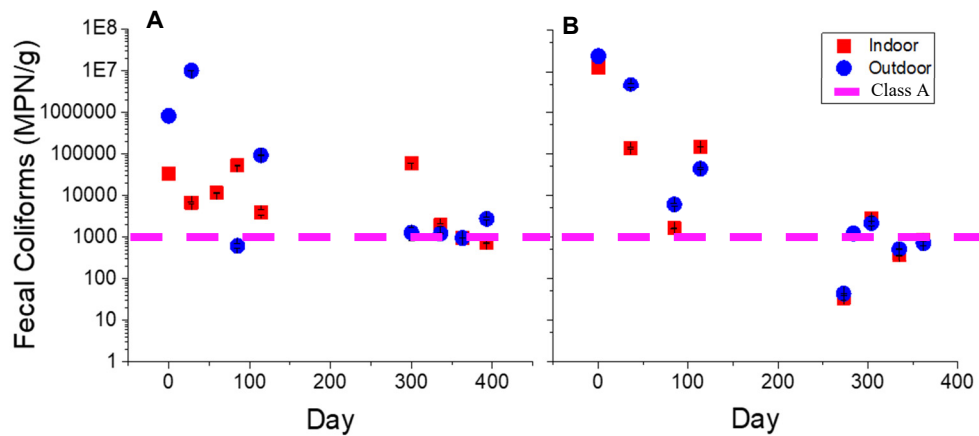
Figure 2-23. Fecal Coliforms at **A)** PLWSA and **B)** GIWA. Fecal coliform reduction at both plants follows similar trends with pathogens decreasing after winter storage.

Similar trends for *Ascaris* ova were observed at both plants. 2nd stage viable *Ascaris* ova remained constant at both plants and did not reach the Class A requirement of a 2-$\log_{10}$ reduction (**Figure 2-24**). Variability in all *Ascaris* ova samples is large, likely associated with the wide error and variability associated with the Bowman method. *Ascaris* ova have been shown to be inactivated to Class A levels through warmer climates[59-63] or a longer storage time of 3 years or more[62,65,66].
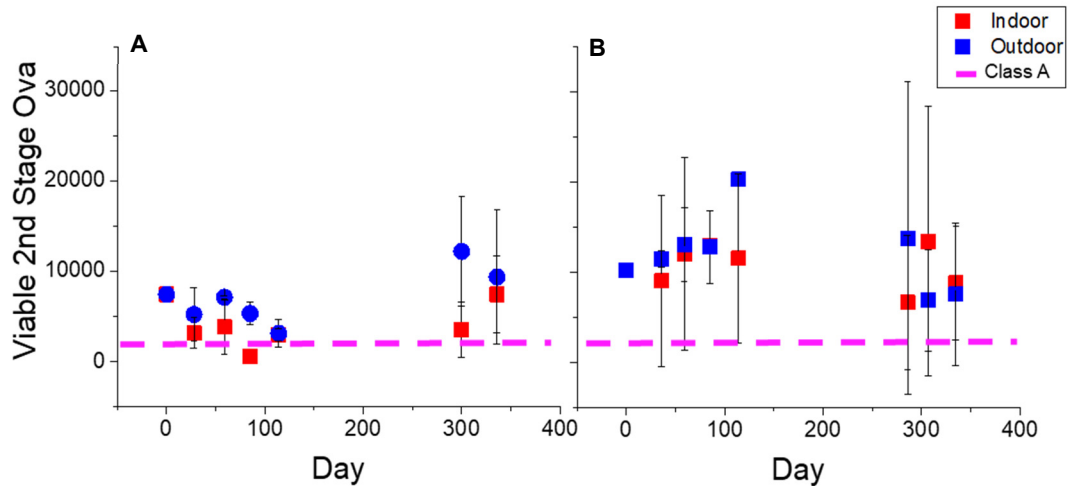
Figure 2-24. Viable 2nd Stage Ascaris Ova at **A)** PLWSA and **B)** GIWA. Levels remained steady and did not decrease to Class A levels.

No clear trends were observed with the coliphage inactivation data, and therefore it was not added to this report. Pathogens in the biosolids were affected by all of the physical/chemical parameters measured during the study. High temperatures and freeze/thaw cycles are known to inactivate microorganisms. Drying of biosolids can dehydrate microorganisms and inactivate pathogens. Volatile solids act as an organic food source for microorganisms, and low levels can cause inactivation. High pH levels can increase the toxic form of ammonia, while low pH levels increase the toxic form of volatile fatty acids.

2.6 Conclusions

Objective 1 combined field- and laboratory-scale experiments to determine the relationship between total solids and pathogen reduction in biosolids subjected to freeze-thaw cycles. During the field study, fecal coliforms reduced after winter freeze-thaw

cycles to undetectable levels. The lab-scale study found that intermediate total solids levels (~16% TS) reduced fecal coliforms to the greatest extent. Observations of significant reductions in fecal coliforms as a result of freeze-thaw cycles in both the field- and laboratory-studies are meaningful for WWTPs that store their biosolids indoors over winter with below-freezing temperatures. Nevertheless, additional testing will be required to confirm the ideal range of the rate of freeze/thaw and the moisture content for pathogen inactivation. Additionally, the impact of multiple freeze-thaw cycles should be evaluated. Supplementary tests should also be performed to examine the effects of freeze-thaw cycles on other indicator organisms besides fecal coliforms.

Objective 2 evaluated pathogen inactivation under long-term storage as a function of environmental conditions. The initial results from the long-term storage pilot-scale study demonstrated changes in environmental conditions, physical-chemical parameters, and microbial populations (August 2016-August 2017). Temperature profiles confirmed that biosolids stored over winter at both GIWA and PLSA underwent multiple freeze-thaw cycles. The main trends observed in physical/chemical parameters over the year were an increase in total solids and a decrease in pH. Fecal coliforms quickly reduced to Class A levels after winter storage, however, *Ascaris* ova did not reach Class A levels after one year of storage. Since Class A requirements were not met, monitoring will continue for several years to verify that pathogen reduction complies with the EPA methods for alternative 6 of Class A biosolids production. Longer storage time, more drastic levels of pH, or higher temperatures would be able to decrease pathogens in the biosolids to a Class A limit. Ultimately, the results of this study should contribute to the

implementation and approval of LCLT treatment processes to allow for the economical

production of Class A biosolids.

3   Arginine Enveloped Virus Inactivation and Potential Mechanisms

3.1   Abstract

Arginine synergistically inactivates enveloped viruses at a pH or temperature that does little harm to proteins, making it a desired process for therapeutic protein manufacturing. However, the mechanisms and optimal conditions for inactivation are not fully understood, and therefore, arginine viral inactivation is not used industrially. Optimal solution conditions for arginine viral inactivation found in the literature are high arginine concentrations (0.7-1 M), a time of 60 minutes, and a synergistic factor of high temperature ($\geq 40°C$), low pH ($\leq$ pH 4), or Tris buffer (5 mM). However, at optimal conditions, full inactivation does not occur over all enveloped viruses. Enveloped viruses that are resistant to arginine often have increased protein stability or membrane stabilizing matrix proteins. Since arginine can interact with both proteins and lipids, interaction with either entity may be key to understanding the inactivation mechanism. Here, we propose three hypotheses for the mechanisms of arginine induced inactivation. Hypothesis 1 describes arginine-induced viral inactivation through inhibition of vital protein function. Hypothesis 2 describes how arginine destabilizes the viral membrane. Hypothesis 3 describes arginine forming pores in the virus membrane, accompanied by further viral damage from the synergistic factor. Once the mechanisms of arginine viral inactivation are understood, further enhancement by the addition of functional groups, charges, or additives may allow the inactivation of all enveloped viruses in mild conditions.

3.2   Introduction

Therapeutic proteins have improved the treatment of diseases including cancers, autoimmunity/inflammation, infections, and genetic disorders[104]. As a result, there has been continued growth in therapeutic protein sales with over 200 therapeutic protein products currently approved[105]. With the growing demand for therapeutic proteins, advancements in the manufacturing process are desired so that large quantities of effective and safe protein products can be produced.

The Food and Drug Administration (FDA) requires two orthogonal virus clearance steps for enveloped and non-enveloped viruses in any biotherapeutic process. This creates a robust system that greatly reduces the chance of non-desired infectious agents from entering the final product. Conventionally, non-enveloped viruses are removed by nanofiltration or chromatographic separation[8,9,11,106-111], while enveloped viruses are inactivated by low pH ($\sim$3.5)[112], solvent/detergent treatment[113] or heat treatment[8,114]. However, conventional processes for enveloped virus inactivation can harm the desired protein product and reduce final yields. Specifically, pH values less than 4.0[114,115], high detergent concentrations[114,116] or temperatures above 37°C[117-122] produce conformational changes, aggregation, or precipitation that destroy the activity of therapeutic proteins. To maintain the stability and structure of proteins during viral clearance, more favorable solution conditions are desired.

One solution to inactivate enveloped viruses without causing aggregation or fragmentation of the therapeutic protein product lies in the addition of the amino acid arginine. Arginine synergistically inactivates enveloped viruses at a less acidic pH ($\geq$ 4)[8-15] or lower temperature (30-40°C)[16] than conventional inactivation methods, increasing

therapeutic protein stability and yield. However, synergistic arginine inactivation is not currently used in industry since the conditions and phenomena for viral inactivation are not clear. Understanding the physical phenomena of arginine viral inactivation could give greater insight into a safe, effective and sustainable way of meeting therapeutic protein viral clearance requirements while maintaining protein stability.

Arginine is a naturally occurring, highly hydrophilic and polar amino acid that is required for protein structure and function[123,124]. Arginine contains a protonated guanidinium group (**Figure 3-1**) that is able to form ionic and hydrogen bonds with proteins and lipids[124-126]. Some common uses of arginine are to prevent protein aggregation[13,127-129] and to translocate through the lipid bilayer[130]. Arginine is used in the biotechnology field for protein refolding[129], protein aggregation suppression[127,131,132], and protein solubilization[133]. Arginine also increases column chromatography elution efficiency[134], is present in high frequency in antimicrobial (AMP) or cell penetrating peptides (CPP)[124], and inactivates enveloped viruses[135].
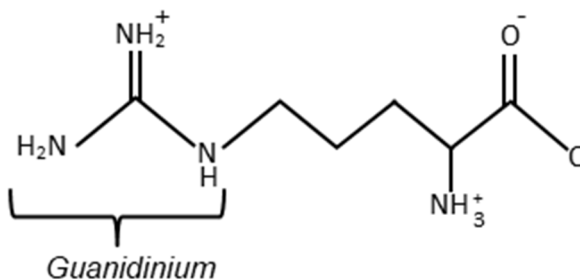
Figure 3-1. Arginine structure at physiological pH. The guanidinium group has a +1 charge while the peptide backbone is amphiphilic.

While there is evidence that arginine interacts with proteins and lipids, there is little theoretical understanding of the interaction with virus. Here, virus inactivation data for arginine and some of its derivatives is summarized. Then, potential hypotheses for the mechanism of virus inactivation is compared to current knowledge of protein and lipid interactions with arginine to elucidate a better understanding of the mechanism of virus inactivation by arginine. Presented are three likely mechanisms. The goal of this paper is to lay out directions of future study on virus inactivation by arginine. Once the mechanism of arginine viral inactivation is better understood, the method has potential to become a commercially viable virus inactivation processes for protein therapeutics.

3.3 Virus Biochemistry

Arginine exclusively inactivates enveloped viruses while having no effect on non-enveloped viruses, signifying that specific virus or host structures are susceptible to arginine[15]. Enveloped and non-enveloped viruses contain a structural array of proteins that form a capsid to protect the nucleic acid cargo. However, the capsid of an enveloped virus is enclosed by a lipid bilayer while non-enveloped viruses expose the viral capsid to the environment without the presence of the lipid bilayer[136].

Enveloped viruses gain their membrane from the host cell. After viral infection, enveloped viruses typically undergo a budding process that results in a portion of the host cell membrane becoming the outer viral envelope[137,138], although the viral lipid bilayer can also originate from the Golgi apparatus[139] or the endoplasmic reticulum[140] in certain cases. Though the lipid bilayer is derived from the host cell in enveloped viruses, proteins incorporated into the viral membrane originate from the viral genetic code[141].

Non-enveloped viruses release from the host cell through membrane disruption without forming an outer envelope[137,138]. Due to the absence of a lipid bilayer, non-enveloped viruses only contain outer proteins that compose the viral capsid. Non-enveloped viruses are generally smaller and more stable than enveloped viruses. Considering the variation in structure and stability, non-enveloped viruses are conventionally removed through filtration or chromatography[8,9,11,106-111], while enveloped viruses are inactivated through chemical or physical processes[8,112-114] in therapeutic protein manufacturing.

3.4 Traditional Enveloped Virus Inactivation

Physical and chemical processes that are licensed to inactivate enveloped viruses in therapeutic protein solutions include heat[8,114], low pH[112] and solvent detergent treatment[113]. Bonds that maintain virus integrity and protein structure are similar, and therefore, conventional methods for virus removal inherently harm the final protein product[142]. To combat negative protein interactions, stabilizers, such as sugars, are commonly added to solution[143]. Sugars stabilize proteins by increasing preferential protein hydration to minimize binding of additional solvent components that may disrupt native protein structure[144]. However, stabilizers must be removed prior to final processing, increasing yield losses, overall cost, and production time[145].

The FDA and EPA require a minimum of a 4 log removal value (LRV), defined in **Eq. 3-1**, for a method to be considered as a virus removal step[146,147]. A 4 LRV results in 99.99% removal of virus, depending on the method of detection, which is typically either by infectious titer or polymerase chain reaction (PCR). In many cases, this requires high

titers of virus to be tested so that the required LRV can be measured within the detection limit of the assay. Low virus titers are rarely, if ever, studied in virus removal verification.

$$LRV = \log_{10}\left(\frac{Virus\ Conc_{Before\ removal}}{Virus\ Conc_{After\ removal}}\right)$$ (Eq. 3-1)

Certified heat treatments in therapeutic protein manufacturing inactivate enveloped viruses by destroying the structural integrity of the virus[148] and altering key viral properties required for infection[149,150]. The temperature necessary for inactivation depends on many factors, including viral structure, time of exposure, and environment[119]. For example, hepatitis C virus is inactivated at 37°C in 2 days and at 56°C in 40 min[117]. Heat inactivation for immunoglobulin, the most common class of protein therapeutics, is 60°C for 10 hours at pH 5.5[142]. Though heat treatments are certified for pathogen inactivation in therapeutic protein manufacturing, mechanisms for viral heat inactivation can mutually harm protein products and therefore are not regularly used in production.

Low pH treatments are commonly used in therapeutic protein manufacturing to inactivate enveloped viruses through lipid hydrolysis[151-153] and protein structural changes[115,154-163]. Values of pH between 3.4 and 4.2 can fully inactivate enveloped viruses given the ideal time frame for the specific virus[112,142]. For example, xenotropic murine leukemia virus is inactivated in 30 min at pH 3.8[164]. Though low pH treatments are very effective at inactivating enveloped viruses, inactivation mechanisms may harm proteins. Added stabilizers are used to increase protein yields during inactivation, however, this adds additional downstream costs for removal.

Solvent detergent treatments inactivate enveloped viruses by solubilizing the lipid bilayer[142] through the addition of non-volatile organic solvents or detergents. Viruses including HIV (human immunodeficiency virus), BVDV (bovine viral diarrhea virus) and SuHV-1 (pseudorabies) have been successfully inactivated through solvent detergent treatment[145]. Though solvent detergent treatment produces little to no protein loss, a downstream step is required to remove added chemicals which increases production costs[145]. Currently all conventional enveloped virus inactivation treatments either harm proteins or add downstream costs, creating a need for improved processing.

3.5   Virus Inactivation with Arginine

Compared to conventional methods, arginine inactivates enveloped viruses under conditions that do less harm to therapeutic proteins. Additionally, downstream removal of arginine is not required since it is often found in formulations[165], lowering processing and analytical costs. Low pH treatments of pH 3.5 or less often cause protein degradation or fragmentation[10,11,13]. However, when low pH is paired with arginine, viral inactivation occurs at a more protein friendly pH of 4.0 or greater. Heat treatments without arginine for hepatitis virus require 10 hours at pH 5.5 and 60°C[142]. When arginine is paired with heat, a less elevated temperature is necessary (30-40°C) for enveloped viral inactivation in a shorter period of time (60 min), generating fewer adverse effects on the therapeutic proteins[16]. Arginine itself has been shown to cause minimal fragmentation of proteins at high temperatures and oxygen content, likely due to the production of NOx[166]. However, arginine largely interacts positively with proteins by suppressing aggregation, increasing solubility, and preventing protein binding[167]. The use of arginine in protein solutions

leads to enhanced recovery of proteins[166]. Though arginine improves protein yields during virus inactivation[11], optimal conditions for full inactivation of all enveloped viruses is not known, hindering its use in manufacturing.

A range of enveloped and non-enveloped viruses have been tested for inactivation by arginine and many are shown in **Table 3-1**[11,168-175]. These viruses are models for a variety of human viruses that contain different structures. Key viral differences include the occurrence of an outer envelope, genome, and size.

Table 3-1. Properties of Tested Viruses

Virus	Acronym	Envelope	Genome	Size (nm)
Minute virus of mice	MMV	No	DNA	18-24
Poliovirus	Polio	No	RNA	22-30
Herpes simplex virus 1	HSV-1	Yes	DNA	110-200
Herpes simplex virus 2	HSV-2	Yes	DNA	110-200
Pseudorabies	SuHV-1	Yes	DNA	120-200
Xenotropic murine leukemia virus	XMuLV	Yes	RNA	100-120
Influenza virus	-	Yes	RNA	100-300
Sendai virus	-	Yes	RNA	150-200
Newcastle disease virus	NDV	Yes	RNA	150-350

Compounds tested for viral inactivation at pH 4 include arginine, butyroyl-arginine, citrate and NaCl (**Figure 3-2**). Molecular structures can be found in **Table 3-2**[74,75]. Virus inactivation by arginine and butyroyl-arginine was first compared to survey molecules with a guanidinium group but different charges. Butyroyl-arginine is a derivative of arginine that contains a guanidium group, a net charge of zero at physiological pH, and a capped amine. Butyroyl-arginine produced similar or higher virus inactivation in comparison to arginine for all viruses **(Fig. 2)**[10]. The charge distribution on butyroyl-arginine allows for dense, self-aggregated clusters to form, which likely explains the enhanced virus inactivation[10]. Neither arginine nor butyroyl-

arginine inactivated poliovirus, a non-enveloped virus. Arginine and its derivatives do not affect non-enveloped viruses, suggesting that inactivation occurs through lipid bilayer interactions.
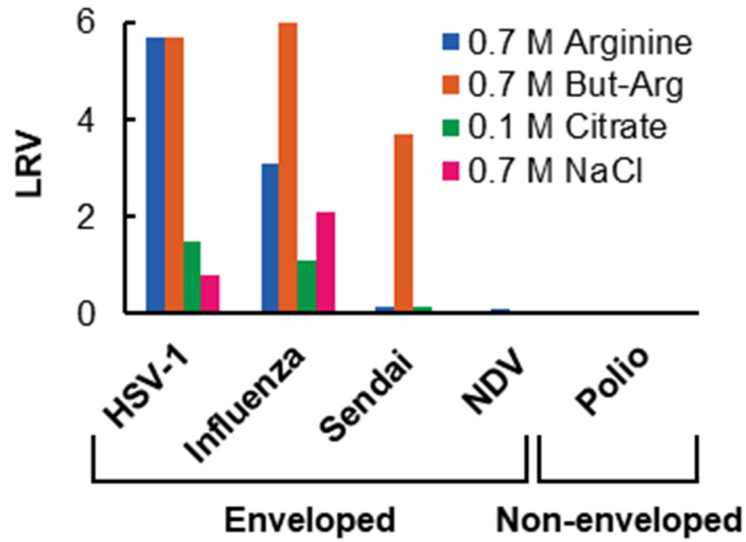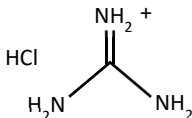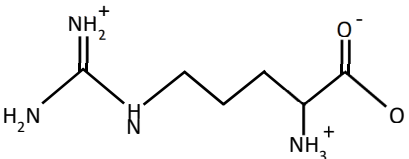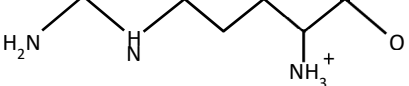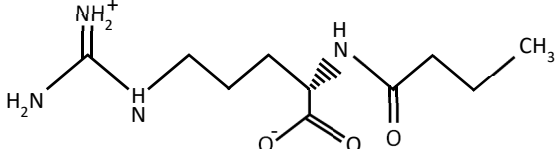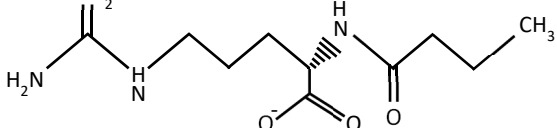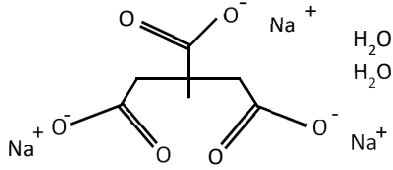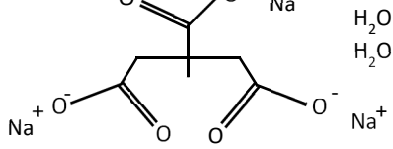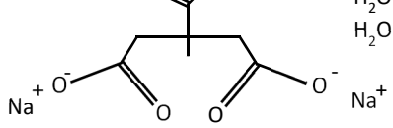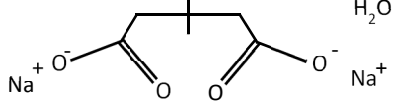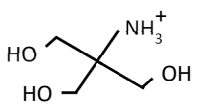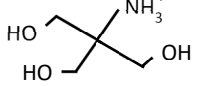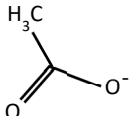
Figure 3-2. Viral inactivation at pH 4.0 on ice for 60 min with enveloped and non-enveloped viruses. Different enveloped viruses showed various levels of inactivation by arginine, while non-enveloped viruses were unaffected. Duplicates or triplicates were performed for all data points. (Reformatted[10,15])

Table 3-2. Properties of Solutes and Buffers

*Partial average charges exist at pH values close to the pK$_a$

Solute	Structure	pK$_a$	Charge Below pK$_a$*
Guanidine HCl		12.55	+1
Arginine		2.41	+2
		9.15	+1
		12.41	0
Butyroyl-Arginine		3.73	+1
		12.14	0

Buffer	Structure	pK$_a$	Charge Below pK$_a$*
Sodium Citrate		3.05	0
		4.65	-1
		5.35	-2
		13.95	-3
Sodium Chloride	Cl⁻ Na⁺	N/A	N/A
Tris Buffer		8.95	+1
		14.16	0
Acetate Buffer		4.54	0

NaCl and citrate produced lower viral inactivation than arginine and its derivates at pH 4. The consistently lower inactivation over all viruses by NaCl (**Figure 3-2**) demonstrates that ionic strength is not the only mechanism contributing to virus inactivation with arginine. Citrate also inactivated viruses to low levels at pH 4. Interestingly, citrate is commonly used to inactivate enveloped viruses during low pH treatment at pH 3.5[15]. Either the increased acidity or the charge difference on citrate must enhance inactivation at pH 3.5 over pH 4. At a pH of 3.5, most of the citrate molecules have a -1 charge, which may strengthen inactivation. As the pH increases to 4, nearing the pK_a of 4.65, some of the citrate molecules will gain an additional negative charge[176,177].

Although arginine and its derivatives produce high inactivation for some enveloped viruses, not all enveloped viruses are fully inactivated. The clear difference in inactivation levels suggests that arginine preferentially interacts with certain viral properties. Specifically, arginine must favor properties of HSV-1 due to its high inactivation. HSV-1 is a large enveloped DNA virus with a diameter of 110 to 200 nm[168,175]. HSV-1 has a highly ordered structure (**Figure 3-3**) where the envelope encloses a tegument protein layer, containing over 20 identified proteins[168]. Tegument proteins participate in a range of viral functions from viral assembly to host cell entry[178]. Complex formation between HSV-1 glycoproteins and cell receptors initiates the fusion between the host cell and viral membranes, leading to viral capsid uptake[179].

Influenza virus has proteins and an infection process that differ from HSV-1, likely explaining the lesser inactivation. Influenza virus is an enveloped RNA virus with a diameter of 100-300 nm[169,180]. Three proteins are imbedded in the lipid bilayer,

including the hemagglutinin (HA), neuraminidase (NA)[181], and matrix-2 (M2)[180]. The

hemagglutinin protein must undergo proteolytic cleavage by host cell proteases prior to

membrane fusion[182]. Surrounding the nucleocapsid, a matrix protein called matrix-1 (M1)

connects the lipid bilayer to the viral core[169], shown in **Figure 3-3**. The integration of M1

into the lipid bilayer stabilizes the virus structure more than the free-floating tegument

proteins in HSV-1. Influenza virus infection is also different than HSV-1. Infection

begins through attachment of the cleaved HA protein to sialic acid receptors on the host

cell membrane, followed by uptake through the low pH endosomal pathway[183]. The low

pH prompts the virus and endosomal membrane to fuse, causing the release of the

nucleocapsid into the cytoplasm[180].
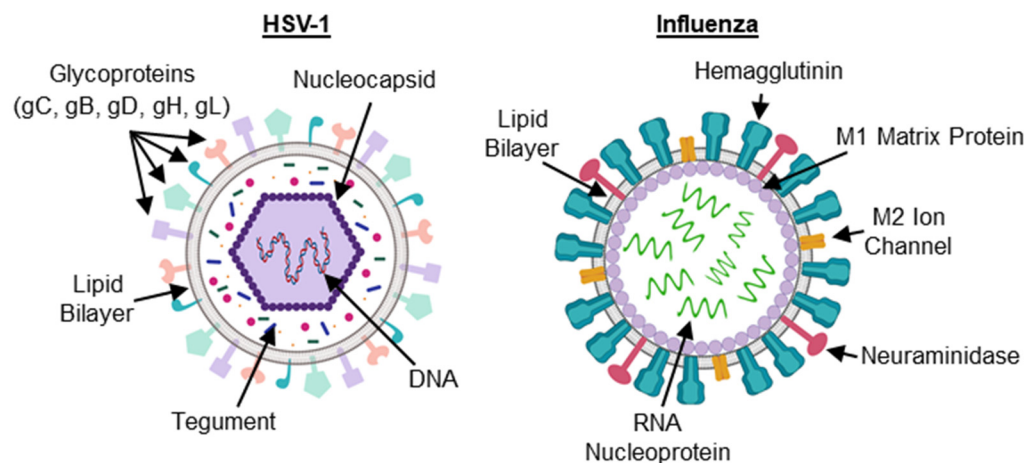
Figure 3-3. Comparison of HSV-1 and influenza virus structure. HSV-1 contains a tegument of proteins between the nucelocapsid and the lipid bilayer. Influenza virus contains a M1 matrix protein that stabilizes the lipid bilayer by connecting the viral core to the membrane. (Images created in BioRENDER)

Sendai virus and NDV belong to the paramyxovirus family, and undergo a similar infection process to influenza virus[184]. Sendai virus and NDV are RNA viruses with diameters of 150-350 nm[171]. Two spike-like glycoproteins, including a fusion protein (F) and a hemagglutinin-neuraminidase protein (HN), are imbedded in the lipid bilayer. Similar to influenza virus, the lipid bilayer of Sendai virus and NDV overlays the matrix protein, M1, that encloses the nucleocapsid[185]. Proteolytic cleavage of the F and HN protein, either intracellularly or extracellularly, is required for virulence[186,187]. Distinct from influenza virus, infection of Sendai and NDV are independent of the low-pH endosomal pathway.

A clear difference between viruses that are highly inactivated by arginine (HSV-1), compared to viruses that show lower inactivation (influenza A virus, Sendai virus, and NDV), is the presence of the M1 matrix protein, and the requirement of proteolytic cleavage prior to infection. The M1 matrix protein tightly associates the lipid bilayer to the viral core, aiding in membrane stabilization[188]. A highly stabilized bilayer may hinder the direct penetration of arginine into the lipid bilayer. On the other hand, increased protein stability prior to proteolytic cleavage may suppress arginine from denaturing that protein. Prior to proteolytic cleavage, the influenza virus uncleaved HA is highly acid-stable[189]. Increased stability of the uncleaved HA proteins would prohibit detrimental arginine-protein interactions. It is hypothesized that the presence of a M1 matrix protein or the increased protein stability prior to proteolytic cleavage prevents arginine from fully inactivating some viruses.

3.5.1 Charge and pH

While virus properties may affect the levels of arginine inactivation, what is special about the arginine molecule to cause virus inactivation? Arginine contains a guanidinium moiety that is able to form ionic and hydrogen bonds with proteins and lipids[124-126], likely aiding in virus inactivation. Various guanidine-based solutes with different charge patterns can inactivate enveloped viruses. Guanidine-based solutes that have been tested for enveloped virus inactivation are shown in **Table 3-2**. Guanidine hydrochloride at a pH of 5 completely inactivates HSV-1 in 10 min[177], but this required a concentration of 6 M. Concentrations of guanidine hydrochloride below 2 M are not effective in virus inactivation[118]. The next potent solute is arginine, which inactivates HSV-1 completely at pH 4 at a concentration of 0.7-1 M in 60 min[13-15]. The most potent arginine derivative is butyroyl-arginine, which can highly inactivate viruses where arginine fails, including influenza virus, at pH 4 and a concentration of 0.7 M in 60 min[10]. At a pH between 4 and 5, guanidine hydrochloride has a +1 charge, arginine has a +1 charge and is zwitterionic, and butyroyl-arginine has a neutral charge and is zwitterionic. Since guanidine hydrochloride requires the highest concentration to inactivate virus, charge or the multiple binding sites on guanidine are not the dominating factors in the antiviral properties of arginine.

The zwitterionic properties of arginine and butyroyl arginine likely enhance viral inactivation through strong lipid binding and self-interactions. Alone, guanidinium is able to form multiple hydrogen bonds with lipids[190]. However, in combination with the strong charge distribution of arginine, the hydrogen binding of guanidinium to lipids is strengthened[190]. Additionally, the opposite charge distribution on arginine and butyroyl-

arginine can cause the formation of clusters due to self-aggregation[191]. Clusters can also form through like-charge pairing of guanidinium moieties[192,193].

Clusters magnify localized concentrations, strengthening protein[127] and lipid interactions[194-198]. Specifically, arginine clusters crowd out hydrophobic protein-protein interactions to prevent aggregation[199-201]. Preventing aggregation is one mechanism to stabilize proteins. Stabilized proteins may not undergo the conformational changes needed to initiate the virus infection cycle[202]. Arginine clusters can also weaken lipid bilayers, resulting in translocation through the lipid bilayer[124,130,203]. It is hypothesized that viral inactivation by arginine is due to protein or lipids interactions, and therefore, strengthening these interactions would increase inactivation.

Butyroyl-arginine is the most effective arginine-derivative, conceivably due to its cluster forming structure. Butyroyl-arginine contains one positive and one negative charge that occupy different ends of the molecule to enhance self-interactions. Arginine contains an additional positive charge, which would reduce the density of clusters due to charge repulsion. The lesser viral inactivation of arginine as compared to butyroyl-arginine is presumably explained by the efficacy to form clusters.

The buffer used to control the pH during inactivation experiments may combine with arginine to enhance viral inactivation. Buffers that have been used in arginine inactivation experiments are found in **Table 3-2**. Tris buffer added to arginine at neutral pH inactivates XMuLV and SuHV-1[11]. Several experiments at pH 4 with acetate buffer have been shown to inactivate a variety of viruses[9,12-15]. The charge on added buffers can interact with proteins, lipids, or DNA to aid in viral inactivation. In addition to charge,

functional groups, such as the amine group on Tris, are hypothesized to interact with viral proteins and lipids[204,205], aiding in inactivation.

3.5.2 Concentration and Time

Synergistic inactivation by arginine is amplified at higher concentrations. The LRV of HSV-1 increases with solute concentration, shown in **Figure 3-4A**. Arginine has a solubility of ~1 M, limiting the concentrations that can be tested. The need for high concentrations of arginine suggest that the interactions of arginine with the lipid bilayer structure are weak[15]. Furthermore, high arginine concentrations imply that dense arginine clusters are required for viral inactivation[194-198].

When arginine synergizes with low pH, inactivation occurs in less than 60 minutes for HSV-1[15]. HSV-1 was reduced by 5 LRV in under 20 min at pH 4 (**Figure 3-4B**). In comparison, a gradual increase with 0.1 M citrate resulted in only 1.3 LRV over 60 min. The fast rate of arginine-induced viral inactivation indicates that the mechanism occurs over a short period of time and is not due to pH alone.
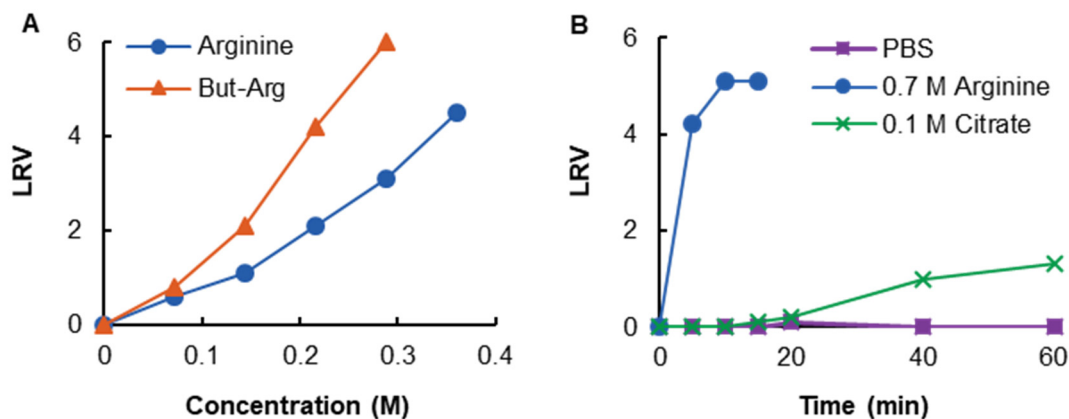
Figure 3-4. **A)** Viral inactivation of HSV-1 as a function of arginine and butyroyl-arginine concentration. Increasing the concentration of arginine derivatives leads to higher virus inactivation. Inactivation occurred at pH 4.0 on ice for 60 min with 20 mM acetate buffer. (**B**) Viral inactivation of HSV-1 as a function of time at pH 4 on ice. PBS control at pH 7. Low pH arginine inactivation occurs under 60 min. Duplicates or triplicates were performed for all data points. (Reformatted[15])

3.5.3 Synergistic Factors: pH, Temperature, Buffers

Arginine synergizes with acidic pH to inactivate enveloped viruses. At pH 4, HSV-1 is equally inactivated by arginine and butyroyl-arginine to ~6 LRV, shown in **Figure 3-5A**. However, as pH continues to increase, viral inactivation decreases across all solutions. A pH of at least 4.0 is required to synergize with arginine for enveloped viral inactivation.

The viral inactivation of influenza virus with cleaved hemagglutinin (CHA) spike proteins and uncleaved hemagglutinin (UCHA) spike proteins (**Figure 3-5B & C**), was found to differ. CHA was inactivated to much higher levels than UCHA at pH 4 with arginine. On the other hand, butyroyl-arginine produced high inactivation in both CHA and UCHA at pH 4. Even up to pH 4.5, butyroyl-arginine highly inactivated CHA influenza virus.
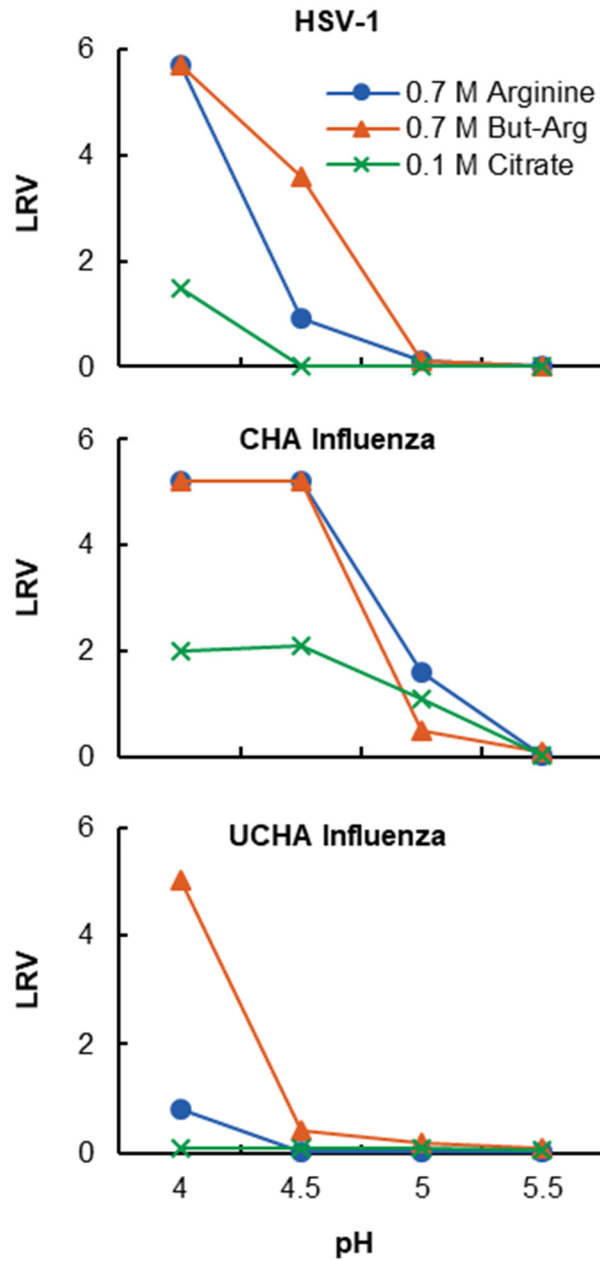
Figure 3-5. Viral Inactivation of HSV-1, CHA influenza virus and UCHA influenza virus as a function of pH on ice for 60 min. As pH increases, arginine induced viral inactivation decreases. Duplicates or triplicates were performed for all data points. (Reformatted[10,15])

The difference of arginine inactivation for CHA and UCHA indicates a dependence on protein structure. CHA spike proteins are required for uptake of influenza virus into the host cell, while UCHA must experience proteolytic cleavage to form CHA prior to cell uptake[10,180]. CHA proteins undergo essential conformational changes during the low pH endosomal pathway required for cell fusion[189]. UCHA proteins do not undergo low pH conformational changes as a result of increased acid stability, hindering viral infection[202]. It is speculated that arginine and low pH can denature the CHA protein, while having no effect on the acid-stable UCHA protein. It may also be true that arginine further stabilizes the CHA protein, inhibiting the required conformational change during the low pH endosomal pathway to undergo infection. Considering that the magnitude of viral inactivation is contingent on protein structure, the synergistic effects of arginine may interact with proteins.

There are multiple cases where a difference in membrane proteins, such as with UCHA and CHA influenza virus, could influence arginine interactions with the lipid bilayer. For example, protein structure can modify packing density of the surrounding lipids[206]. With a looser lipid packing, arginine-lipid interactions would be enhanced to increase inactivation[206]. Furthermore, negative charges on proteins may attract arginine, preventing arginine from interacting with the lipid bilayer to induce viral inactivation. Considering the data as a whole, as pH increases, the effectiveness of arginine decreases, leaving open the hypothesis that arginine interacts with envelope proteins or the lipid bilayer.

High temperature, like low pH, can synergize with arginine to inactivate enveloped viruses. The temperature dependence on viral inactivation of HSV-2 is shown

79

in **Figure 3-6**. For reference, HSV-2 and HSV-1 are very similar in structure and function. Classification of these virus types is based on antigenic differences, or how viral proteins are modified to avoid an immune response[207]. Temperatures higher than 35°C initiated the synergistic effect of arginine at a pH of 4.4. Increasing the temperature to 40°C improved arginine synergistic viral reduction by 2.3 LRV. Citrate followed a similar trend to arginine but with a consistently lower inactivation. On the contrary, 0.1 M citrate/0.6 M NaCl produced insignificant inactivation up to a temperature of 40°C. This data suggests that an increase in ionic strength decreases the effect of temperature and pH on HSV-2 inactivation in contact with citrate. Again, it appears that ionic strength is not the dominating force responsible for virus inactivation at higher temperatures. The addition of salt ions to intermediate concentrations is largely known to increase protein stability[208]. At intermediate salt concentrations, the added charges from salt can decrease unfavorable interactions in solutions that could denature a protein[209,210]. Salts can also shield the charge on citrate, and that charge may be an important factor in the antiviral mechanism of citrate. Conclusively, arginine produced the highest viral inactivation compared to citrate and NaCl with increasing temperature.
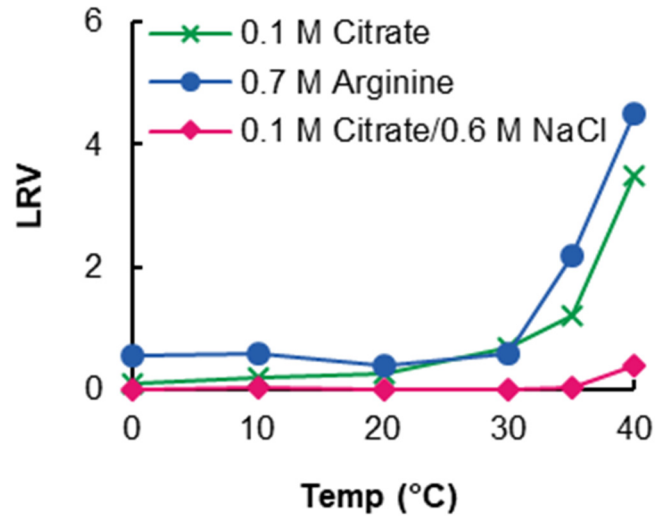
Figure 3-6. Viral inactivation of HSV-2 as a function of temperature at pH 4.4. At 35°C, arginine begins to synergize with temperature to inactivate HSV-2. (Reformatted[14])

Similar to temperature and pH, Tris buffer seems to synergize with arginine to inactivate enveloped viruses. The inactivation of SuHV-1, X-MLV, and MMV at neutral pH for 60 min at 4°C with 5mM Tris buffer is shown in **Figure 3-7**. SuHV-1 and X-MLV are both enveloped viruses that were inactivated to near 4 LRV. The following data is the only example in literature where neutral pH and arginine inactivated enveloped viruses, and therefore, it is assumed that Tris buffer is the synergistic factor. MMV is a non-enveloped virus and was negligibly inactivated when exposed to arginine and Tris, consistent with results that arginine has little effect on non-enveloped viruses[10]. Compared to conventional inactivation methods, Tris buffer paired with arginine at neutral pH and 4°C maintains the full activity of proteins[11], making it a desired process in therapeutic protein manufacturing.
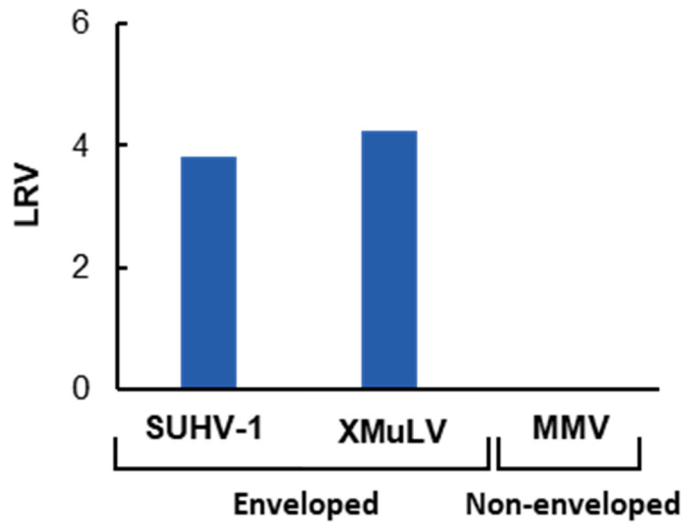
Figure 3-7. Viral inactivation with 1M arginine and 5 mM Tris buffer at pH 7.0 for 60 min at 4°C. At a neutral pH, arginine can synergize with Tris buffer to inactivate enveloped viruses. (Reformatted[11])

It is curious as to how Tris synergizes with arginine at neutral pH to inactivate viruses. Tris undergoes multiple interactions that may disrupt biological processes to aid in inactivation[211]. For example, Tris is toxic to rat nerve cells at concentrations as low as 10 mM[212]. Interactions of Tris with lipid bilayers may explain the observed toxicity. When exposed to a phospholipid bilayer at room temperature, Tris buffer increased lipid disorder[213]. Similarly, in strains of *Escherichia coli*, Tris buffer increased membrane permeability, leading to a loss of cell membrane components[214]. On the contrary to the above studies, in supported lipid bilayers, atomic force microscopy measurements demonstrated that Tris buffer reduced membrane stress, while other ions, such as Ca^{2+}, increased membrane stress[215]. Though there are mixed results on the effects to lipid bilayers, Tris buffer does interact with membranes.

Aside from lipid bilayers, Tris undergoes additional interactions in biological solutions. Tris can stabilize proteins through electrostatic and hydrogen bonding[216,217] and can associate with DNA[218]. The positive charge and primary aliphatic amine group of Tris, shown in **Table 3-2**, are thought to be the root cause of multiple interactions[204,216,218,219]. Charges on molecules interact with proteins and lipids[215,220-224], while primary aliphatic amines interact with several compounds including DNA[204,216,218,219]. Either through lipid bilayer, protein or DNA interactions, Tris is thought to synergize with arginine to inactivate enveloped viruses.

At optimal solution conditions and synergistic abilities, arginine is an effective means of inactivating some enveloped viruses. High concentrations (0.7-1M) and a time of 60 minutes combined with the synergistic factor of high temperature, low pH, or Tris buffer is needed for maximum virus inactivation. After gaining a comprehensive understanding of arginine interactions with proteins and viruses, we list three hypotheses for the mechanisms of synergistic arginine viral inactivation.

3.6   Hypotheses for Synergistic Arginine Viral Inactivation

We propose three mechanisms for arginine induced enveloped viral inactivation and go into greater detail on the potential phenomenon involved (**Figure 3-8**). Hypothesis 1 describes arginine-protein interactions leading to the loss of viral infectivity. Hypothesis 2 describes the destabilization of the viral membrane by arginine. Hypothesis 3 describes pore formation by arginine, followed by further viral damage from the synergistic factor.
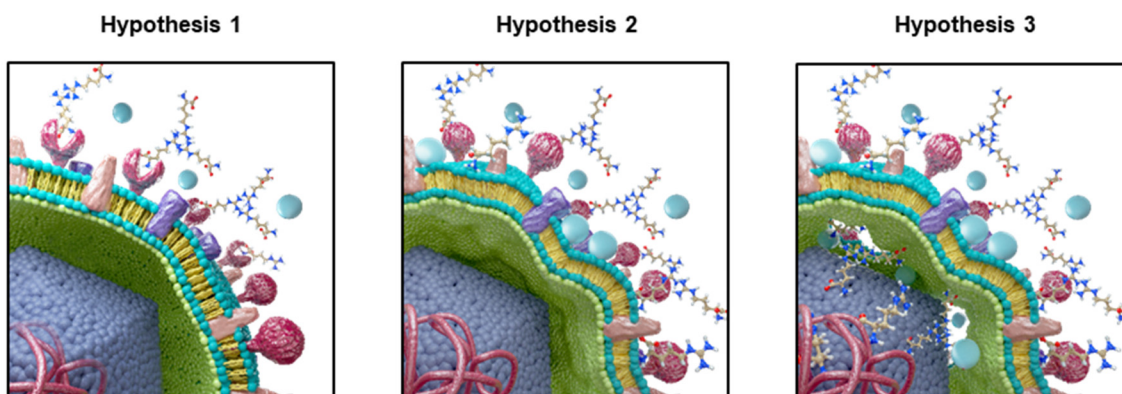
Figure 3-8. Hypotheses on the virus inactivation mechanism of arginine. It is hypothesized that viral inactivation occurs by either the **1)** disruption of protein activity, **2)** destabilization of the lipid bilayer, or **3)** pore formation in the lipid bilayer. Arginine is shown as its molecular structure and the synergistic factor is represented as a blue sphere. Examples of synergistic factors are low pH, temperature or buffer molecules.

3.6.1   Hypothesis 1: Arginine with Synergistic Factor Interacts with Viral Proteins

Hypothesis 1 states that arginine synergizes with Tris, low pH or temperature to directly inhibit protein function. There are two ways in which proteins are speculated to lose their function by arginine. First, the synergy of arginine is thought to denature or fracture viral proteins. Second, arginine may bind to or crowd out proteins to prevent required conformational changes or attachment to host cell receptors[225]. Regardless of the process, the loss or inability of viral proteins to undergo necessary functions induced by arginine will hinder viral infection.

The combination of arginine with the synergistic factor may disrupt protein structure. Low pH and high temp are common protein denaturants, though, the levels used with arginine have little effect on proteins[10,11,13,16]. Combined with arginine, the effects of low pH or high temp to destabilize proteins may be enhanced. Arginine contains multiple binding opportunities that possibly disrupt protein structure. The

cationic guanidinium group of arginine has the capacity to form up to six hydrogen bonds with anionic species[226]. The binding of the guanidinium group to the carbonyl oxygen on the protein backbone can structurally stabilize a protein's secondary and tertiary structure[227]. But when arginine is external to the protein, the bonds holding the secondary and tertiary structure may favor binding to the external arginine rather than internal bonds, leading to protein fracturing or denaturation. In solution, water surrounds proteins to create a hydration shell that maintains protein structure[228]. When arginine binds to proteins through hydrogen and cation-π bonds[129,191,201,229], the protein hydration shell is likely disrupted, leading to protein destabilization. Arginine is also highly common in salt bridges[230]; the presence of arginine in solution could disrupt or create new salt bridges in proteins, altering protein structure.

Though it seems plausible that arginine and the synergistic factor denatures proteins, other evidence suggests that this is the weakest of the hypotheses. Tris buffer was shown to synergize with arginine to inactivate virus at neutral pH[11] (**Figure 3-7**). Tris is known to stabilize proteins[216,217], suggesting that there are no harmful effects on protein conformation. Arginine is also largely known to prevent protein aggregation and enhance protein solubility[13,127-129]. By binding to proteins through hydrogen and cation-π bonds, arginine collects on the surface to prevent protein aggregation[129,191,201,229]. Despite the positive effects on proteins, arginine has been shown to slightly fracture proteins through NO_x production at high temperatures ($\geq 40°C$)[166]. However, NO_x production by arginine is too insignificant at or below room temperature to denature a protein[166]. This would rule out denaturation as the cause for inactivation on ice or at 4°C (**Figure 3-2**,

Figure 3-4, **Figure 3-5**, **Figure 3-7**) Overall, it is unlikely that the synergistic effects of arginine denature proteins.

Though it is unlikely that arginine denatures proteins, arginine may prevent host cell fusion. Binding of arginine to membrane proteins could render the protein unrecognizable to the host cell receptor to obstruct cell fusion. Levels of inactivation across viruses could be explained by the capacity for arginine-protein binding. Glycoproteins with negatively charged species and aromatic residues would enhance arginine binding[129,191,201,229]. Additionally, the synergistic factor could promote conditions for arginine-protein binding. For example, a drop in pH can alter the charge of amino acid residues on the membrane proteins, allowing arginine to bind to the protein.

In addition to protein binding, arginine molecules in solution tend to self-aggregate into clusters[191,192]. Arginine-arginine clusters are thought to occur due to like-charge pairing of guanidinium moieties[192,193] or hydrogen bonding from head to tail[191]. These clusters are known to crowd out protein-protein or protein-surface interactions[167,199,201,231]. Correspondingly, arginine clusters would crowd out protein interactions with host cell receptors. Crowding may or may not entail protein binding. If no protein binding occurred, the effects would be reversible by dilution of arginine, though this is not the case. When diluting arginine samples prior to plaque assays, inactivation effects for enveloped viruses remained[15]. For this reason, arginine-protein binding would be required to reduce virus infectivity.

In support of arginine-protein interactions, inactivation levels vary across viruses with different proteins[10]. For example, arginine at pH 4 highly inactivated influenza virus containing CHA proteins while lower inactivation resulted for influenza virus containing

UCHA[10]. UCHA differs from CHA in structure and stability[202] UCHA spike proteins must undergo proteolytic cleavage to modify into CHA structure prior to cell uptake[189]. Due to the increased stability, UCHA proteins do not undergo the essential conformational changes required for cell fusion that CHA endures during the low pH endosomal pathway[202]. The structure and stability of CHA compared to UCHA could explain differences in inactivation levels. Arginine may destabilize the CHA proteins to prevent host cell binding, while having limited effect on the stable UCHA protein. Alternatively, arginine may further stabilize CHA to hinder endosomal low-pH conformational changes that are required for host cell infection. For this reason, CHA and UCHA influenza virus inactivation data may support either arginine-induced protein denaturation or protein stabilization.

Similar to UCHA of influenza, NDV and Sendai virus are not highly inactivated by the synergistic effects of arginine[10,15]. Also similar to UCHA, NDV and Sendai both require proteolytic cleavage of glycoproteins prior to infection. In contrast to influenza, NDV and Sendai proteins do not undergo low pH conformational changes after proteolytic cleavage. Accordingly, stabilization of NDV or Sendai virus proteins would not inhibit infectivity because conformational changes are not required for infection, favoring protein denaturation as the root cause of inactivation. If we disregard protein denaturation as the mechanism, arginine may be more likely to bind to the proteins of NDV, Sendai, and influenza to inhibit host cell fusion. Overall, it is not easy to explain the difference in NDV, Sendai, and influenza virus inactivation by protein denaturation.

Protein denaturation or inhibition of host cell binding may be fundamental to arginine-induced inactivation. However, one of the largest pieces of evidence against

hypothesis 1 is that the synergistic activities of arginine do not affect non-enveloped viruses[10,15]. Similar to enveloped viruses, non-enveloped viruses have external proteins that induce host cell recognition and uptake[225]. For hypothesis 1 to have significance, arginine would have some effect on non-enveloped virus infectivity.

3.6.2 Hypothesis 2: Arginine with Synergistic Factor Interacts with Viral Lipids

According to hypothesis 2, viral inactivation manifests through the interactions of arginine and the synergistic factor (Tris, high temp or low pH) with the lipid bilayer to induce membrane deformations. Deformations to the lipid bilayer may completely destabilize the outer viral membrane to result in viral inactivation. Alternatively, lipid bilayer deformations may prompt conformational changes to membrane proteins, resulting in a loss of viral infectivity.

The synergistic activities of arginine exclusively inactivate enveloped viruses while non-enveloped viruses remain unharmed[10,15], suggesting that mechanisms for viral inactivation involve the lipid bilayer. In support of hypothesis 2, arginine does interact with the lipid bilayer through binding[124-126] and lipid deformations. Specifically, arginine-rich peptides deform membranes in order to translocate into the cell for drug delivery[190,191,232-234]. At low arginine concentrations, endocytosis has been observed as the sole route for arginine peptide translocation[235]. However, studies show that at high arginine concentrations, direct penetration of arginine peptides is favorable over endocytosis[197,235,236]. Although arginine peptides do have a different charge/size ratio in comparison to a single arginine molecule, the guanidinium group on arginine is a large component of peptide activity[237]. Membrane deformations result from the guanidinium

moiety binding to negative charges on the lipid bilayer, and/or the hydrophilic peptides interacting with the hydrophobic lipids[190,191,232-234]. Arginine side chains also maintain their charge when exposed to the hydrophobic membrane environment where no other amino acid can, aiding further in membrane deformations[237]. The transport of arginine peptides through lipid bilayers has been extensively studied where single arginine molecules have not[198]. It is useful to use arginine peptides as a model for arginine to further expose the mechanism of arginine inactivation.

Loosening of lipid packing increases peptide uptake, indicating that arginine deforms the lipid bilayer for translocation[234,238-241]. High cholesterol content in lipids decreases membrane fluidity and translocation of arginine[238 203,206]. In the presence of the hydrophobic cation pyrenebutyrate, which is suspected to loosen lipid packing and increase membrane fluidity, arginine uptake increased in the lipid bilayer[234,239-241]. Virus size can also affect membrane curvature and lipid packing density. A mild degree of lipid curvature exists in viral membranes with a large diameter. Mild curvature leads to loosely packed lipids that deform and bend in response to arginine interactions[194]. In contrast, the drastic curvature of small diameter membranes forms tightly packed lipids that are difficult to distort[194]. This is schematically shown in **Figure 3-9**[194,242]. Curvature is not likely an issue for cells or bacteria due to their large size in comparison to most viruses. However, when exploring the interaction of arginine with small macromolecules, like viruses, this curvature may play a role in the selective penetration of arginine into the lipid bilayer.
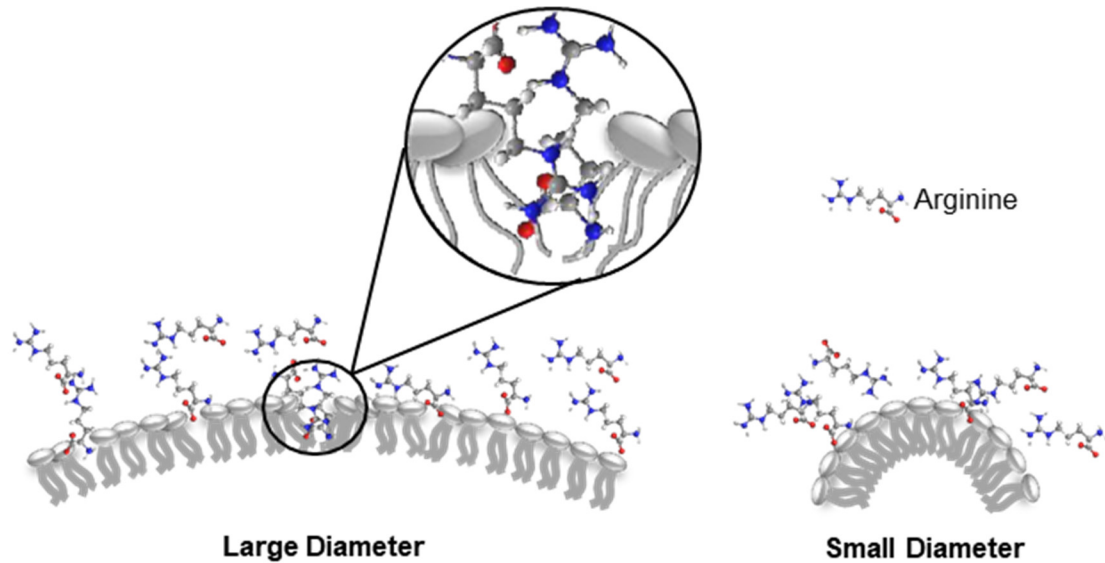
Figure 3-9. Hypothesized interaction of arginine with large and small diameter membranes. The open spacing of lipids in a large diameter membrane increases susceptibility to arginine deformations. Oppositely, the tightly packed lipids of a small diameter membrane are difficult for arginine to manipulate.

The synergistic factors of low pH, high temperature, and Tris buffer all disrupt the lipid bilayer, favoring hypothesis 2. Low pH[151-153] and high temperature[148] invoke lipid hydrolysis. Tris disorders and disassembles the lipid bilayer[213,214]. However, Tris buffer has also been shown to increase membrane stability[215]. Considering all inactivation factors that disrupt the lipid bilayer, it is likely that the synergistic inactivation mechanisms of arginine involves the viral membrane.

Differences in inactivation levels observed across viruses can be attributed to lipid bilayer deformations. When analyzing synergistic arginine inactivation data, viruses that endure low inactivation (Sendai, influenza, NDV) all contain the M1 matrix protein[10,15]. The M1 matrix protein integrates the membrane to the viral core, increasing lipid bilayer stability[188]. Increased lipid bilayer stability decreases viral susceptibility to membrane

90

defects to increase viral survival when exposed to arginine. However, this would not explain the high inactivation levels of CHA influenza and low inactivation of the UCHA influenza virus in response to arginine and low pH[10]. Arginine combined with low pH may deform the membrane to the extent of destabilizing integral membrane proteins. UCHA has increased stability in comparison to CHA[189]. Therefore, UCHA may retain its structure in response to membrane defects while CHA is denatured. Protein structure can also alter packing density of lipids at the protein-lipid interface[206]. The differences in structure between UCHA and CHA influence the surrounding lipid packing density to affect arginine inactivation. The fact that arginine peptides and synergistic factors are known to affect lipid bilayers, in combination with viral inactivation data, support hypothesis 2.

3.6.3 Hypothesis 3: Arginine Forms Pores in the Lipid Bilayer

Hypothesis 3 considers arginine-induced pore formation in the lipid bilayer as the fundamental component in viral inactivation. Similar to membrane deformations, pore formation may destabilize the lipid bilayer to disrupt membrane proteins or overall virus integrity. Alternatively, pores in the lipid bilayer may allow the passage of the synergistic factor through the lipid bilayer and into the viral core, leading to degradation of viral genetic material.

In several studies, arginine-rich peptides have been shown to cross the lipid bilayer through the formation of a water pore[124,194,197,198,234,242]. Pores are hypothesized to form in a similar manner to membrane deformations, through electrostatic or hydrophilic interactions[190,191,232-234]. For example, preferential binding to negative charges in

91

zwitterionic lipids (common in mammalian membranes) results in lipid sorting and membrane tension. Membrane tension can lead to lipid flip flop and membrane multilamellarity, eventually forming a pore[130]. In comparison to direct translocation by membrane deformations, translocation through a pore is thought to require less energy, and is therefore more advantageous[205,242]. Multiple arginine molecules can cross through a pore at one time, lowering the translocation energy[198,242,243]. Additionally, passing through a pore can lower arginine translocation energy through avoidance of the hydrophobic lipid core[198,242,243]. Similar to membrane deformations, pores in the lipid bilayer may destabilize the membrane and associated membrane proteins. This would coincide with the data for low inactivation of viruses containing the M1 matrix protein[10,15], along with the increased stability of UCHA influenza virus at low pH[10].

Arginine-induced pores may additionally allow for the synergistic factor to pass through the protective lipid bilayer, causing oxidation or cleavage of virus capsid proteins or nucleic acids. The membrane of an enveloped virus protects the capsid and nucleic acids against environmental factors[244,245]. A pore in the membrane may allow hydronium ions in a low pH solution[245], Tris buffer[218], or high temperature[246] to disrupt the genetic material and inactivate the virus. However, the levels of pH and temperature used during arginine synergistic viral inactivation are not known to cause DNA degradation[245,246]. Due to the lower energy requirement for a pore formation in comparison to membrane deformations, arginine likely forms a pore to result in viral inactivation.

3.6.4   Future Study

It will take a concerted effort and multiple experiments to shed light on the mechanism of arginine in virus inactivation. The first is to determine if the virus structure has been compromised after treatment. This simple test has not been reported in the literature. To specifically test hypothesis 1, protein binding experiments can determine if a protein is still active after arginine exposure. Heparin is a common cell receptor for virus, and changes in heparin binding could be used to explore the changes in cell attachment[247]. However, changes in heparin binding could also support hypothesis 2, since lipid instability could cause changes in membrane bound proteins, disrupting binding events.

To assess hypothesis 2 and 3, nanoindentation can measure changes in virus stiffness[248]. If the virus stiffness decreases after arginine exposure, the lipid bilayer is being compromised either by deformation or pore formation. If virus stiffness and heparin binding are reduced, then hypothesis 2 is most likely. To discern hypothesis 2 from hypothesis 3, the integrity of the genetic material in the virus can be assessed. The reduction in genetic material for would provide evidence that the integrity of the membrane has been compromised, as described in hypothesis 3. While literature supports all of the hypothesis, it is possible to better discern the mechanism of arginine inactivation if more effort is put into this area.

3.7   Conclusions

The process of synergistic arginine enveloped viral inactivation provides greater protein stability and increased therapeutic protein yields in comparison to conventional

methods[8-16], making arginine a desirable pathogen removal step in therapeutic protein manufacturing. Although there are multiple studies on the synergistic effects of arginine, information has not been compiled to determine the mechanisms and optimal conditions for viral inactivation. Through analyzing literature data, optimal solution conditions for the synergistic ability of arginine include high concentrations (0.7-1M), a time of 60 minutes, and a synergistic factor of high temperature (40°C), low pH (pH 4), or Tris buffer (5 mM)[8-16]. However, these optimal solutions conditions do not inactivate all enveloped viruses evenly, suggesting that inactivation mechanisms are contingent upon certain viral structures. Viral structures that were highlighted to reduce the synergistic inactivation of arginine included increased protein stability and the presence of a matrix protein that integrates the capsid to the lipid bilayer. Three hypotheses were proposed for the mechanisms of synergistic arginine inactivation that explained the lower inactivation levels for viruses containing stabilized membrane proteins and lipid bilayers. Hypothesis 1 describes the viral inactivation by arginine through the inhibition of vital protein function. Hypothesis 2 describes viral inactivation by arginine through the destabilization of the viral membrane. Hypothesis 3 describes pore formation induced by arginine, accompanied by further viral damage from the synergistic factor to inactivate the virus. Due to the undisputable fact that arginine solely effects enveloped viruses, it is likely that either hypothesis 2 or 3 is correct. However, additional data is required for a definite understanding of synergistic arginine inactivation. When the mechanisms are fully known, viral inactivation by arginine may be further enhanced by the addition of functional groups, charges, or molecules to completely inactivate all enveloped viruses.

4 Physiochemical Properties of Enveloped Viruses and Arginine Dictate Inactivation

4.1 Abstract

Therapeutic protein manufacturing would benefit by having an arsenal of ways to inactivate viruses. There have been many publications on the inactivation ability of arginine at pH 4.0, but the mechanism of this inactivation has not been elucidated. This study explored virus structure, arginine-derivatives, arginine clustering, hydrophobicity, and buffer type on enhancing inactivation by arginine. Virus structure considerably influenced arginine inactivation. Large diameter viruses (SuHV-1, HSV-1) with loosely packed lipids were highly inactivated, whereas small diameter viruses (EAV, BVDV) with tightly packed lipids were negligibly inactivated by arginine. SuHV-1 experienced the highest inactivation of the viruses tested, with full inactivation at pH 7 and 1 M arginine. Membrane cholesterol sensitivity likely explains the inactivation difference between SuHV-1 and HSV-1. To increase the inactivation of viruses resistant to arginine, arginine-derivatives, and arginine peptides were tested. A greater capacity for clustering (butyroyl-arginine and R_8 peptide) and added hydrophobicity (butyroyl-arginine and $CapA_6R$ peptide) enhanced virus inactivation. Pyrenebutyrate, a hydrophobic cation, improved the inactivation of EAV by arginine. Dynamic light scattering (DLS) and transmission electron microscopy (TEM) detected increases in virus size after arginine exposure, supporting lipid expansion or arginine binding as the mechanism for inactivation. Conclusively, viruses with a large diameter and high cholesterol sensitivity were inactivated by arginine to the greatest extent. For viruses resistant to arginine, hydrophobicity and arginine-clustering enhanced inactivation.

4.2 Introduction

Therapeutic proteins are a progressive treatment option for cancers, autoimmunity/inflammation, infections, and genetic disorders[104]. When therapeutic proteins are produced from mammalian cells, there is potential for the presence of infectious viruses in solution[249]. Therefore, viral clearance is crucial in the manufacturing of therapeutic proteins to ensure infectious viruses do not spread to clinical patients. FDA regulations require a minimum of two orthogonal downstream viral clearance processes during manufacturing[250]. Typically, orthogonal processes include a filtration step to remove nonenveloped viruses and an inactivation step to remove enveloped viruses[249]. Low pH treatment is commonly used to inactivate enveloped viruses because of its simple, effective, and robust nature[249]. Currently, low pH treatment requires pH values $\leq$ 4.0[251], with pH values $\leq$ 3.6 being the most effective[249]. Unfortunately, acidic pH levels below 4 can sometimes damage proteins in therapeutic solutions[252]. Therefore, there is a need for an enveloped virus inactivation process that occurs at less acidic conditions.

Arginine can inactivate enveloped viruses at pH ≥ 4[10,15], increasing protein stability and reducing product aggregation propensity in comparison to conventional low pH treatment. However, optimal conditions for full inactivation of all enveloped viruses by arginine are not known[17]. Several studies demonstrate the inactivation of enveloped viruses by 0.7-1 M arginine after 1 hour at pH 4, with diminishing effects above pH 4[10,15]. However, not all enveloped viruses are equally inactivated under these conditions. For example, after 1 hour at pH 4 with 0.7 M arginine, HSV-1 is fully inactivated while influenza is only inactivated to 3.1 LRV. Sendai and Newcastle disease virus (NDV) experience insignificant inactivation at those conditions[10,15]. A stabilized lipid bilayer or

stabilized membrane proteins are hypothesized to lessen the inactivation effects of arginine[17]. Lipid bilayer stability can be influenced by lipid packing density or integrated proteins. In the case of Influenza, NDV, and Sendai virus, lipid bilayer stability is increased through the action of matrix proteins that integrate the lipid bilayer to the viral core. These viruses also all contain uncleaved glycoproteins that have increased stability[169,186,187]. Since viruses resistant to arginine contain both stabilized lipid bilayers and proteins, it is unclear if arginine is interacting with the lipid bilayer, proteins, or both to inactivate enveloped viruses.

Recently, pseudorabies virus (SuHV-1) and xenotropic murine leukemia virus (X-MLV) were inactivated at pH 7 in a solution of 1 M arginine and 5 mM Tris after 1 hour at 4°C[11]. In comparison to conventional low pH processes, inactivation at neutral pH maintains the stability of proteins, and therefore, is desired for viral clearance in therapeutic protein manufacturing. This is the only example in the literature where arginine inactivated a virus at neutral pH and below 35°C[16]. The main differences between this singular study and the numerous studies that demonstrated inactivation by arginine at pH 4 were the buffers and viruses tested. Acetate or no buffer was used with inactivation studies at pH 4[10,15], while Tris buffer was used at neutral pH. HSV-1 and influenza virus were tested at pH 4 and above[10,15], while SuHV-1 and X-MLV were tested at neutral pH[11]. The conflicting results in the literature lead to uncertainty in how arginine inactivates viruses at pH 7. Inactivation may be the result of virus structure or solution conditions.

Another key to arginine virus inactivation appears to be related to charge and hydrophobicity. Butyroyl-arginine, an arginine-derivative with a net charge of zero

between pH 3.73-12.14 and a hydrophobic capped amine, was equally or more effective than arginine in inactivating enveloped viruses over all conditions tested[10]. Because of its pure zwitterionic nature, butyroyl-arginine more readily forms self-clusters compared to arginine, which has an extra positive charge at physiological pH[10]. Arginine clusters support lipid and protein interactions to strengthen inactivation[17]. Additionally, the increased hydrophobicity of butyroyl-arginine may promote uptake into the lipid bilayer[239]. Improved clustering or hydrophobicity enhances inactivation by arginine, supporting the idea that solution conditions can enhance inactivation.

Arginine fully inactivates some enveloped viruses at pH 4[10,15] and pH 7[11]. However, not all enveloped viruses are highly inactivated by arginine under conditions reported in the literature. Viral membrane structures or glycoprotein stability appear to affect arginine inactivation. Additionally, the charges or functional groups on arginine or the buffer influence inactivation. Overall, it is not clear what factors optimize inactivation by arginine. This study goes into depth to explore virus structure, arginine-derivatives, arginine clustering, hydrophobicity, and buffer type on the inactivation of enveloped viruses by arginine. Pseudorabies virus (SuHV-1), herpes simplex virus (HSV-1), equine arteritis virus (EAV), and bovine viral diarrhea virus (BVDV) were tested for inactivation under various solution conditions. This study improves our understanding of arginine inactivation of enveloped viruses and helps to define the ability of arginine to inactivate enveloped viruses while retaining therapeutic protein stability during manufacturing.

4.3 Materials and Methods

4.3.1 Materials

For cell culture and viral assays, Eagle's medium essential media (EMEM), Dulbecco's modified eagle medium (DMEM), phosphate buffer saline (PBS, pH 7.2), sodium bicarbonate, penicillin/streptomycin (pen/strep, 10,000U/ml), sodium pyruvate (100mM) and trypsin/EDTA were purchased from Life Technologies (Carlsbad, CA). Fetal bovine serum (FBS, Canada origin) for cell culture was purchased from HyClone^{TM} GE Healthcare (Pittsburg, PA). Horse serum (New Zealand Origin) and glycerol for cell culture were purchased from Sigma Aldrich. MTT salts (2-(3,5-diphenyltetrazol-2-ium-2-yl)-4,5-dimethyl-1,3-thiazole; bromide, 98%) were purchased from Alfa Aesar^{TM} (Haverhill, MA) and sodium dodecyl sulfate (SDS, BioReagent, ≥98.5%) was purchased from VWR (Radnor, PA) for MTT assays.

Chemicals used during viral inactivation assays included L-arginine monohydrochloride (99%) and agmatine sulfate (97%) purchased from ThermoFisher Scientific (Waltham, MA) and 1-pyrenebutyric acid (PYB, 97%) and dimethyl sulfoxide (Hybri-Max^{TM}, sterile filtered, ≥ 99.7%) purchased from MilliporeSigma (St. Louis, MO). Peptides were synthesized by Biomatik (Wilmington, Delaware) to mimic clustering and hydrophobic conditions. Peptide capA$_6$R contained a six-chain hydrophobic alanine tail linked to an arginine, capped with an acetyl group at the N-terminus and amidated at the C-terminus. It was received as the trifluoroacetic acid (TFA) salt at >80% purity. Peptide R$_8$ is a chain of eight arginine molecules, which was received as the TFA salt at >95% purity.

Buffers of MES sodium salt (99% Acros Organics^{TM}), sodium acetate anhydrous (fused crystals/certified ACS), Tris hydrochloride (molecular biology grade), and potassium phosphate (ACS AR Crystal, Macron Fine Chemicals^{TM}) were purchased from ThermoFisher Scientific. Buffers of sodium acetate ($\geq$ 99% bioreagent), acetic acid (glacial), and citric acid monohydrate were purchased from MilliporeSigma. Buffers of sodium citrate tribasic dihydrate, glycineamide hydrochloride ($\geq$ 99% AT), Trizma® Base ($\geq$ 99% bioperformance certified), glycine (99% for molecular biology), tricine, and sodium phosphate dibasic heptahydrate (ACS reagent, 98-102%) were generously donated by MilliporeSigma. Solution pH was adjusted with sodium hydroxide (NaOH) from MilliporeSigma and hydrochloric acid (HCl) from ThermoFisher Scientific.

For the cholesterol assay, methyl-β-cyclodextrin (BioReagent, suitable for cell culture) was purchased from MilliporeSigma and the Amplex Red Cholesterol Assay Kit was purchased from ThermoFisher Scientific. For transmission electron microscopy imaging, glutaraldehyde (Grade 1, 70% in H$_2$0) was purchased from MilliporeSigma, and uranyl acetate was purchased from ThermoFisher Scientific.

4.3.2 Methods

4.3.2.1 Cells and Viruses

Bovine turbinate cells (BT-1, ATCC CRL-1390), rabbit-kidney cells (RK-13, ATCC CCL-37), and Vero cells (ATCC CCL-81) were purchased from ATCC. Bovine viral diarrhea virus (BVDV) strain NADL was purchased from the United States Department of Agriculture Animal and Plant Health Inspection Service (USDA APHIS). Equine arteritis virus strain Buvyrus (EAV, ATCC VR-796), human herpesvirus 1 strain

F (HSV-1, ATCC VR-733), and suid herpesvirus 1 strain Aujeszky (SuHV-1, ATCC VR-135) were purchased from ATCC. All cells were incubated at 5% CO_2 and 100% humidity during infectivity assays.

BT-1 cells were cultured in DMEM media supplemented with 1% v/v pen/strep, 1% v/v sodium pyruvate, and 10% v/v horse serum at 37°C and 5% CO_2. Cells were split every 3-4 days (or when 70% confluent) at a 1:3 ratio. BVDV was added at a concentration of 10^5 MTT_{50}/ml to BT-1 cells at 80% confluency in supplemented DMEM media for virus propagation in a cell culture flask. Once BVDV was added to the BT-1 cells, the flask was left on a roto-shaker at low speed for one hour. After shaking, the virus suspension was removed from the 75 cm^2 flask and 15 mL of fresh media was added to the infected cells. The infected flask was incubated at 37°C for 72 hours. After, the monolayer was scraped with a cell scraper and the media was collected in a centrifuge tube. The tube was spun down at 5500xg for 15 min at 4°C. The supernatant was collected as the propagated virus sample and 10% v/v glycerol was added for storage at -80°C.

RK-13 cells were cultured in EMEM media supplemented with 1% pen/strep, and 10% FBS and incubated at 37°C and 5% CO_2[253]. Cells were split every 2-3 days (or when 70% confluent) at a 1:3 ratio. EAV was added at a concentration of 10^5 MTT_{50}/ml to RK-13 cells at 70% confluency in supplemented EMEM media in a cell culture flask. The flask was shaken at low speeds on a roto-shaker for 1 hour. After shaking, the virus suspension was removed from the flask and fresh media was added. The cells were left to incubate at 37°C for 3-5 days or when 100% cytopathic effect (CPE) was observed. Flasks were then frozen at -80°C and thawed at room temperature for two freeze-thaw

cycles. Glycerol was added at a concentration of 10% to the final virus suspension and frozen at -80°C for storage.

Vero cells were cultured in EMEM media supplemented with 1% pen/strep, and 10% FBS and incubated at 37°C and 5% CO_2. Cells were split every 2-3 days (or when cells reached 70% confluency) at a 1:5 ratio. For HSV-1 propagation, the virus was added at a concentration of $10^{3.56}$ MTT_{50}/ml into Vero cells at a confluency of 70% in DMEM supplemented with 1% pen/strep, 1% sodium pyruvate and 2% FBS. The HSV-1 infected flask was shaken for 1 hour on a roto-shaker. After shaking, the virus suspension was removed from the flask and fresh media was added. The flask was incubated at 35°C for 3-5 days until 100% CPE was observed. Flasks underwent two freeze-thaw cycles at -80°C and room temperature[254]. HSV-1 virus suspensions were collected from the flask and stored at -80°C with 10% glycerol. For SuHV-1 propagation, 10^4 MTT_{50}/ml was added to 70% confluent Vero cells in EMEM supplemented with 1% pen/strep, and 10% FBS. The flask was shaken for 1 hour on a roto-shaker. After shaking, the virus suspension was removed from the flask and fresh media was added. The flask was incubated at 37°C for 3-5 days until 100% CPE was observed. Flasks were subjected to two freeze-thaw cycles at -80°C and room temperature. SuHV-1 virus suspensions were collected from the thawed flasks and stored at -80°C with 10% glycerol.

4.3.2.2 Virus Quantification and Purification

Virus titer was determined through an MTT colorimetric cell viability assay, as described previously[255]. The MTT assay uses absorbance readings to determine the concentration of virus that reduces the cell viability by 50%. Briefly, 96-well plates were

seeded at a density of 2 x 10^5 cells/ml (for BT-1/BVDV), 8 x 10^4 cells/ml (for RK-13/EAV), 10^5 cells/ml (for Vero/HSV-1), or 8 x 10^4 cells/ml (for Vero/SuHV-1). After 22-26 hours, cells were infected with their respective virus sample and serially diluted across the plate at a 1:5 ratio in virus culture media. Plates were incubated for six days at 37°C for BT-1 (BVDV), RK-13 (EAV), and Vero (SuHV-1) and 35°C for Vero (HSV-1). After incubation, MTT salts were added to the 96-well plate, incubated for four additional hours followed by the addition of SDS at a pH of 2. Between 4-12 hours after the SDS addition, the absorbance of each well was read with a microplate reader (BioTek, Winooski, VT) at a wavelength of 550 nm to determine the 50% infectious dose, reported as MTT_{50}/ml[255]. Final viral concentrations were reported as a log_{10} reduction value (LRV), defined in **Eq. 4-1**.

$$LRV = \log_{10} \left(\frac{Virus\ Conc_{Before\ treatment}}{Virus\ Conc_{After\ treatmentl}} \right) \qquad \textbf{(Eq. 4-1)}$$

Purification of viruses was performed using a $3M^{TM}$ Emphaze^{TM} AEX Series Hybrid Purifier BVR1 that contained a pore size of 0.2μm, generously gifted by $3M^{TM}$ (Minneapolis, MN). The filter was prepared by loading 20 mM phosphate buffer at pH 7 until the buffer exited the air vent. The crude virus was mixed with an equal volume of 20 mM phosphate buffer at pH 7 and loaded into the filter at a total volume of 40 ml. The virus was then eluted with 20 mM phosphate buffer with 0.5 M NaCl at pH 7. Eluate was collected in 5 ml fractions and tested for virus recovery. The fraction with the highest virus titer was used for succeeding assays. Protein reduction was measured for the HSV-1 sample by the Bradford assay[256].

4.3.2.3 Inactivation Assays

All arginine and/or buffer solutions were prepared less than 24 hours before the experiment and stored at 4°C. Solutions were prepared with ultrapure water (resistivity of ≥ 18 MΩ cm) obtained from a Thermo Fisher Nanopure filtration system and sterilized before biological assays with a 0.2 µm syringe filter or a 0.2 µm bottle top filter purchased from VWR. Respective acid and base solutions were mixed for each buffer to achieve a final concentration of 20 mM and a pH of 4 or 7, calculated by the Henderson-Hasselbalch equation (**Eq.4- 2**). Acetate buffer was prepared by mixing sodium acetate anhydrous with acetic acid. Tris buffer was prepared by mixing Tris hydrochloride with Trizma® Base. Citrate buffer was prepared by mixing sodium citrate tribasic with citric acid monohydrate. The final solution pH was adjusted with 1M HCl or 1 M NaOH. For all assays, EAV was added at a concentration between 10^6-10^7 MTT$_{50}$/ml. BVDV, HSV-1, and SuHV-1 were added at concentrations between 10^7-10^8 MTT$_{50}$/ml. Triplicates were taken at each time point to obtain accurate representation.

$$pH = pK_a + \log\left(\frac{[A^-]}{[HA]}\right) \qquad \textbf{(Eq. 4-2)}$$

For inactivation studies of arginine or agmatine, 1M arginine or agmatine at pH 4 or 7 was prepared with 20 mM Tris, acetate, or no buffer. Viruses were added to the appropriate solution at a 1:10 v/v ratio in a 1.5 ml sterile microcentrifuge tube. Solutions were vigorously mixed with a vortex after virus addition and before sampling. Solution pH did not change after virus addition. Samples were stored at 4°C and assessed for virus titer with the MTT assay at various time points.

For inactivation by arginine peptides, peptides were dissolved in DMSO less than 1 hour before experiments to avoid error in measurement. Final solutions contained 10% DMSO with 7.6 mM CapA$_6$R, 0.95 mM R$_8$, or 7.6 mM arginine buffered with 20 mM Tris. The virus was added to the final solution at a 1:10 v/v ratio in a 1.5 ml sterile microcentrifuge tube. Solutions were mixed after virus addition and again before sampling with a vortex. Solutions were stored at 4°C and virus inactivation was measured after 1 hour.

For arginine inactivation studies with added PYB, solutions were prepared by dissolving PYB into DMSO less than 1 hour prior to experiments to avoid error in measurements. Final solutions contained 10% DMSO with 1 M arginine, 10 mM PYB, and 20 mM Tris buffer at pH 7 or 20 mM acetate buffer at pH 4. PBS with 10% DMSO and 10 mM PYB was tested as a control. Mock solutions were created for comparison that contained the same components as the primary solutions without PYB. The virus was added to the appropriate solution at a 1:10 v/v ratio in a 1.5 ml sterile microcentrifuge tube. Solutions were vigorously mixed with a vortex after virus addition, and again before sampling. Solutions were stored at 4°C and virus inactivation was measured after 1 hour.

4.3.2.4 Dynamic Light Scattering (DLS) and Transmission Electron Microscopy (TEM)

The size distribution of HSV-1 and SuHV-1 after arginine exposure was measured by DLS with a Malvern Zetasizer Nano ZS (Westborough, MA). DLS evaluated the hydrodynamic diameter of the virus particles after exposure to arginine

samples at 1 and 24 hours. Samples were placed in disposable cuvettes (200 acrylate, 280-900 nm, 3.5 mL volume) purchased from Spectrocell (Oreland, PA) at a volume of 1 ml. The Malvern Zetasizer Nano ZS was set to a material refractive index of 1.450 and an absorption of 0.00. All dispersants were set to a temperature of 21°C at a viscosity of 1 cP. A refractive index of 1.378 was used for arginine samples and a refractive index of 1.335 was used for PBS samples. The refractive index was measured by a digital refractometer from Reichert (NY, catalog # 13940000).

Purified virus samples or purified virus samples with 1 M arginine were prepared for TEM imaging according to university biosafety procedures by crosslinking proteins through fixation with 7.4 v/v% glutaraldehyde for 1 hour[257]. Samples were then placed onto a plasma-treated carbon type-B 300 mesh copper TEM grid (Ted Pella catalog #01813), and allowed to attach for 2 minutes. Following virus attachment, the grid was rinsed with ultrapure water and negatively stained with 2 w/v% uranyl acetate in ultrapure water. After a 2-minute staining period, the grid was washed again with ultrapure water and dried in a desiccator for at least 24 hours before imaging. An FEI 200kV Titan Themis scanning transmission electron microscope (S-TEM) operating at 80kV was used to obtain electron micrographs.

4.3.2.5 Amplex Red Cholesterol Assay

Purified HSV-1 and SuHV-1 samples were split into two 1 ml aliquots and treated in parallel. To extract cholesterol from the samples, methyl-β-cyclodextrin (MβCD) was added at a concentration of 5 mM to the first aliquot in PBS buffer. The second aliquot for each virus was left unaltered in PBS buffer. All aliquots were incubated at 37°C for 1

hour. After incubation, virus titer and cholesterol levels were quantified. Virus titer was quantified through the MTT assay described earlier. Cholesterol was measured in duplicates with the Amplex Red Cholesterol Assay following manufacturer's instructions. Triplicates for every sample were measured. Separate mock samples for each virus were tested to give a representative level of cholesterol in solution without the virus. Mock samples contained a solution of cells that underwent the same propagation and purification method as their respective virus.

4.3.2.6 Statistical Analysis

Statistical analysis of the data was performed in MATLAB using a two-sample Student's t-test to compare the means of two independent groups. The test assumed equal variances between the two samples. A significance level of $p < 0.05$ was used. All data sets were tested in triplicate.

4.4 Results and Discussion

4.4.1 Model Viruses

The inactivation of four enveloped viruses was compared to determine the influence of viral physical properties on viral-arginine interactions. The viruses were chosen based on genomic properties, size, isoelectric point, and structure, with details shown in **Table 4-1** and **Figure 4-1**. SuHV-1 and HSV-1 belong to the *Herpesviridae* family and are similar in size, structure, and function[168,258]. SuHV-1 causes Aujeszky's disease in pigs[21], while HSV-1 produces oral or genital lesions in humans[20]. Both are large enveloped viruses with diameters of 110-200 nm[170]. Distinctive to herpesviruses,

the nucleocapsid contains double-stranded DNA and is encircled in a tegument protein matrix that contains over 20 identified proteins[168,258]. The mature capsid and tegument layer is enclosed within a lipid bilayer bearing approximately 11 glycoproteins[168,258].

EAV is a small enveloped virus with a diameter of 50-70 nm belonging to the *Arteriviridae* family[259]. EAV is infectious in horses with symptoms including fever, depression, skin rash and abortion in pregnant mares[260]. The virion is composed of a positive-sense single-stranded RNA coated in a nucleocapsid protein (N) and enveloped by a lipid bilayer[259]. The envelope is complexed with integral membrane proteins including E, ORF5a, GP2, GP3, GP4, GP5, and M[260].

BVDV is a small enveloped virus with a diameter of 40-50 nm belonging to the Flaviviridae family[261]. Dengue virus, yellow fever virus and hepatitis C virus are also part of the Flaviviridae family, thereby making BVDV ideal for modeling significant human viruses[262]. The virion contains a positive-sense single-stranded RNA enclosed in a nucleocapsid protein. The surrounding lipid bilayer contains two glycoproteins, E1 and E2, that are necessary for cell entry[261].

Table 4-1. Properties of Tested Enveloped Viruses

Virus	Genome	Diameter (nm)	Isoelectric Point
Pseudorabies Virus (**SuHV-1**)	dsDNA	110-200[170]	~7.5[263]
Herpes Simplex Virus 1 (**HSV-1**)	dsDNA	110-200[170]	~4.9[264]
Equine arteritis Virus (**EAV**)	(+)ssRNA	50-70[259]	N/A
Bovine Viral Diarrhea Virus (**BVDV**)	(+)ssRNA	40-50[261]	4.3-4.5[265]
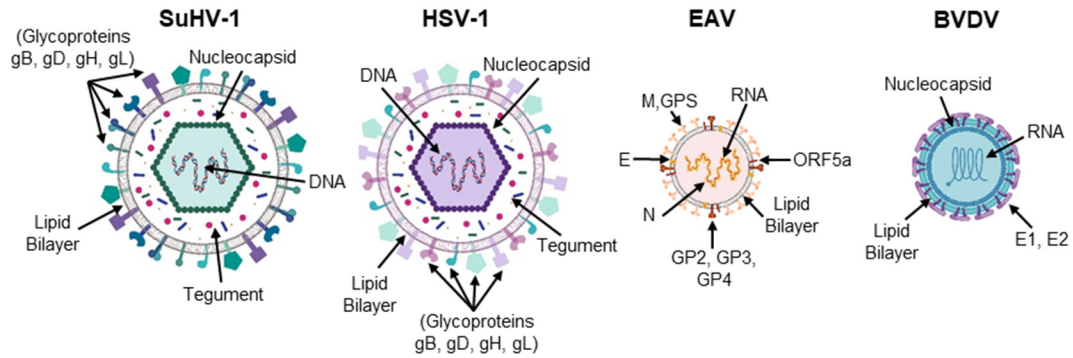
Figure 4-1. Structure of SuHV-1, HSV-1, EAV and BVDV. HSV-1 and SuHV-1 are large enveloped viruses containing a tegument protein layer. EAV and BVDV are small enveloped viruses. Images created in Biorender.

4.4.2 Virus Physiochemical Properties Influence Arginine Interactions

Viral properties, including a stabilized lipid bilayer or stabilized membrane proteins, influence the inactivation efficacy of arginine[17]. However, it is unknown if arginine is interacting with proteins or lipids to induce viral inactivation. Inactivation levels of the viruses detailed in Table 1 were compared to elucidate the mechanisms of arginine. The inactivation of SuHV-1, HSV-1, BVDV, and EAV was tested at pH 4 and pH 7 with various solvents (**Fig 4-2**). Tabular data can be found in **Table A1**. SuHV-1 and HSV-1 are commonly used in arginine inactivation studies, and therefore, were tested for comparison to literature[10,11,15]. Particularly, SuHV-1 was chosen to recreate inactivation by arginine at neutral pH[11]. BVDV and EAV were selected to determine the effect of arginine on small enveloped viruses. Acetate and Tris were chosen to determine the influence of buffers on inactivation at pH 4 and 7[10,11,15]. Citrate inactivates enveloped viruses at pH 3.5[15] and was used as a comparison to conventional methods.
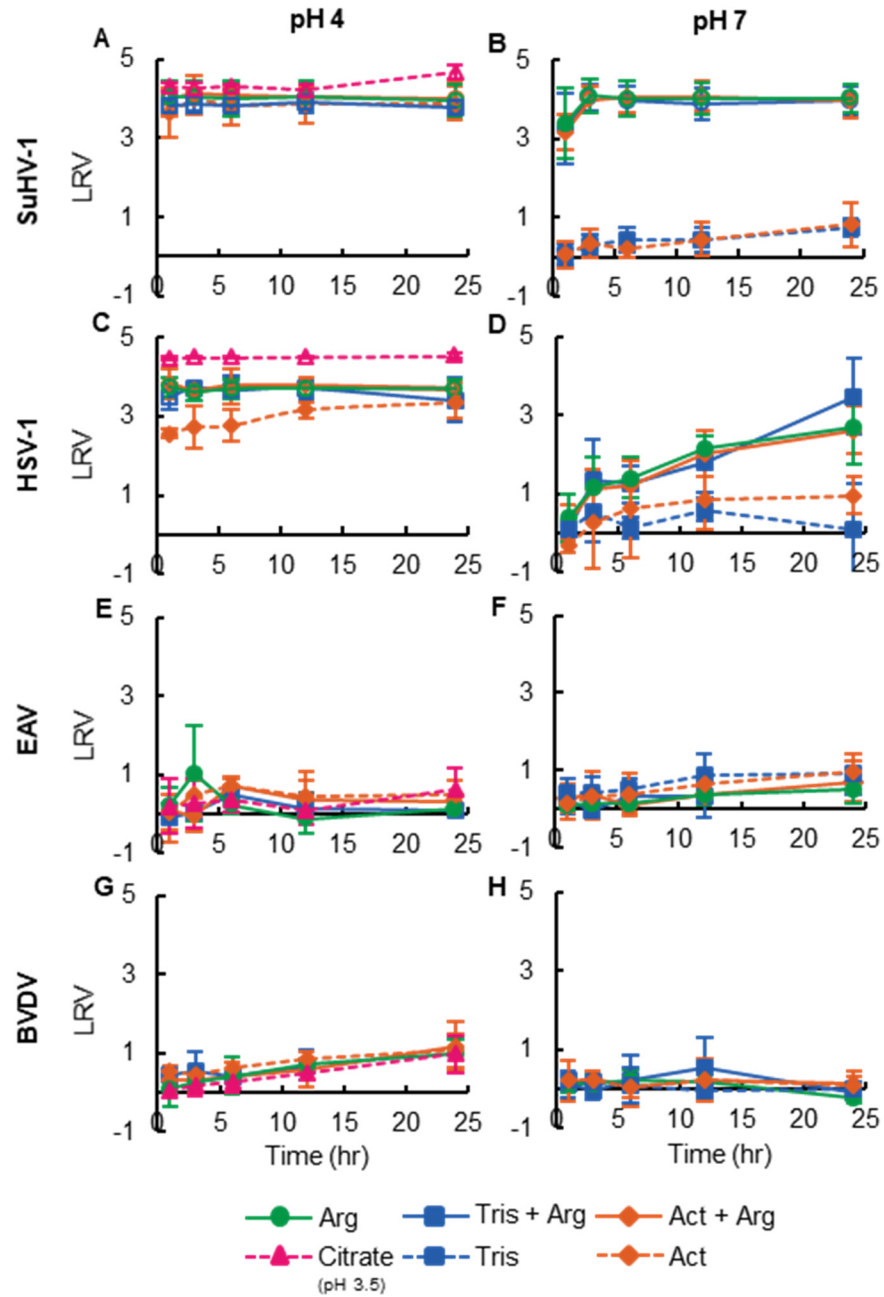
Figure 4-2. Inactivation of enveloped viruses by arginine (arg). Inactivation occurred at either pH 4 (1st column), pH 7 (2nd column) or pH 3.5 (citrate) at 4°C over 24 hours. Arginine concentration was 1 M and Tris, acetate (act), and citrate concentrations were 20 mM. Open circles represent limit of detection. Tris buffer was not tested at pH 4 since it would not remain at pH 4. All data points are in triplicate and the error bars represent the standard deviation. Tabular data can be found in **Table A1**.

Different viruses had distinct inactivation patterns. As shown in **Fig. 4-2**, SuHV-1 was inactivated to its limit of detection by all solutions within 1 hour at pH 4. Complete inactivation without arginine reveals that 20 mM acetate alone at pH 4 inactivates SuHV-1. HSV-1 was inactivated to its limit of detection with all arginine solutions at pH 4 within 1 hour. Without arginine, acetate buffer inactivated HSV-1 to 3.35 ± 0.37 LRV after 24 hours, verifying that arginine is required for complete inactivation of HSV-1 at pH 4. At pH 7, SuHV-1 was completely inactivated by all solutions containing arginine within 3 hours, replicating the data from McCue et al. and confirming that full inactivation was independent of buffer[11]. Unlike at pH 4, acetate and Tris buffer alone produced negligible inactivation of SuHV-1. For HSV-1 at pH 7, inactivation increased to 3.46 ± 0.96 LRV after 24 hours with arginine buffered in Tris. Buffer solutions without arginine at pH 7 produced minimal inactivation of HSV-1. EAV and BVDV were inactivated to low levels (below 1 LRV) at pH 4 and pH 7 over all solution conditions tested. At pH 3.5, citrate fully inactivated HSV-1 and SuHV-1, but had little effect on EAV or BVDV. At pH 3.5, 0.1 M citrate has been shown to fully inactivate HSV-1[15].

The clear difference in inactivation capacity between large (HSV-1 and SuHV-1) and small (BVDV and EAV) enveloped viruses supports the theory that arginine interacts with the lipid bilayer to inactivate viruses. Large diameter membranes have a mild degree of curvature that leads to loosely packed lipids, while small diameter membranes have a large degree of curvature, creating tightly packed lipids[194]. Loosely packed lipids are hypothesized to bend and deform easily in response to arginine[17], supported by the high inactivation of the larger viruses. The tightly packed lipids of small membranes restrict

deformation by arginine to hinder inactivation. This is supported by the low inactivation of EAV and BVDV. Overall, the data support the hypothesis that arginine interacts with the lipid bilayer to inactivate viruses.

Though it is clear that membrane diameter is key in arginine inactivation, what creates the difference in inactivation levels between SuHV-1 and HSV-1 at pH 7? Interestingly, SuHV-1 is more thermal stable than HSV-1[266], which is the opposite of what would be expected from their arginine sensitivity. The two viruses have different charges at pH 7 (HSV-1 has an isoelectric point of ~4.9[264], where SuHV-1 has an isoelectric point of ~7.5[263]), creating distinct electrostatic binding potentials. Though SuHV-1 and HSV-1 contain comparable glycoproteins, many are structurally or functionally different[267]. Therefore, arginine may disrupt an essential protein in SuHV-1 where it does not in HSV-1.

Differences in lipid bilayer cholesterol may explain the higher inactivation of SuHV-1 compared to HSV-1 by arginine. Cholesterol in the lipid bilayer controls membrane stability and aids in viral infection[268]. Cholesterol is singularly contained in the lipid bilayer or can interact with sphingolipids to form lipid rafts. Singular cholesterol and lipid rafts support many viral functions including membrane stability and protein interactions[269]. SuHV-1 may contain less cholesterol than HSV-1, resulting in a less stable membrane. Arginine would deform a less stable membrane to a greater extent to result in higher inactivation. Alternatively, arginine may promote cholesterol loss or migration, disrupting the infection process. The bending and deformation of lipids by arginine may disrupt cholesterol in the membrane to hinder infection. For example, membrane deformations have been shown to cause migration of cholesterol in lipid

113

bilayers[270]. SuHV-1 may require cholesterol to a greater extent than HSV-1 during infection, resulting in higher inactivation by arginine as a result of cholesterol loss or migration. Overall, the charge, glycoproteins, or cholesterol content may explain the discrepancy in arginine inactivation of SuHV-1 and HSV-1.

The effect of cholesterol depletion on virus inactivation was studied to explore differences between HSV-1 and SuHV-1 resulting in varying levels of arginine inactivation. Viral cholesterol may influence inactivation by arginine as a result of membrane stability or the requirement of cholesterol in the infection process. To begin the cholesterol assay, purified HSV-1, SuHV-1, and mock samples were subjected to 5 mM methyl-β-cyclodextrin (MβCD) to deplete cholesterol, or no MβCD for 1 hour at 37°C. MβCD sequesters cholesterol in its hydrophobic pocket to extract it from membranes[271]. Past studies have used MβCD to remove cholesterol from the viral or cellular membrane to observe effects on viral infectivity[268,272]. Cholesterol levels in all samples decreased to low levels following MβCD exposure (**Fig. 4-3A & B**). Tabular data can be found in **Table A2**. Similar cholesterol levels were observed in mock and viral samples after purification. Therefore, cholesterol levels do not represent virus cholesterol exclusively, but a combination of virus and cell fragment cholesterol remaining in solution. Though we cannot deduce exact cholesterol levels in the virus, we can confirm that overall solution cholesterol was reduced to low levels after MβCD exposure.
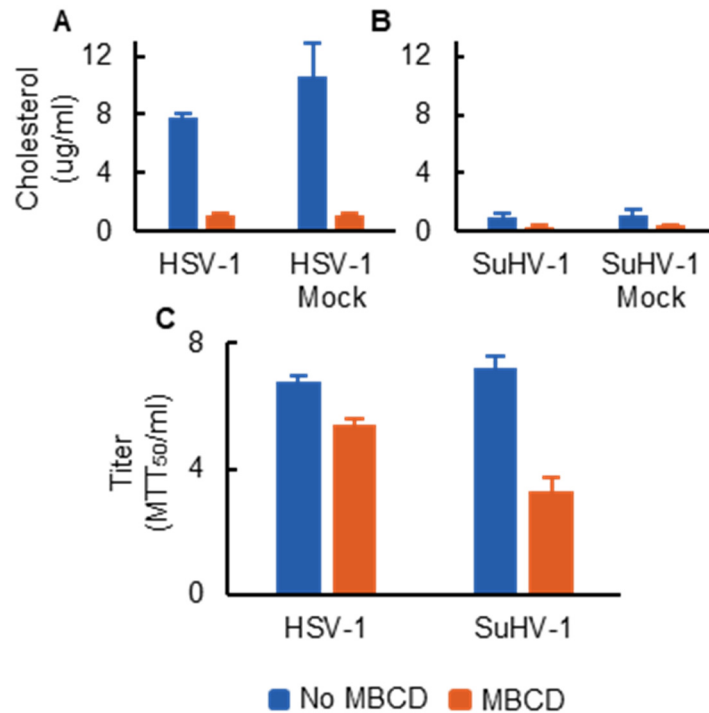
Figure 4-3. Effect of cholesterol depletion on the infectivity of HSV-1 and SuHV-1. Purified virus and mock samples of (A) HSV-1 and (B) SuHV-1 were incubated for 1 hour at 37°C at pH 7with either 5mM methyl-β-cyclodextrin (MβCD) or no MβCD. Cholesterol was reduced in all samples containing MβCD to low levels. (C) Infectivity changes after MβCD exposure. Mock samples contained Vero cells that underwent identical propagation and purification as virus samples. All data points are in triplicate and the error bars represent the standard deviation. Tabular data can be found in **Table A2**.

The reduction of cholesterol in the viral membrane inactivated SuHV-1 to a greater extent than HSV-1. HSV-1 infectivity reduced by 1.4 LRV while SuHV-1 reduced by 4 LRV after MβCD exposure (**Fig. 4-3C**). Cell toxicity in response to MβCD concentration can be found in **Fig. A1**. Again, the data in **Fig. 4-3A & B** represent a reduction of viral cholesterol and not a quantitative measure of viral cholesterol resulting from imperfect purification. This means that the LRVs are not representative of viral cholesterol levels but instead a loss of viral cholesterol. The high LRV of SuHV-1

115

suggests that cholesterol, or cholesterol-rich lipid rafts, play a larger role in the infection process of SuHV-1 compared to HSV-1. These results are consistent with the inactivation results by arginine, where SuHV-1 was inactivated to a greater extent compared to HSV-1 at pH 7. This consistency supports the hypothesis that arginine deforms the viral membrane to remove or disrupt cholesterol. The disruption of viral cholesterol may highly affect SuHV-1 because of the requirement for cholesterol in membrane stability or protein function. Though there may be other factors in play, the higher susceptibility of SuHV-1 to inactivation is likely associated with membrane cholesterol loss by arginine.

4.4.3   Solution Properties to Enhance Inactivation of Viruses by Arginine

Not all enveloped viruses are fully inactivated by the synergistic effects of arginine[10,11,15]. The results from **Fig. 3-2** show that BVDV and EAV are not inactivated by 1M arginine under any conditions. Correspondingly, past studies show that influenza, Sendai, and Newcastle disease virus (NDV) are not fully inactivated with 0.7 M arginine at pH 4 on ice for 60 min[10,15]. For this reason, various solution properties were tested to determine if viral inactivation by arginine could be enhanced. We explored solution properties by altering the charges on arginine, artificially inducing clustering, and adding hydrophobic molecules to arginine or the solution. In addition to enhancing inactivation, modifying solution conditions may also provide insight into mechanisms of arginine inactivation.

4.4.3.1 Inactivation with Arginine Derivatives

The guanidinium moiety on arginine is essential for virus inactivation. Guanidinium has an affinity for hydrogen and can form ionic bonds with proteins and lipids[124]. Other properties of arginine, such as charge or hydrophobicity, may also be crucial for viral inactivation. Charges on arginine affect electrostatic interactions between the virus and arginine itself for cluster formation[124,191]. Hydrophobicity is suspected to loosen lipid packaging to allow arginine to easily bend and deform lipid bilayers[239]. To observe the effect of charge and hydrophobicity on arginine viral inactivation, the inactivation of three guanidinium-containing arginine derivatives with separate charge patterns were compared. The three derivatives were arginine, agmatine, and butyroyl-arginine, and their structures are illustrated in **Fig. 4-4A**. Agmatine is arginine with the carboxylic acid removed. Butyroyl-arginine is arginine with the amine capped with a hydrophobic butyryl group. At pH 4 and 7, arginine is zwitterionic with a + 1 charge, agmatine has a + 2 charge, and butyroyl-arginine is zwitterionic with a neutral charge[176].
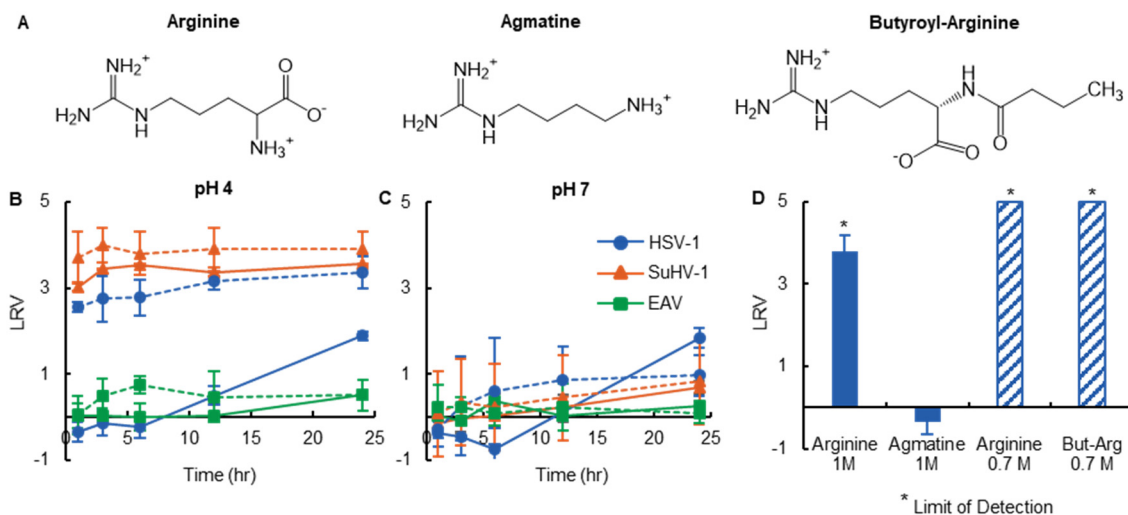
Figure 4-4. Inactivation of enveloped viruses with arginine derivatives. (A) The structure of arginine, agmatine, and butyroyl-arginine. All arginine-derivatives contain a guanidinium group but each has a different charge pattern. Inactivation of HSV-1, SuHV-1, and EAV in response to agmatine buffered with acetate at (B) pH 4 and (C) pH 7. Solid lines represent agmatine solutions buffered with acetate, dashed lines represent solutions without agmatine. Inactivation occurred at 4°C over 24 hours. Agmatine concentration was 1 M and acetate concentration was 20 mM. (D) Arginine, agmatine, and butyroyl-arginine inactivation of HSV-1 after 1 hour at 4°C or on ice. Slashed bar graphs of 0.7 M arginine and but-arg adapted from Katsuyama et al. *Limit of detection. All data points are in triplicate and the error bars represent the standard deviation. Tabular data can be found in **Table A3** and **A4**.

The inactivation of HSV-1, SuHV-1, and EAV with 1 M agmatine was compared at pH 4 and 7 in **Fig. 4-4B&C**. Tabular data can be found in **Table A3.** At pH 4, agmatine produced negligible inactivation of EAV and HSV-1, while 3.55 ± 0.01 LRV occurred for SuHV-1 after 24 hours. The inactivation of EAV and SuHV-1 at pH 4 with agmatine (solid line) were similar to the control solution (dashed line), indicating that agmatine did not inactivate the virus. The inactivation of HSV-1 at pH 4 with agmatine was much lower than the control solution, demonstrating the stabilizing effect of agmatine on HSV-1. At pH 7, agmatine and the controls inactivated all viruses to around

1 LRV, demonstrating no effect of agmatine on virus inactivation. When looking at the data as a whole, agmatine fails to inactivate enveloped viruses.

The inactivation efficacy of arginine, agmatine, and butyroyl-arginine is compared in **Fig 4-4D**. Tabular data can be found in **Table A4**. The butyroyl-arginine data was reformatted from Katsuyama et al.[10]. Solutions containing 1 M arginine, 0.7 M arginine[10], and 0.7 M butyroyl-arginine[10] fully inactivated HSV-1 at pH 4 after 1 hour, while 1 M agmatine produced negligible inactivation. Butyroyl-arginine and arginine inactivate HSV-1 to the same levels at pH 4. However, as pH increases to 4.5, butyroyl arginine is over 2-LRVs more effective than arginine at inactivating HSV-1 (data not shown)[10]. Butyroyl-arginine is the most effective at inactivating enveloped viruses, followed by arginine. Agmatine is the least effective in inactivating the tested viruses.

The difference in inactivation efficacy between butyroyl-arginine, arginine, and agmatine is likely explained by added hydrophobicity and/or clustering. Clustering of arginine can strengthen protein[127] and lipid interactions[197] to support inactivation. The zwitterionic charge on butyroyl-arginine and arginine allow for the formation of clusters through self-aggregation. However, the two positive charges on agmatine are not optimal for clustering, consistent with the lesser inactivation capacity observed. Butyroyl-arginine has an ideal charge pattern for clustering as a result of one positive and one negative charge on opposite ends of the molecule[10]. Though arginine can also form clusters, it is not as effective as butyroyl-arginine as a consequence of its extra positive charge[17]. Butyroyl-arginine also contains a hydrophobic moiety where arginine and agmatine do not[15]. The increased hydrophobicity of butyroyl-arginine can strengthen interactions with

lipids, which may aid in inactivation[10,15], demonstrated by increased inactivation by butyroyl-arginine.

The difference between agmatine and arginine is charge based. Inactivation differences between agmatine and arginine are likely a result of clustering. Agmatine is not zwitterionic, therefore, clusters cannot form by electrostatic interaction. The inability of agmatine to form clusters is likely the root cause of low inactivation. However, this same lack of clustering and a high positive charge may be the reason for agmatine appearing to provide virus stabilization in the presence of low pH (**Fig. 4-4B**). Acidic pH commonly inactivates viruses through lipid hydrolysis[153] or protein denaturation[154]. However, with agmatine at pH 4, HSV-1 was demonstrated to be further stabilized (**Fig. 4-4B**). The positive charges on agmatine may bind to negative charges on HSV-1 to counteract deterioration at acidic pH. Through HSV-1 has a positive net charge at pH 4 with its pI being ~4.9[264], negative charges on the virus still exist. SuHV-1 has a higher overall positive charge related to its higher pI, and therefore, may not be stabilized by the positive agmatine charges. Arginine derivatives with added hydrophobicity, enhanced clustering, or both lead to increased enveloped virus inactivation. Therefore, we decided to study each effect independently.

4.4.3.2 Inactivation Based on Charge and Hydrophobicity

Hydrophobicity or clustering of arginine derivatives appears to enhance viral inactivation. To further evaluate these properties, arginine peptides were synthesized specifically for this work with added hydrophobicity or forced arginine clustering. Hydrophobicity is suspected to loosen lipid packaging to support membrane deformations

by arginine[239], while clustering strengthens arginine interactions with lipids and proteins[127,197]. CapA6R and R8 peptides were tested for inactivation, and their structures are shown in **Fig. 4-5A**. CapA6R contains an arginine molecule linked to a six-chain hydrophobic alanine tail. The peptide is capped on both ends to expose a single positive charge on the guanidinium moiety. The single charged peptide avoids clustering to exclusively model added hydrophobicity. CapA6R has been previously studied for its antimicrobial activity[205]. The R8 peptide simulates the clustering of eight arginine molecules. This peptide has been studied for drug delivery as a cell-penetrating peptide and was chosen for its high cell penetration efficiency[273].
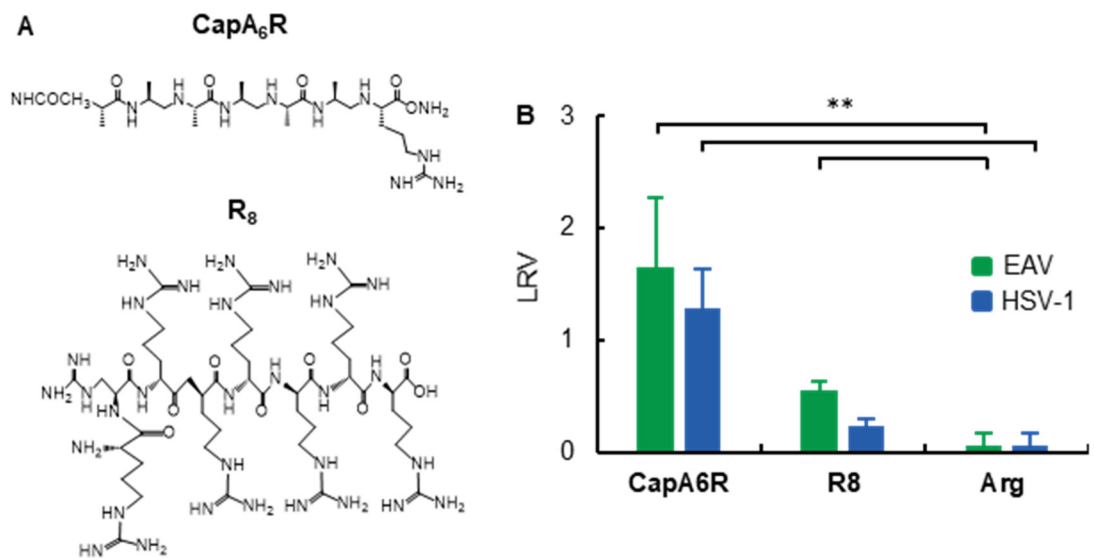
Figure 4-5. Virus inactivation with arginine peptides. (A) Peptide structure of CapA$_6$R and R$_8$. (B) Virus inactivation tested after 1 hour at pH 7 at 4°C in Tris buffered solutions with 10% DMSO. Arginine and CapA6R concentrations were 7.6 mM. R8 concentration was 0.95 mM which is equivalent to an arginine concentration of 7.6mM. Tris concentration was 20 mM. The brackets with ** represent statistically different means with a $p<0.05$ by the Student's t-test. All data points are in triplicate and the error bars represent the standard deviation. Tabular data can be found in **Table A5**.

The inactivation of EAV and HSV-1 by $CapA_6R$, R_8, and arginine was compared in **Fig. 4-5B**. Tabular data can be found in **Table A5**. Enveloped virus inactivation increases with arginine concentration[15], and therefore, an equivalent arginine concentration of 7.6 mM for all species was applied for equal comparison. This low concentration of peptide was used to demonstrate a change in the inactivation mechanism because of costs restraints, and not to provide a method for high virus inactivation. Solutions were buffered with Tris at pH 7 and exposed to arginine or arginine peptides for 1 hour. As a result of high hydrophobicity, $CapA_6R$ was dissolved in DMSO and added to the final solution at a concentration of 10% DMSO. For equal comparison, 10% DMSO was added to each solution. $CapA_6R$ produced the highest inactivation, followed by R_8, with arginine producing the lowest inactivation at the concentration tested. By the two-sample Student's t-test, $CapA_6R$ inactivated EAV and HSV-1 to greater levels than arginine, with p-values of 0.0255 and 0.009, respectively. R_8 inactivated EAV a greater level than arginine, with a p-value of 0.0075. Inactivation of HSV-1 by R_8 was not statistically different than the arginine control, with a p-value of 0.145. Interestingly, both $CapA_6R$ and R_8 inactivated EAV to a greater extent than HSV-1. Commonly, HSV-1 is highly inactivated, whereas EAV is not inactivated by arginine solutions (**Fig. 4-2**). The data supports that added hydrophobicity and clustering enhance the inactivation of enveloped viruses under conditions where conventional arginine inactivation is low.

The increased hydrophobicity of $CapA_6R$ resulted in the highest inactivation levels of HSV-1 and EAV as compared to arginine. To determine if hydrophobicity could further enhance inactivation, pyrenebutyrate (PYB), a hydrophobic counter-anion, was added to arginine solutions. PYB is commonly used to increase the uptake of arginine

cell-penetrating peptides across the lipid bilayer by electrostatically binding to arginine[239]. Added hydrophobicity is thought to allow for easier translocation of arginine through the hydrophobic core of the lipid bilayer[239].

The inactivation of EAV and HSV-1 with PYB is shown in **Fig. 4-6**. Tabular data can be found in **Table A6**. Inactivation occurred at 4°C after 1 hour. PYB enhanced the inactivation of EAV by 1.58 ± 0.29 LRV compared to the control with arginine and Tris buffer at pH 7. However, EAV inactivation was not enhanced by PYB at pH 4, and HSV-1 inactivation was not enhanced by any PYB solution. The difference in inactivation capacity of EAV at pH 4 and 7 is likely explained by the charge on PYB. PYB has a -1 charge at pH 7 and is neutral at pH 4[176]. The negative charge at pH 7 may bind to the positive charges on arginine or EAV for enhanced inactivation. The greater inactivation of EAV over HSV-1 by PYB may also be a result of the virus charge. The isoelectric point of HSV-1 is ~4.9[264], whereas the isoelectric point of EAV is unknown. If the isoelectric point of EAV is higher than HSV-1, the charges on EAV at pH 7 may be more positive to allow for the binding of PYB. The difference in inactivation of EAV and HSV-1 suggest that PYB is binding to the lipid bilayer to loosen the lipid packing, instead of binding to arginine itself to aid in translocation.
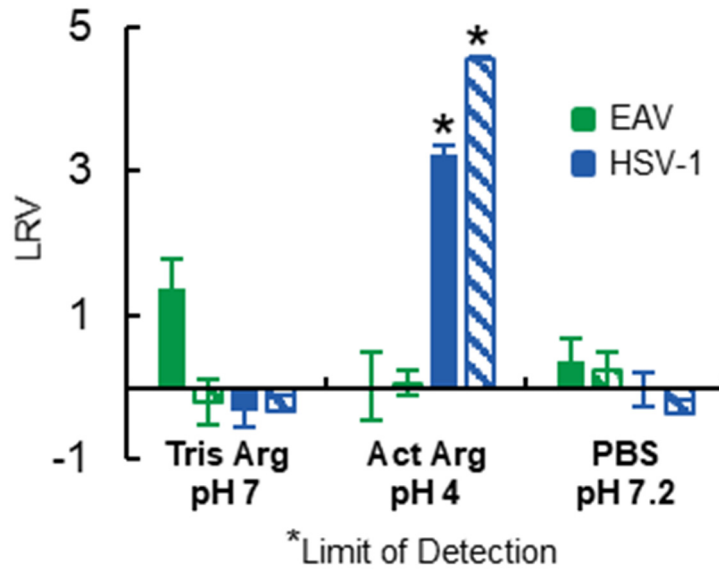
Figure 4-6. Inactivation of EAV and HSV-1 by arginine and pyrenebutyrate (PYB). Solid bars represent samples with PYB and 10% DMSO, dashed bars represent mock samples with only 10% DMSO. Inactivation occurred after 1 hour at 4°C. PYB was at 10 mM, arginine was at 1 M, and Tris and acetate were at 20 mM concentration. *Limit of detection. Note that the limit of detection for HSV-1 in Vero cells was lowered by PYB. All data points are in triplicate and the error bars represent the standard deviation. Tabular data can be found in **Table A6**.

Though PYB did increase EAV inactivation at pH 7, complete inactivation was not reached. When PYB has been used to enhance the uptake of peptides into the cell, the concentrations of PYB were larger than the peptide (15μM for PYB and 1.5 μM for peptides)[239]. Here, PYB was 100X less concentrated than arginine as a consequence of its solubility limit. If higher concentrations of hydrophobic cations could be used, arginine inactivation can be hypothesized to be enhanced to fully inactivate all viruses.

4.4.4 Functional Groups and Charges on Buffers

Since charge interactions of PYB and arginine derivatives with the virus influence inactivation, the effect of buffer functional groups and charge were explored. It has been shown previously that 1M arginine with Tris buffer at pH 7 can fully inactivate SuHV-1[11]. Properties of Tris that may aid in the inactivation of viruses include the amine group, charge, or high-fat solubility. Amine groups interact with various compounds[218], charges dictate electrostatic interactions, and increased fat solubility can increase diffusion into lipid bilayers[274]. However, all arginine solutions fully inactivated SuHV-1 at pH 7 (**Fig. 4-2**), suggesting the synergy of Tris is not the mechanism causing high inactivation.

Various buffers were tested to model Tris and acetate to determine if specific properties aid in the inactivation of HSV-1 (**Fig. 4-7**). Tabular data can be found in **Table A7**. Buffers were chosen for their potential inactivation properties. Structure and pK_a values of the tested buffers can be found in **Table A8**[176]. Glycine mimicked the amine group on Tris. Glycineamide mimicked the +1 charge and amine group on Tris. Tricine has a similar structure to Tris, but lower-fat solubility[275]. MES mimicked the charge on acetate. Despite the differences, all buffers inactivated viruses to similar levels. Overall, the data suggest that specific properties of buffers do not aid in viral inactivation by arginine.
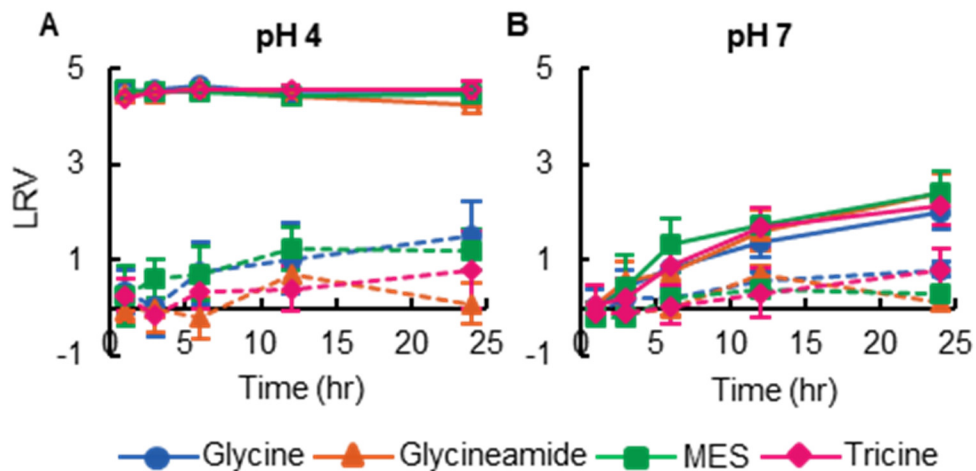
Figure 4-7. Inactivation of HSV-1 with buffer mimics. Solid lines represent buffered solutions with arginine, dashed lines represented buffered solutions without arginine. Buffer mimics showed similar inactivation to Tris and acetate used with arginine. Inactivation occurred at either (A) pH 4 or (B) pH 7 at 4°C. Arginine concentration was 1 M. Glycine, glycineamide, MES, and Tricine concentration were 20 mM. Open circles represent the limit of detection. All data points are in triplicate and the error bars represent the standard deviation. Tabular data can be found in **Figure A7**.

4.4.5 Viral Structural Changes after Arginine Exposure

The hypotheses for the mechanisms of viral inactivation by arginine all infer viral structural changes[17]. Viral structure is speculated to change by complete disassembly, aggregation[13], deformation of proteins/lipids[13], or simply arginine binding[15]. DLS measurements and TEM images evaluated viral structural changes after arginine exposure to elucidate inactivation mechanisms.

Size differences of HSV-1 and SuHV-1 before and after arginine exposure were measured by DLS (**Fig 4-8A**). This data is also presented in **Figure A3** in a different form for clarification. Both viruses increased in size after exposure to arginine. Viruses were exposed to arginine at 1 or 24 hours at pH 4 or 7. PBS at pH 7.4 was used as a control for no arginine exposure. When HSV-1 was exposed to arginine at pH 4, size

increased by 110 ± 25 nm after 1 hour and 243 ± 37 nm after 24 hours. Size changes to

HSV-1 at pH 4 and 7 over all conditions were comparable. Changes to SuHV-1 were

similar, with the largest size increase of 123 ± 62 nm with arginine buffered with Tris at

24 hours. Size changes in control PBS solutions were minimal for both viruses over 24

hours (**Fig. A2**). The peak at 1 nm is likely the arginine molecule itself. Similar to DLS

measurements, TEM images showed increased virus size after arginine exposure (**Fig. 4-**

8B). HSV-1 was 158 nm and SuHV-1 was 179 nm before arginine exposure. After

arginine exposure, HSV-1 increased to 526 nm while SuHV-1 increased to 358 nm. TEM

measurements were obtained by measuring the size of the virus in the images shown. An

increased viral size could be the result of expanding lipids or viral swelling by lipids

bilayer deformations. Additionally, the binding of large arginine clusters to viral particles

could increase the size of the viral particle. However, the data suggest that virus

disassembly or viral aggregation is not the cause of inactivation.
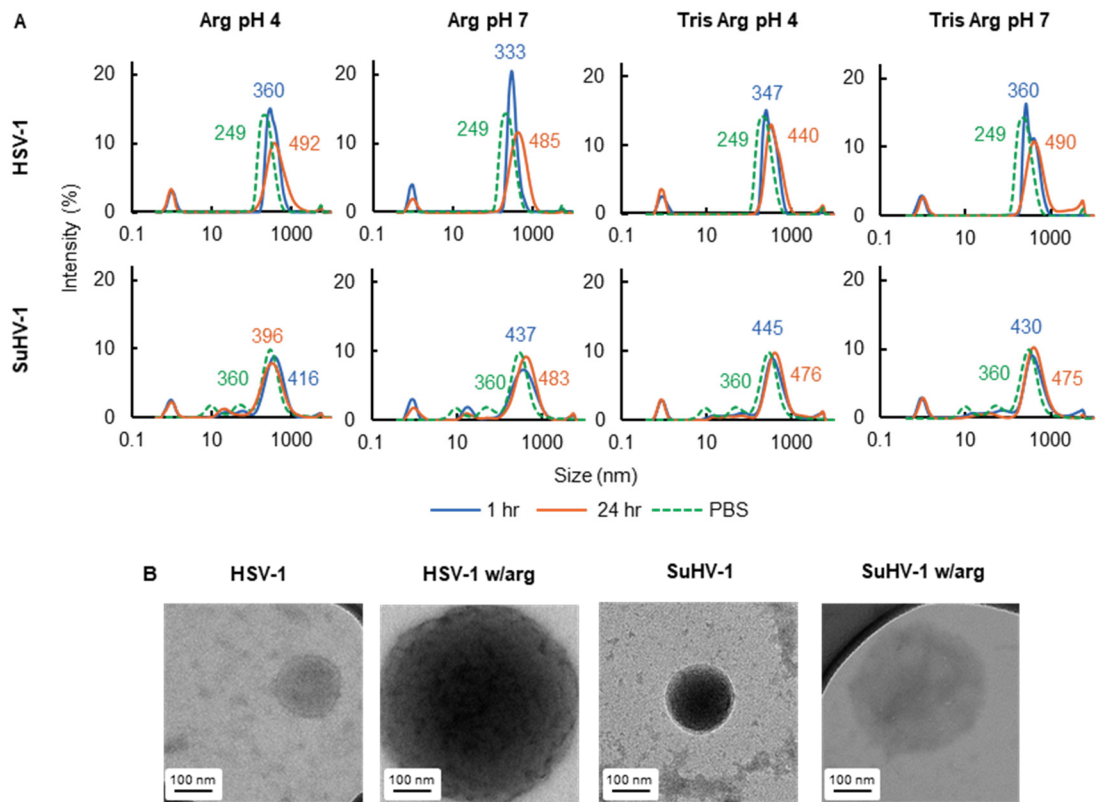
Figure 4-8. Size changes of HSV-1 and SuHV-1 after arginine exposure. (A) DLS after 1 and 24 hours and (B) TEM after 1-hour arginine exposure at 4°C at pH 4. Arginine was at 1 M, Tris was at 20 mM, and PBS was at pH 7.4. Inactivation occurred at 4°C. All data points for DLS measurements are in triplicate.

4.5 Conclusions

Inactivation of enveloped viruses by arginine maintains the structure and stability of therapeutic proteins, making it a desired viral clearance process in protein manufacturing[10,11,15]. Arginine had been found to stabilize therapeutic proteins while inactivating enveloped viruses. However, not all enveloped viruses are inactivated by arginine to safe levels for clinical use[17]. This study investigated virus structure, properties

of arginine, buffer type, and viral changes to further elucidate the mechanisms by which the inactivation of enveloped viruses is enhanced by arginine.

Viral structure influenced the inactivation capacity of arginine. Large diameter viruses (SuHV-1 and HSV-1) were highly inactivated by arginine, while small diameter viruses (EAV and BVDV) were negligibly inactivated by arginine. The difference in inactivation is hypothesized to be the result of lipid packing density[17]. Large diameter viruses have loosely packed lipids for easy deformation by arginine and small diameter viruses have tightly packed lipids that restrict deformation by arginine[17]. However, virus size does not solely explain the inactivation differences between SuHV-1 and HSV-1. SuHV-1 was completely inactivated at pH 7 by arginine with all buffer types, similar to the results from McCue et al.[11], whereas HSV-1 was only partly inactivated (3.7 LRV). SuHV-1 and HSV-1 are comparable viruses from the *Herpesviridae* family[168,258], therefore, it is difficult to discern differences that influence inactivation by arginine. Removal of membrane cholesterol inactivated HSV-1 by 1.4 LRV and SuHV-1 by 4 LRV. SuHV-1 may have a higher sensitivity to cholesterol reduction as a result of the requirement for cholesterol in membrane stability or protein function[268,272]. Bending and deforming the viral membrane likely disrupts lipid rafts and cholesterol. Therefore, inactivation by arginine because of lipid bilayer deformations would be enhanced with a higher sensitivity to cholesterol reduction. Overall, loosely packed lipids or high cholesterol sensitivity of enveloped viruses support inactivation by arginine.

Various solution properties were tested to enhance the inactivation of viruses that are naturally resistant to arginine. Charge and functional groups on arginine-derivatives were assessed to determine the influence on inactivation. Butyroyl-arginine was the most

129

effective, followed by arginine, and agmatine was the least effective. The ability to form dense clusters and the hydrophobic capped amine of butyroyl-arginine likely aid in inactivation. To dig deeper into these effects, arginine peptides were tested to model added hydrophobicity ($CapA_6R$) and forced arginine clustering (R_8). Both $CapA_6R$ and R_8 enhanced inactivation over arginine itself, with $CapA_6R$ being the most effective. Since added hydrophobicity continually enhanced inactivation, pyrebutyrate, a hydrophobic cation, was added to arginine solutions. PYB improved inactivation of EAV but not of HSV-1 when exposed to arginine. This difference was likely the result of virus charge. Additionally, the impact of buffers with various functional groups and charges were explored during inactivation by arginine. Buffers had no obvious effects on inactivation. Collectively, the data indicate hydrophobicity and arginine clustering enhance the inactivation of enveloped viruses.

Viral structural changes after arginine exposure were examined by DLS and TEM. Both methods detected increasing virus size after arginine exposure for 1 or 24 hours. The results demonstrate that virus disassembly or virus aggregation do not explain inactivation. The increase in virus size may result from lipid expansion or arginine binding. Lipid expansion would result from arginine bending and deforming the viral membrane. On the other hand, arginine binding to viral proteins or lipids would also display an increased virus size. These insights correlate with earlier results where added hydrophobicity and arginine clustering enhanced inactivation. Hydrophobicity loosens lipid packaging to support lipid bilayer deformations[239] whereas arginine clusters strengthen lipid and protein interactions[127,197]. To narrow down the mechanisms further, these findings can be related to the impacts of virus structure on inactivation. Viruses

130

with loosely packed lipids or the requirement for membrane cholesterol are highly inactivated by arginine. These viral properties would enhance inactivation through bending and deforming the viral membrane. Combining the data as a whole, lipid bilayer deformation is the likely mechanism for virus inactivation by arginine though no mechanism can be completely ruled out.

The results from this study support lipid bilayer deformation as the mechanisms for viral inactivation by arginine. This mechanism can be enhanced by added hydrophobicity or arginine-clustering to inactivate viruses that are resistant to arginine. Though optimal conditions for full inactivation of all viruses were outside the scope of this work, this study provided insight into increasing inactivation by arginine. Additional testing is required to optimize hydrophobicity, arginine-clustering, and charge for full inactivation of all enveloped viruses. For example, increasing the concentrations of arginine-peptides or added hydrophobic molecules may enhance inactivation. By adding new components to arginine solutions, it would also be useful to look into the impact of inactivation conditions on the final product quality.

4.6 Acknowledgements

131

College of New York for his guidance on HSV-1 growth, quantification, and propagation.

5 Influence of Buffer Type and Concentration on Virus Inactivation during Low pH Treatment

5.1 Introduction

Viral safety is a major concern in biotherapeutic manufacturing. Infectious human viruses may be present in solution when mammalian cells are used to produce biotherapeutic products[249]. To ensure viral safety is met and infections do not spread to clinical patients, regulations require the use of two orthogonal downstream viral removal processes during manufacturing[112,250,276,277]. A filtration and an inactivation step are commonly used to remove nonenveloped and enveloped viruses[249]. Low or high pH, solvent/detergent, heat gamma irradiation, or ultraviolet radiation treatments are examples of enveloped viral inactivation processes[251]. Low pH is simple and effective, and therefore, is typically used in manufacturing with treatments of pH ≤ 3.6 being most effective[249]. However, acidic pH levels under 4 can damage essential cells, tissues, or proteins in biotherapeutic solutions[252]. For this reason, there is a demand for a robust inactivation process at less acidic conditions.

Under specific operating parameters, virus inactivation has occurred at pH 4 or above where conditions are less detrimental to the stability of essential solution components[252]. Operating parameters influencing virus inactivation at pH 4 include temperature, incubation time, and solutions conditions[278]. It is standard with increasing temperature and incubation time that virus inactivation is enhanced[278,279]. However, solution conditions including protein concentration, buffer type, and buffer concentration, have a more complicated influence on virus inactivation[278]. High (30 mg/ml) or low protein concentrations (0 mg/ml) increase inactivation of viruses at acidic pH[278].

133

Concentration and type of buffer in solution also influence virus inactivation, though the effectiveness can depend on several solution properties[249,251,252,278-280].

There are many examples in the literature where the concentration and/or type of buffer influence the inactivation capacity of viruses in low pH solutions. **Table 5-1** compares buffer effectiveness during the inactivation of viruses at low pH. It is evident from previous work that buffer concentration and type largely influence the inactivation of viruses at acidic pH. Buffer concentration can influence buffer effectiveness. For example, citrate was most effective at low concentrations (0.15 M) in inactivating Influenza A virus while acetate was most effective at high concentrations (0.6M). Virus type also influences buffer effectiveness. Pseudorabies virus (SuHV-1) was fully inactivated by acetate, citrate and glycine[279]. Acetate was the most effective buffer in inactivating xenotropic murine leukemia virus (XMuLV)[279]. Citrate was most effective buffer in inactivating murine leukemia virus[251]. Viral inactivation depends not only on the buffer type, but additionally on buffer concentration, virus type, and pH.

Table 5-1. Examples of Low pH Inactivation with Buffers.

Buffer	Virus	Conditions	Results	Reference
NaCl, Phosphate, Acetate, and Citrate	Influenza A	• 0.15-0.9 M buffer • pH 5 • 5 min • 30° C	Citrate most effective at low concentrations (0.15 M) while acetate was the most effective at high concentrations (0.6M).	Nishide et al[252]
Acetate, Citrate, and Glycine/phosphate	XMuLV	• pH 3.9 • 30 min • 20° C	Acetate fully inactivated X-MLV while citrate or glycine/phosphate produced low inactivation.	Durno et al[278]
Acetate titrated with acetic acid or phosphoric acid	XMuLV	• 25-100 mM buffer • pH 3.7 • 10 min	Inactivation increased with acetic acid titrant and buffer concentration.	Chinnia et al[249]
Acetate, Citrate, and Glycine	SuHV-1 and XMuLV	• 50 mM buffer • pH 3.7 • 17° C	Complete inactivation of PRV occurred with all buffers after 4 min. Complete inactivation of X-MLV occurred with glycine and acetate after 2 min, and with citrate after 15 min.	Gillespie et al[279]
Acetate, Citrate, and Glycine	Murine Leukemia Virus	• pH 3.9 • 15-25° C	Citrate was the most effective and glycine was the least effective for inactivation.	Cameron et al[251]

In this study the influence of buffer type, buffer concentration and time at pH 4 on the inactivation of four viruses is examined. Buffers tested include citrate, acetate, and

glycine at concentrations of 20-500 mM. Data collected will provide insight into the matrix conditions required for high inactivation of viruses at pH 4 to improve biotherapeutic manufacturing.

5.2 Materials and Methods

5.2.1 Materials

Buffers used during inactivation assays included sodium acetate ($\geq$ 99% bioreagent), acetic acid (glacial), and citric acid monohydrate purchased from Millipore Sigma (St. Louis, MO). Glycine (99% for molecular biology) and sodium citrate tribasic were generously donated from Millipore Sigma. Chemicals for cell culture assays included Eagle's medium essential media (EMEM), Dulbecco's modified eagle medium (DMEM), phosphate buffer saline (PBS, pH 7.2), sodium bicarbonate, penicillin/streptomycin (pen/strep, 10,000U/ml), sodium pyruvate (100mM) and trypsin/EDTA, purchased from life technologies (Carlsbad, CA). Fetal bovine serum (FBS, Canada origin) was purchased from HyCloneTM GE Healthcare (Pittsburg, PA), and horse serum (New Zealand Origin) was purchased from Sigma Aldrich. For the virus titer determination by MTT assay, MTT salts (2-(3,5-diphenyltetrazol-2-ium-2-yl)-4,5-dimethyl-1,3-thiazole; bromide, 98%) were purchased from Alfa AesarTM (Haverhill, MA) and sodium dodecyl sulfate (SDS, BioReagent, $\geq$98.5%) was purchased from VWR (Radnor, PA). The pH of buffer solutions was adjusted with sodium hydroxide (NaOH), purchased from Millipore Sigma and hydrochloric acid (HCl), purchased from ThermoFisher Scientific.

5.2.2   Methods

5.2.2.1   *Cells and Viruses*

Vero cells (CCL-81), rabbit-kidney cells (RK-13, CCL-37), and porcine kidney cells (PK-13, CRL-6489) were purchased from ATCC. Suid herpesvirus 1 (SuHV-1) strain Aujeszky (VR-135), human herpesvirus 1 (HSV-1) strain F (VR-733), and equine arteritis virus (EAV) strain Buvyrus (VR-796) were purchased from ATCC. Porcine parvovirus (PPV) strain NADL-2 was generously gifted by Dr. Ruben Carbonell from North Carolina State University in Raleigh, NC. Each cell line was incubated at 5% CO_2 and 100% humidity at 37°C during virus propagation or infectivity assays, except Vero cells infected with HSV-1 were incubated at 35°C. EAV was propagated in RK-13 cells, HSV-1 was propagated in Vero cells and SuHV-1 was propagated in Vero cells, as described previously (Chapter 4). PPV was propagated in PK-13 cells, as described previously[255].

5.2.2.2   *Virus Quantification*

The MTT colorimetric cell viability assay was used to calculate virus titer[281]. First, 96-well plates were seeded with 8 x 10^4 cells/well for the combination of Vero cells for SuHV-1 titer, RK-13 cells for EAV titer, and PK-13 cells for PPV titer. A density of 10^5 cells/well was required for Vero cells for HSV-1 titer. Plates seeded with cells were incubated at 37°C, 5% CO_2, and 100% humidity before virus infection. Following 22-26 hours of incubation, 25 ul of the virus sample was added to the first column of the 96-well plate and serially diluted at a 1:5 ratio down the plate. Plates were incubated for six days at 37°C for SuHV-1, EAV, and PPV and 35°C for HSV-1. After, MTT salts were

added to each well to detect live cells by the production of purple formazan. Plates were placed back into the incubator for 4 hours, and then SDS at a pH of 2 was added to each well and incubated for an additional 4-12 hours to allow SDS to solubilize the formazan crystals. Absorbance was measured in each well at a wavelength of 550 nm by a microplate reader (BioTeK, Winooski, VT). Final viral concentrations were calculated as the 50% infectious dose (MTT_{50}/ml) and reported as a log_{10} reduction value (LRV), defined in **Eq. 5-1**.

$$LRV = \log_{10}\left(\frac{Virus\ Conc_{Before\ removal}}{Virus\ Conc_{After\ removal}}\right)$$ (**Eq. 5-1**)

5.2.2.3 Buffer Inactivation Assays

To begin inactivation assays, glycine, acetate, and citrate were prepared at concentrations of 20mM, 100mM, 250mM, and 500 mM. Buffer solutions were made with ultrapure water (resistivity of $\geq$ 18 MΩ cm) collected from a Thermo Fisher Nanopure filtration system. Acetate buffer was prepared by mixing sodium acetate anhydrous with acetic acid to concentrations that yielded the final buffer molarity at pH 4, calculated by the Henderson-Hasselbalch equation (**Eq. 5-2**)[282]. Citrate buffer was prepared by mixing sodium citrate tribasic with citric acid monohydrate to concentrations that yielded the final molarity at pH 4, calculated by the **Eq. 5-2**[282]. Glycine buffer was prepared with glycine. 1M NaOH and 1M HCl were used for final adjustments to pH 4. Buffers were sterilized before biological assays with a 0.2 μm syringe filter from VWR (Radnor, PA).

$$pH = pK_a + \log\left(\frac{[A^-]}{[HA]}\right) \qquad\qquad \textbf{(Eq. 5-2)}$$

To begin inactivation assays, 100 µl of model virus and 900 µl of the appropriate

buffer were mixed in a 1.5 ml sterile ultracentrifuge tube. SuHV-1, HSV-1, and PPV

were added at concentrations of 10^7-10^8 MTT$_{50}$/ml and EAV was added at a

concentration of 10^6-10^7 MTT$_{50}$/ml. The addition of the virus did not alter the solution

pH. Samples were stored at 4°C, and virus titer was measured at 0.5, 1, 2, 3, and 6 hours

with the MTT assay.

5.3   Results and Discussion

5.3.1   Model Virus and Buffers

Pseudorabies virus (SuHV-1), herpes simplex virus 1 (HSV-1), equine arteritis

virus (EAV), and porcine parvovirus (PPV) were chosen as model viruses. Properties of

viruses are listed in **Table 5-2**. SuHV-1 and HSV-1 are both large enveloped viruses with

diameters of 110-200 nm belonging to the *Herpesviridae* family[168,170,175,258].

Herpesviridae are double-stranded DNA viruses containing a capsid surrounded by a

tegument protein matrix and enclosed in a lipid bilayer[258,267]. EAV is a small enveloped

virus from the *Arteriviridae* family with a diameter of 50-79 nm[259]. EAV contains a

positive-sense single-stranded RNA coated in a nucleocapsid protein[259] and enveloped by

a lipid bilayer[260]. PPV is a small non-enveloped virus with a diameter of 18-26 nm[283].
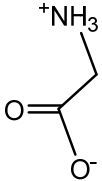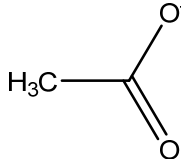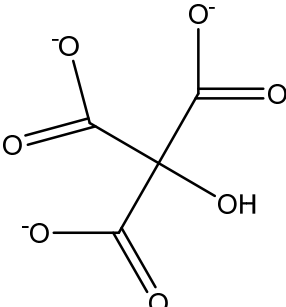
PPV belongs to the *Parvoviridae* family and contains single-stranded DNA[284].

Table 5-2. Properties of Tested Viruses

Virus	Acronym	Envelope	Diameter (nm)	Isoelectric Point	Genome
Pseudorabies Virus	SuHV-1	Yes	110-200[170]	~7.5[263]	dsDNA
Herpes Simplex Virus 1	HSV-1	Yes	110-200[168,175]	~4.9[264]	dsDNA
Equine Arteritis Virus	EAV	Yes	50-70[259]	N/A	(+)ssRNA
Porcine Parvovirus	PPV	No	18-26[283]	4.8-5.1[283]	ssDNA

Citrate, acetate, and glycine were used as buffers during virus inactivation at pH 4. All buffers are weak electrolytes that have been used in the literature to inactivate viruses at low pH [249,251,252,278,279]. Structure, pK_a, and charges of the buffers are listed in **Table 5-3**. Glycine is a simple non-essential amino acid containing a hydrogen atom side chain[285]. Acetate is monocarboxylic acid anion formed as a salt from acetic acid and a base[286]. Citrate is commonly used as a buffer in inactivating viruses during low pH treatment at pH 3.5[15]. Glycine and acetate have a dominant charge of 0 while citrate has a dominant charge of -1 at pH 4.

Table 5-3. Properties of Tested Buffers[176]

Buffer	Structure	pK$_a$	Dominant charge below pK$_a$
Glycine		2.31	+1
		9.27	0
Acetate		4.54	0
Citrate		3.13	0
		4.76	-1
		6.40	-2

5.3.2 Inactivation Capacity of Buffers at pH 4

The inactivation of viruses at pH 4 with glycine, acetate, and citrate buffer at 20 mM, 100mM, 250 mM, and 500 mM was assessed. Inactivation experiments were co conducted at 4°C and the LRV for each virus was measured at 0.5, 1, 2, 3, and 6 hours. Both viral and buffer properties influenced inactivation as follows.

The inactivation of SuHV-1 by glycine, acetate, and citrate is shown in **Fig. 5-1**. The effectiveness of glycine increased with buffer concentration and time, but never fully

141

inactivated SuHV-1. Glycine at 20 mM produced negligible inactivation, while inactivation increased over time at all other concentrations, reaching a maximum of 4.13 LRV after 6 hours at 500 mM glycine. Acetate fully inactivated SuHV-1 at concentrations of 250mM or above after 30 min. Full inactivation, or limit of detection, is represented by open shapes. Acetate at 20 mM and 100 mM inactivated SuHV-1 to similar levels after 6 hours to 4 LRV and 3.76 LRV, respectively. Inactivation increased over time with 20 mM and 100 mM acetate to 3 hours and then leveled off. Citrate concentrations $\geq$ 100 mM completely inactivated SuHV-1 within 30 min. Citrate at 20mM reduced SuHV-1 by 3.3 LRV after 6 hours, but similar inactivation of 3.5-$\log_{10}$ occurred after 1 hour. Citrate was the most effective buffer, followed by acetate, and the least effective was glycine in inactivating SuHV-1 at pH 4.
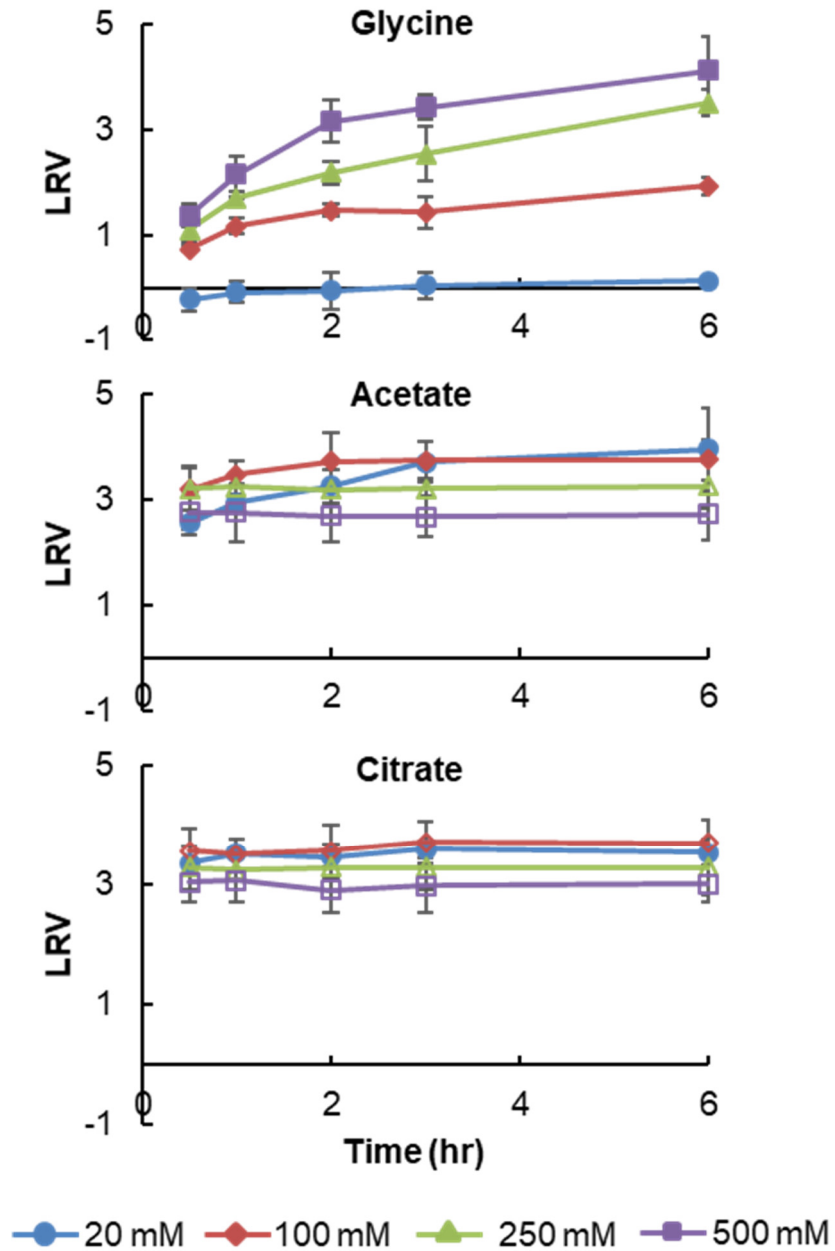
Figure 5-1. Inactivation of SuHV-1 by various concentrations of glycine, acetate, and citrate at pH 4. Citrate is the most effective, and after 30 min all concentrations of 100 mM or above fully inactivate SuHV-1. Acetate is the next effective with concentrations of 250 or above fully inactivate SuHV-1. Glycine is the least effective at inactivating SuHV-1. The limit of detection is signified by open shapes. Data points were measured in triplicates and error bars represent standard deviation.

Inactivation of HSV-1 was influenced by buffer concentration and type (**Fig. 5-2**). Inactivation of HSV-1 by 20 mM glycine was negligible but increased at concentrations ≥ 100 mM to 1.78 LRV after 6 hours. Acetate never fully inactivated HSV-1, up to 4 LRV, at any concentration, where it did fully inactivate SuHV-1 at concentrations ≥ 250mM. After 1 hour, inactivation at all acetate concentrations leveled out, whereas 20 mM produced 3.08 LRV, 100 mM produced 3.6 LRV, 250 mM produced 3.4 LRV, and 500 mM produced 3.7 LRV. The effectiveness of citrate in inactivating HSV-1 increased with concentration. Inactivation by 20 mM citrate increased over time to 3.2 LRV after 6 hours. Inactivation by 100 mM citrate increased drastically after 1 hour to 4.22 LRV, and reached 4.6 LRV after 6 hours. Citrate at 250 mM fully inactivated HSV-1 after 1 hour, and 500 mM citrate fully inactivated HSV-1 after 30 min. Conclusively, citrate was the most effective at inactivating HSV-1, followed by acetate, and the least effective was glycine.
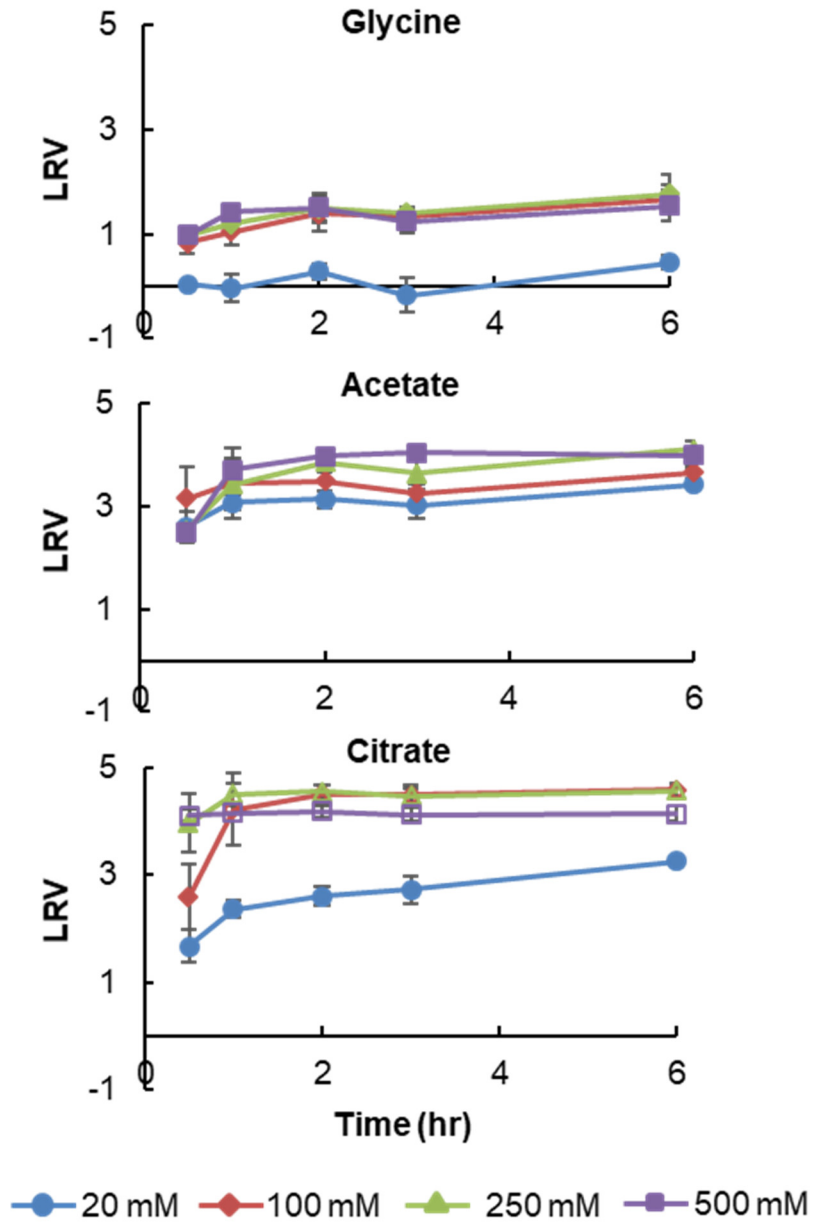
Figure 5-2. Inactivation of HSV-1 by various concentrations of glycine, acetate, and citrate at pH 4. Citrate is the most effective, and at 1 hour all concentrations of 100 mM or above fully inactivate HSV-1. Acetate is the next effective, and glycine is the least effective at inactivating HSV-1. The limit of detection is signified by open shapes. Data points were measured in triplicates and error bars represent standard deviation.

Inactivation of EAV (**Fig. 5-3**) and PPV (**Fig. 5-4**) was negligible at all buffer concentrations at pH 4 after 6 hours. Properties of EAV and PPV may hinder inactivation by buffers at pH 4. EAV is a small enveloped virus, creating a lipid bilayer that is tightly packed for increased membrane stability[17]. This highly stabilized virus may restrict inactivation compared to larger viruses (SuHV-1 and HSV-1) that contain loosely packed lipids[17]. PPV is a non-enveloped virus, meaning it does not contain a lipid bilayer and the protein capsid is directly exposed to the environment[225]. Lipid bilayers are more sensitive to environmental degradation than proteins, and therefore non-enveloped viruses tend to be more stable than enveloped viruses[225]. The stability or absence of the lipid bilayer likely protects EAV and PPV from inactivation by buffers at pH 4.
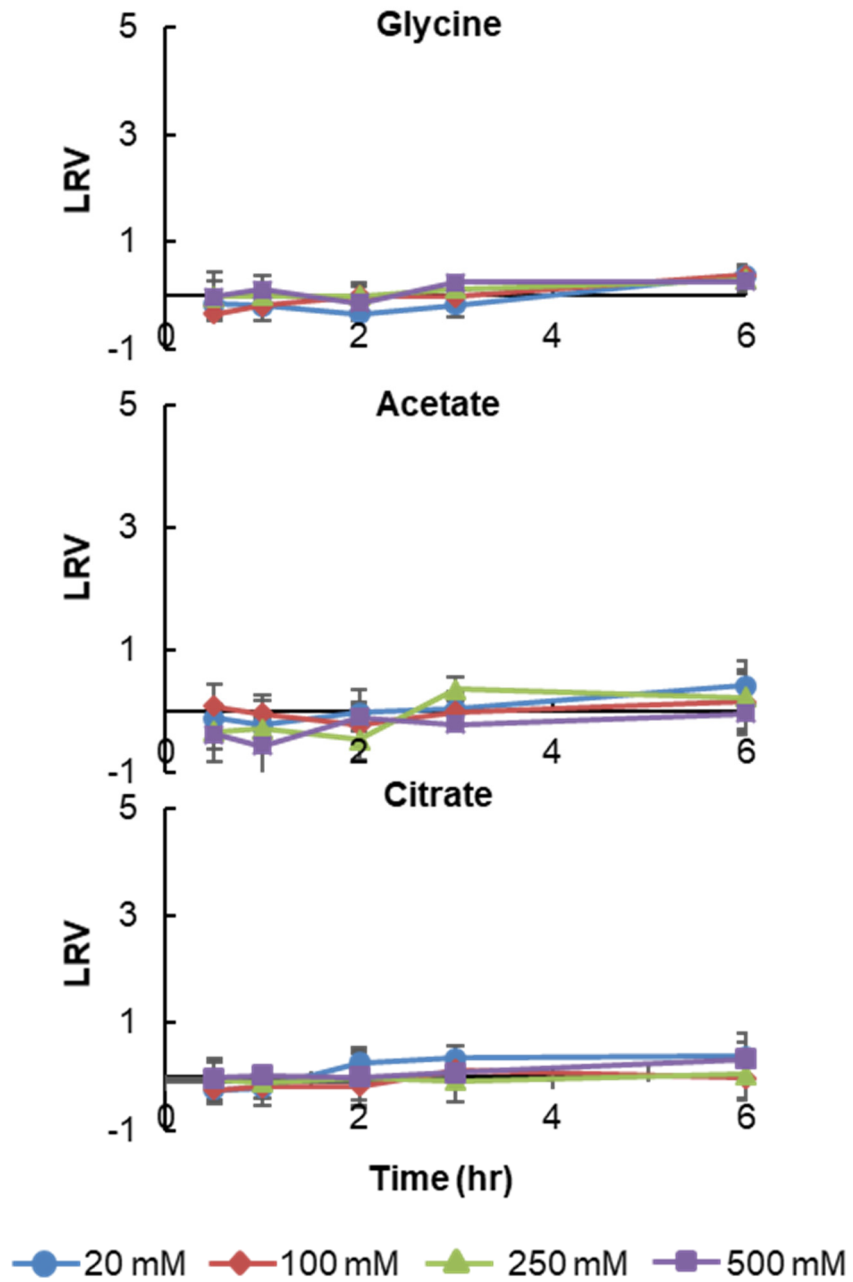
Figure 5-3. Inactivation of EAV by various concentrations of glycine, acetate, and citrate at pH 4. All buffers and concentrations did not inactivate EAV. Data points were measured in triplicates and error bars represent standard deviation.
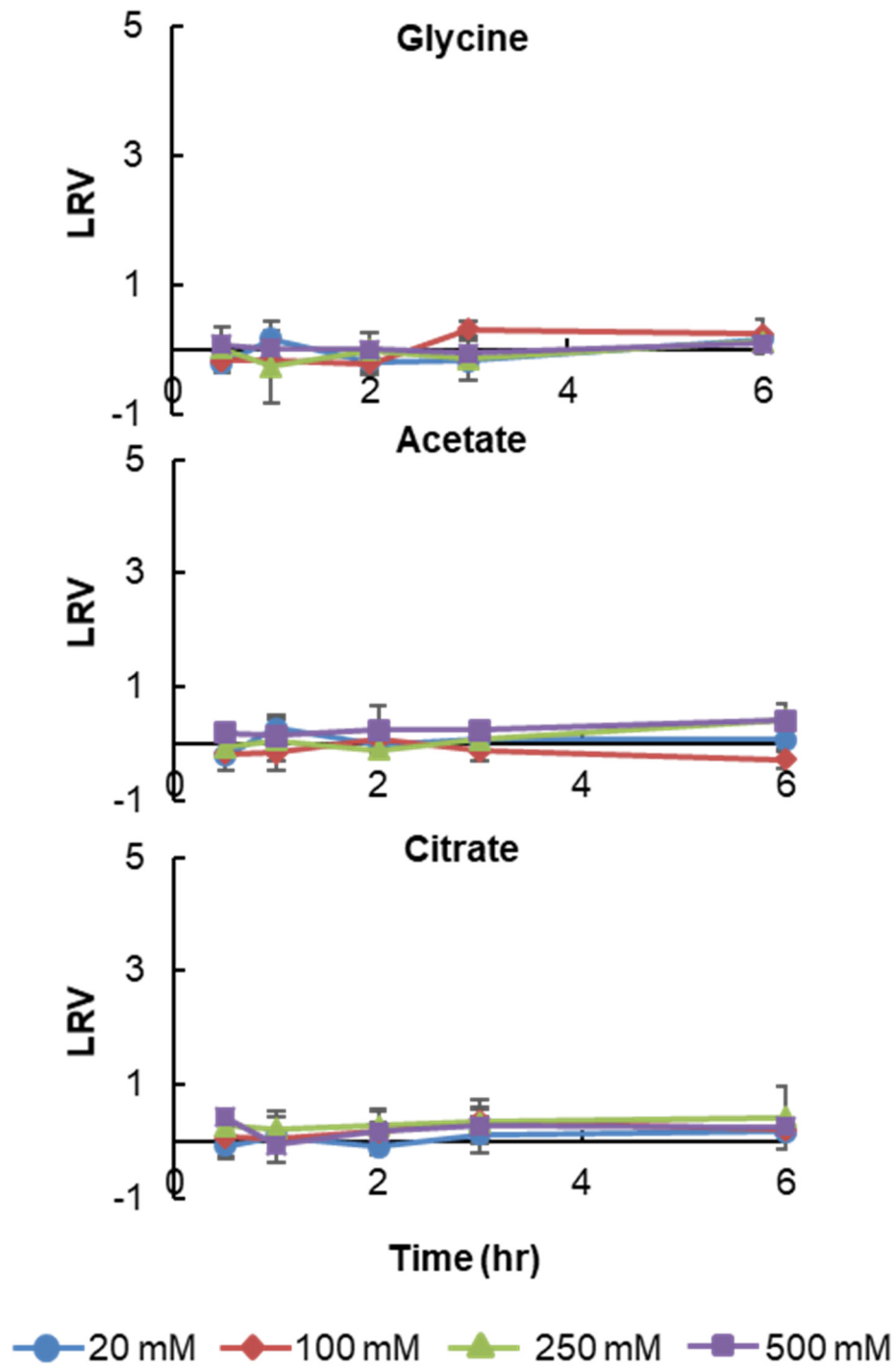
Figure 5-4. Inactivation of PPV by various concentrations of glycine, acetate, and citrate at pH 4. All buffers and concentrations did not inactivate PPV. Data points were measured in triplicates and error bars represent standard deviation.

5.3.3 Variables Influencing Inactivation at pH 4

Inactivation levels are dependent on the virus type, buffer type, and buffer concentration (**Fig. 1-4**). SuHV-1 was inactivated to the greatest extent, followed by HSV-1, and both EAV and PPV were negligibly inactivated under all buffer conditions. Negligible inactivation of EAV and PPV is likely explained by the absence or increased stability of the lipid bilayer. However, this does not explain the higher inactivation of SuHV-1 over HSV-1. For both SuHV-1 and HSV-1, citrate was the most effective and glycine was the least effective buffer in inactivation. Increasing buffer concentration either enhanced inactivation or had no effect on inactivation, but never decreased inactivation. The dependence for inactivation on virus type, buffer type, and buffer concentration provides insight into mechanisms of inactivation.

Inactivation effectiveness correlates to buffer and virus charges (**Table 1 & 2**). Citrate is the most negatively charged buffer at pH 4 with a dominant charge of -1. Acetate has a dominant charge of 0, however, partial charges of -1 exist since pH 4 is close to the pK$_a$ of 4.54. Glycine is the least negative at pH 4 with a dominant charge of 0. As a whole, higher negative buffer charges result in enhanced inactivation of SuHV-1 and HSV-1. In regards to virus charge, SuHV-1 has an isoelectric point (pI) of ~7.5[263], whereas HSV-1 has an isoelectric point of ~4.9[264] (**Table 1**). The higher pI of SuHV-1 leads to greater positive charges on the virus in comparison to HSV-1 at pH 4. The greater positive charge of SuHV-1 likely promotes electrostatic interactions of the negative charges of citrate or acetate to result in higher inactivation compared to HSV-1.

Negative buffer charges and positive virus charges appear to correlate to high inactivation, therefore, electrostatic interactions between the buffer and the virus likely

influence inactivation. It is reported that charges on buffers may weakly bind to viruses through electrostatic interactions to modify surface properties such as proteins[209,210,252,287]. At low or intermediate buffer concentrations (millimolar), binding may stabilize viral proteins by reducing unfavorable interactions[209,210,288]. Oppositely at high concentrations, binding appears to promote an increase in repulsive forces that destabilize viral proteins[287,288]. Brorson et al. demonstrated membrane and capsid structure changes of X-MLV with transmission electron microscopy images as a result of inactivation at pH 3.8 with acetate or citrate buffer[289]. Overall, buffers likely bind to the virus at high concentrations (typically molar levels) to destabilize viral proteins causing inactivation.

5.3.4 Conclusions

Low pH treatments are commonly used in biotherapeutic manufacturing to inactivate enveloped viruses[249]. There is a need for an enveloped virus inactivation at pH ≥ 4 to maintain the stability of biological products in solution. This study investigated the influence of time, buffer properties, and virus properties on the inactivation of four model viruses at pH 4.

Inactivation levels were dependent on time, virus-type, buffer-type, and buffer concentration. SuHV-1 reached full inactivation with acetate concentrations of ≥ 250 mM and citrate concentrations ≥ 100 mM after 30 min. Of the viruses tested, HSV-1 was inactivated to the next greatest extent where full inactivation occurred at citrate concentrations ≥ 250 mM after 1 hour. EAV and PPV were negligibly inactivated over all solution conditions, consisted with the literature, this is likely a result of the stabilized

lipid bilayer of EAV and no lipid bilayer of PPV. The increasing inactivation levels from glycine, to acetate, to citrate for SuHV-1 and HSV-1 correspond to the increasing negative charges on the buffer. Similarly, the greater inactivation of SuHV-1 over HSV-1 corresponds to the greater positive virus charge. Electrostatic interactions between the negatively charged buffers and positively charged viruses likely destabilize viral proteins to result in inactivation[209,210,252,287].

Inactivation of viruses at pH 4 is a function of virus and buffer properties. Viral structures, including a stabilized lipid bilayer, can resist inactivation at pH 4. Resistant viruses likely require harsher conditions for full inactivation. For viruses that are not resistant to pH 4 inactivation, enhancing electrostatic interactions between the buffer and the virus can increase inactivation levels.

6 Conclusions and Future Work

6.1 Conclusions

Infectious diseases considerably impact worldwide health[1]. For example, the 2019 novel coronavirus (SARS-CoV-2) sparked a global pandemic by causing a deadly respiratory disease[3]. The SARS-CoV-2 outbreak reminds us that even though society enacts practices to protect the public from infectious diseases[4], challenges in treatment and prevention remain. For this reason, continual improvements to health measures must be made to control infectious diseases. Wastewater treatment and viral clearance during pharmaceutical applications are examples of health measures that can be improved to prevent the spread of infectious diseases.

Chapter 2 investigated a low-cost, low-tech biosolids treatment method to improve the sustainability of wastewater treatment operations. Many WWTPs are looking to upgrade their biosolids treatment processes to Class A standards to open additional avenues for sustainable reuse. However, current options for upgrades to biosolids treatment typically require high-cost, high-tech processes that are not feasible for smaller WWTPs with limited resources. Therefore, there is a need for a low-cost, low-tech process that produces high-quality biosolids. During this study, a low-cost, low-tech treatment option for Class A biosolids was investigated through long-term storage in northern climates. The effects of freeze/thaw cycles, temperature, moisture, volatile solids, ammonia, and pH on pathogen inactivation were evaluated for one year. After one year of long-term storage at two northern WWTPs, fecal coliforms decreased to regulatory standards but *Ascaris* ova remained constant. Therefore, more than one year of

storage in northern climates is required for Class A biosolids treatment to affect proper helminth ova inactivation. Freeze/thaw cycles significantly reduced fecal coliform levels in all biosolids tested. Specifically, 16% TS produced the highest inactivation of fecal coliforms during freeze/thaw cycles. Ultimately, the results of this study provided information on minimum process parameters for low-cost, low-technology biosolids treatment.

Chapter 3 hypothesized the mechanisms for enveloped virus inactivation by arginine. Enveloped virus inactivation by arginine maintains protein stability, and therefore, is a desirable process in therapeutic protein manufacturing[8-16]. However, optimal conditions for full inactivation of all enveloped viruses by arginine are not known. Viruses containing stabilized membranes or stabilized proteins are not highly inactivated by arginine[17]. For this reason, arginine may be interacting with proteins or lipids to inactivate viruses. Three hypotheses were developed to explain the potential mechanisms of inactivation by arginine. Hypothesis 1 described inactivation by arginine through inhibition of protein function. Hypothesis 2 described inactivation by arginine as a result of viral membrane destabilization. Hypothesis 3 described inactivation by arginine through membrane pore formation. To reject a hypothesis, the effect of arginine on protein function or membrane stability needs to be determined. Understanding the mechanisms of arginine will provide insight into developing treatment methods that enhance
virus inactivation.

Chapter 4 examined the influence of viral and arginine properties on inactivation. Viral membrane structures largely affected inactivation by arginine. Viruses with stable

membranes (EAV and BVDV), resulting from small diameter membranes with tightly packed lipids, were negligibly inactivated by arginine. Viruses with less stable membranes (HSV-1 and SuHV-1), resulting from large diameter membranes with loosely packed lipids, were highly inactivated by arginine. Additionally, viruses that were sensitive to membrane cholesterol reduction were also inactivated to high levels by arginine. Overall, the mechanism of membrane deformation was supported by the influence of viral membrane properties on arginine inactivation. In regards to arginine structure, hydrophobicity and arginine-clustering increased inactivation of viruses resistant to arginine. An increasing virus size after arginine exposure was measured by DLS and TEM images, alluding to lipid expansion or arginine binding as the mechanism for inactivation. Overall, the data from this study supports lipid bilayer deformation as the mechanism of arginine inactivation and added hydrophobicity or arginine-clustering to enhance inactivation.

Chapter 5 investigated buffer type and concentration on the inactivation of several enveloped viruses at pH 4. Similar to arginine, viruses with highly stable membranes (EAV) or no membranes (PPV) were negligibly inactivated at pH 4. Full inactivation (~5 LRV) occurred for viruses with less stable membranes (SuHV-1 and HSV-1) at pH 4 under various buffer conditions. Citrate produced the highest inactivation, and glycine produced the lowest inactivation of SuHV-1 and HSV-1. Increasing electrostatic interactions between the virus and buffer enhanced inactivation. Conclusively, this study provided insight into the conditions (buffer type and time) for virus inactivation by buffers at pH 4 which preserves biopharmaceutical protein activity as opposed to lower pH treatments.

6.2 Future Work

Meaningful results for the improvement of pathogen inactivation in biosolids and pharmaceutical applications are presented in this dissertation. However, gaps in information remain that hinder the further development and widespread use of the pathogen inactivation processes studied. Future research into biosolids treatment, virus inactivation by arginine, and low pH virus inactivation by buffers are required to create well-established processes.

6.2.1 Biosolids Treatment

To develop a universal long-term storage Class A biosolids treatment, additional freeze-thaw and long-term storage studies are required. To start, studies to predict the influence of freeze-thaw conditions on pathogen inactivation are needed. Fecal coliform reduction in biosolids at two WWTPs after one freeze-thaw cycle with total solids contents varying from 5-28% was studied in Chapter 2. Since conditions can vary tremendously across plants, the influence of several variables on pathogen inactivation is required for an understanding of freeze-thaw cycles. Variables to adjust and analyze for pathogen inactivation would include 1) number of freeze-thaw cycles, 2) temperature gradient, and 3) biosolids origin. Furthermore, the effect of freeze/thaw cycles on pathogen inactivation for enteric viruses and *Ascaris* ova is needed for Class A requirements. After the data is collected, the impact of freeze-thaw conditions on pathogen inactivation could be analyzed through multivariate regression to model site-specific WWTP pathogen inactivation.

Further long-term storage field- and lab-scale studies are required to develop a universal low-cost, low-tech Class A biosolids treatment method. Chapter 2 demonstrated the influence of biosolids properties on pathogen inactivation during long-term storage at two WWTPs over one year. Key information was collected on the inactivation of fecal coliforms during winter storage; however, the data indicate that the specific treatment conditions did not minimum Class A treatment requirements. To determine the minimum conditions required for long-term storage at individual WWTPs, it is necessary to conduct field-scale studies across various climates at longer storage times. During the field-scale studies, biosolids properties (VS, TS, ammonia, temperature, VFA, and pathogen content) and environmental conditions (precipitation, humidity, temperature, UV, and wind) should be monitored to determine minimum storage times required to reach Class A standards under different climates and biosolids conditions. The field-scale study could be paired with a lab-scale study to strengthen the data. In the lab-scale study, variables to be altered and quantified for their influence on pathogen inactivation include 1) pH, 2) temperature, 3) ammonia content, 4) VS, 5) VFA, and 6) TS. The data could then be analyzed under multivariate regression to determine the significance of each variable on pathogen inactivation. Additionally, a model could be constructed to predict pathogen inactivation at WWTPs with known biosolids conditions.

6.2.2 Virus Inactivation by Arginine

Greater information on the mechanisms and optimization of enveloped virus inactivation by arginine is needed to create a safe and reliable viral clearance process for therapeutic protein manufacturing.

156

6.2.2.1 Arginine Mechanisms

In Chapter 3, mechanisms for enveloped virus inactivation by arginine were hypothesized including 1) inhibition of protein function, 2) deformation of the lipid bilayer, and 3) holes in the lipid bilayer. Overall, the data collected in Chapter 4 supported the mechanisms of lipid bilayer deformation. However, supplementary studies are necessary to assess and confirm all hypothesized mechanisms.

Experiments to assess protein function and structure before and after arginine exposure are required to evaluate hypothesis 1. Protein binding experiments with enzyme-linked immunosorbent assay (ELIZA), bio-layer interferometry technology (BLITz), or immunohistochemistry could elucidate protein changes after arginine exposure. ELIZA and BLITz work by immobilizing a specific host cell receptor to measure the binding capacity of an associated protein. For example, heparin is commonly used as a cell receptor for viruses, and differences in heparin-binding before and after arginine exposure could signify a disruption in protein function[247]. Immunohistochemistry uses the process of immunostaining to identify specific proteins (antigens) through the binding of antibodies. For example, antibodies that bind to HSV-1 proteins include polyclonal rabbit anti-HSV-1[290] and Monoclonal CHA 437 antibody[291]. Quantifying the protein-antibody binding before and after arginine exposure would elucidate protein changes. Sodium dodecyl sulfate-polyacrylamide gel electrophoresis (SDS PAGE) separates proteins by molecular weight and could illuminate general protein differences in the virus before and after arginine exposure. Though all these studies evaluate hypothesis 1, changes in protein binding or structure could also support

hypothesis 2, since lipid instability may alter the efficacy and function of membrane-bound proteins.

Nanoindentation experiments, such as atomic force microscopy (AFM), could measure changes in virus stiffness to evaluate hypotheses 2 and 3. If the virus stiffness decreases after arginine exposure, the lipid bilayer is being compromised either by lipid deformations or pores. If virus stiffness and protein structure or binding are being changed, then hypothesis 2 is most likely. To test hypothesis 3, the reduction in genetic material after arginine exposure could be measured by polymerase chain reaction (PCR). Holes in the lipid bilayer likely expose the inner virus to harsh outer conditions, degrading the genetic material. While our data supports hypothesis 2, future studies are required to assess all potential hypotheses for the mechanisms of viral inactivation by arginine.

6.2.2.2 Arginine Optimization

Added hydrophobicity and arginine clustering improved viral inactivation by arginine, however, full inactivation of all enveloped viruses was not reached. To determine the optimal conditions for full inactivation of all enveloped viruses by arginine, additional studies are required.

The influence of membrane cholesterol on HSV-1 and SuHV-1 infectivity was examined in Chapter 4. Cholesterol reduction increases membrane fluidity[238 203,206], which may aid in the destabilization of lipids by arginine. To evaluate the effects of membrane cholesterol reduction on inactivation by arginine, future studies are required. To begin the studies, membrane cholesterol would be reduced in several viruses (both

resistant and non-resistant to arginine inactivation) by MβCD. After cholesterol reduction, viruses would be exposed to arginine. LRV would be calculated from the titer before and after arginine exposure. A higher LRV compared to the arginine LRV without cholesterol reduction would signify that an increase in membrane fluidity enhances inactivation by arginine. If this is the case, other membrane disrupters could be used in combination with arginine to produce high inactivation. The membrane disruptor pyrenebutyrate (PYB) was tested at low levels of 10 mM in Chapter 4. PYB loosens lipid packing and increases membrane fluidity[234,239-241], similar to cholesterol reduction. Though PYB did enhance arginine inactivation, it did not fully inactivate viruses due to low solubility limits. Other hydrophobic molecules (isoleucine, valine, or leucine) or membrane disruptors (detergents) with higher solubility limits could be tested to enhance inactivation by arginine.

Testing higher concentrations or different conformations of arginine peptides may uncover conditions for full virus inactivation. Chapter 4 studied the effect of $CapA_6R$ (added hydrophobicity) and R_8 (added arginine clustering) peptides at 7.6 mM equivalent arginine concentration on the inactivation of viruses. Though these peptides inactivated viruses to higher levels than 7.6 mM arginine, the low concentrations were unable to fully inactivate any viruses. Higher concentrations of peptides likely improve inactivation levels. Additionally, different conformations of peptides could be tested. For example, a more hydrophobic amino acid (isoleucine, valine, or leucine) could be replaced for alanine in the tail of $CapA_6R$. Also, larger and smaller arginine peptides could be tested and compared to R_8. Literature shows there may be an ideal number of arginine molecules required to disrupt the lipid membrane[197]. While our results provided insight

into the mechanisms and optimization of inactivation by arginine, additional studies are required to more effectively use arginine.

6.2.3 Low pH Virus Inactivation by Buffers

Additional information is required to determine the effects of buffers on the inactivation of viruses at low pH. Chapter 5 established that viruses with stable membranes or no membrane were resistant to inactivation at pH 4. To determine minimum conditions to inactivate resistant viruses, lower pH values must be tested. For example, testing the inactivation of PPV and EAV with acetate, glycine, and citrate at 500 mM with decreasing pH values below 4 would determine minimum conditions for inactivation. For viruses with less stable membranes, enhancing the electrostatic interactions between the virus and the buffer improved inactivation, however, this was only studied with two viruses. For a greater statistical significance, additional viruses should be tested for inactivation at pH 4 by buffers with several charges. Viruses tested must be large enveloped viruses that are not resistant to inactivation at pH 4 such as Influenza or xenotropic murine leukemia virus. Largely, supplemental tests are required to decipher the minimum conditions for full inactivation of viruses with buffers at low pH.

This dissertation improved public health by determining mechanisms and optimal conditions for pathogen inactivation in wastewater treatment and pharmaceutical applications. While key insights into pathogen inactivation were found, continual research is required to protect public health against infectious diseases.

7 References

1. WHO. The Top Ten Causes of Death
    http://www.who.int/mediacentre/factsheets/fs310/en/. Published 2017. Updated
    January 2017. Accessed.

2. WHO. Infectious Diseases http://www.who.int/topics/infectious_diseases/en/.
    Published 2018. Accessed.

3. CDC. Coronavirus. https://www.cdc.gov/coronavirus/types.html. Published 2020.
    Accessed.

4. The Infectious Diseases Society of America. Infectious Disease
    http://www.idsociety.org. Published 2018. Accessed.

5. Metcalf E. Inc.(2003), Wastewater engineering treatment and reuse. In: McGraw-
    Hill, New York; 1819.

6. Dumont J, Euwart D, Mei B, Estes S, Kshirsagar R. Human cell lines for
    biopharmaceutical manufacturing: history, status, and future perspectives. *CRIT
    REV BIOTECHNOL.* 2016;36(6):1110-1122.

7. Englande A, Reimers R. Biosolids management-sustainable development status
    and future direction. *Water science and technology.* 2001;44(10):41-46.

8. Arakawa T, Yamasaki H, Ikeda K, Ejima D, Naito T, Koyama AH. Antiviral and
    virucidal activities of natural products. *CURR MED CHEM.* 2009;16(20):2485-
    2497.

9. Ikeda K, Yamasaki H, Suzuki Y, Koyama AH, Arakawa T. Novel strategy with
    acidic arginine solution for the treatment of influenza A virus infection. *EXP
    THER MED.* 2010;1(2):251-256.

10. Katsuyama Y, Yamasaki H, Tsujimoto K, Koyama AH, Ejima D, Arakawa T.
    Butyroyl-arginine as a potent virus inactivation agent. *INT J PHARM.*
    2008;361(1-2):92-98.

11. McCue JT, Selvitelli K, Cecchini D, Brown R. Enveloped virus inactivation using
    neutral arginine solutions and applications in therapeutic protein purification
    processes. *BIOTECHNOL PROG.* 2014;30(1):108-112.

12. Naito. Antiviral effect of arginine against herpes simplex virus type 1. *INT J MOL
    MED.* 2009;23(4).

13. Ohtake S, Arakawa T, Koyama AH. Arginine as a Synergistic Virucidal Agent.
    MOLECULES 2010;15(3):1408-1424.

14. Tsujimoto K, Uozaki M, Ikeda K, et al. Solvent-induced virus inactivation by acidic arginine solution. *INT J MOL MED.* 2010;25(3):433-437.

15. Yamasaki H, Tsujimoto K, Koyama AH, Ejima D, Arakawa T. Arginine facilitates inactivation of enveloped viruses. *J PHARM SCI* 2008;97(8):3067-3073.

16. Utsunomiya H, Ichinose M, Tsujimoto K, et al. Co-operative thermal inactivation of herpes simplex virus and influenza virus by arginine and NaCl. *INT J PHARM* 2009;366(1-2):99-102.

17. Meingast C, Heldt CL. Arginine Enveloped Virus Inactivation and Potential Mechanisms. *BIOTECHNOL PROG* 2019.

18. Metcalf E, Eddy R. Wastewater Engineering: Treatment and Reuse, Tata McGraw. In: Hill Publishing Company Ltd, New Delhi; 2003.

19. EPA. Plain English Guide to the EPA Part 503 Biosolids Rule 1994.

20. Boller M. Small wastewater treatment plants—a challenge to wastewater engineers. *WATER SCI TECHNOL.* 1997;35(6):1-12.

21. Sparn B, Hunsberger R. *Opportunities and challenges for water and wastewater industries to provide exchangeable services.* National Renewable Energy Lab.(NREL), Golden, CO (United States);2015.

22. Water C. Running Costs of Wastewater Treatment Plants http://costwater.com/runningcostwater.htm. Published 2017. Accessed.

23. Chellappan S. *Behaviour of viruses in biosolids*: Applied Science, RMIT University 2013.

24. Schwarz KR. *The Fate of Human Enteric Pathogens Following the Land Application of Biosolids in Agriculture* Curtin Univeresity of Technology 2012.

25. Farrell JB, Merrill D, Schafer P. *Producing Class A Biosolids With Low-Cost, Low-Technology Treatment Processes.* IWA Publishing; 2004.

26. S. X. McHaney ER, A Babatola D. Ihrke Cost-Effective Biosolids Dewatering and Pathogen REduction by Solar Drying at the San Jose/Santa Clara Water Pollution Control Plant. . Paper presented at: Management of Water and Wastewater Solids for the 21st Centuring: A GLobal Perspective June 19-22, 1994; Washington D.C

27. Tata P, Lue-Hing C, Bertucci JJ, Sedita SJ, Knafl GJ. Class A biosolids production by a low-cost conventional technology. *WATER ENVIRON RES.* 2000;72(4):413-422.

28. Amani T, Nosrati M, Sreekrishnan T. Anaerobic digestion from the viewpoint of microbiological, chemical, and operational aspects—a review. *ENVIRON REVIEWS.* 2010;18(NA):255-278.

29. Cramer W, Burge W, Kawata K. Kinetics of virus inactivation by ammonia. *APPL ENVIRON MICROB.* 1983;45(3):760-765.

30. Ward R. Mechanism of poliovirus inactivation by ammonia. *J VIROL.* 1978;26(2):299-305.

31. Ward RL, Ashley CS. Identification of the virucidal agent in wastewater sludge. *APPL ENVIRON MICROB.* 1977;33(4):860-864.

32. Fidjeland J, Nordin A, Vinneras B. Inactivation of Ascaris eggs and Salmonella spp. in fecal sludge by treatment with urea and ammonia solution. *J WATER SANIT HYG DE.* 2016;6(3):465-473.

33. Allievi L, Colombi A, Calcaterra E, Ferrari A. Inactivation of fecal bacteria in sewage sludge by alkaline treatment. *BIORESOURCE TECHNOL* 1994;49(1):25-30.

34. Reimers R, Little M, Englande A, McDonell D, Bowman D, Hughes J. Investigation of parasites in sludges and disinfection techniques. In: *Investigation of parasites in sludges and disinfection techniques.* EPA. Health Effects Research Laboratory; 1986.

35. Ghiglietti R, Rossi P, Ramsan M, Colombi A. Viability of Ascaris suum, Ascaris lumbricoides and Trichuris muris eggs to alkaline pH and different temperatures. *PARASSITOLOGIA.* 1995;37(2-3):229-232.

36. Fenlon D, Ogden I, Vinten A, Svoboda I. The fate of Escherichia coli and E. coli O157 in cattle slurry after application to land. *J APPL MICROBIO.* 2000;88(S1).

37. O'SHAUGHNESSY SA, Kim M-Y, Choi CY. Mathematical model to predict pathogen die-off in biosolids. *J RESIDUALS SCI TECH.* 2008;5(2).

38. Öğleni N, Özdemir S. Pathogen reduction effects of solar drying and soil application in sewage sludge. *TURK J AGRIC FOR.* 2010;34(6):509-515.

39. Rouch DA, Mondal T, Pai S, et al. Microbial safety of air-dried and rewetted biosolids. *J WATER HEALTH.* 2011;9(2):403-414.

40. Shanahan EF, Roiko A, Tindale NW, Thomas MP, Walpole R, Kurtböke Dİ. Evaluation of pathogen removal in a solar sludge drying facility using microbial indicators. *INT J ENVIRON RES PU.* 2010;7(2):565-582.

41. Zaleski KJ, Josephson KL, Gerba CP, Pepper IL. Potential regrowth and recolonization of salmonellae and indicators in biosolids and biosolid-amended soil. *APPL ENVIRON MICROB.* 2005;71(7):3701-3708.

42. Lang N, Smith S. Influence of soil type, moisture content and biosolids application on the fate of Escherichia coli in agricultural soil under controlled laboratory conditions. *J APPL MICROBIO.* 2007;103(6):2122-2131.

43. McMahon KD, Stroot PG, Mackie RI, Raskin L. Anaerobic codigestion of municipal solid waste and biosolids under various mixing conditions—II: microbial population dynamics. *WATER RES* 2001;35(7):1817-1827.

44. Brody T. *Nutritional Biochemistry* Academic Press 1999.

45. Abdul P, Lloyd D. Pathogen survival during anaerobic digestion: Fatty acids inhibit anaerobic growth ofEscherichia coli. *BIOTECH LETTERS.* 1985;7(2):125-128.

46. Kunte D, Yeole T, Ranade D. Effect of volatile fatty acids on Shigella dysenteriae during anaerobic digestion of human night soil. *WORLD J MICROB BIOT.* 2000;16(6):519-522.

47. Kunte D, Yeole T, Ranade D. Two-stage anaerobic digestion process for complete inactivation of enteric bacterial pathogens in human night soil. *WATER SCI TECHNOL.* 2004;50(6):103-108.

48. Liu P, Chernyshov A, Najdi T, et al. Membrane stress caused by octanoic acid in Saccharomyces cerevisiae. *APPL MICROBIO BIOTECH.* 2013;97(7):3239-3251.

49. Royce LA, Liu P, Stebbins MJ, Hanson BC, Jarboe LR. The damaging effects of short chain fatty acids on Escherichia coli membranes. *APPL MICROBIO BIOTECH.* 2013;97(18):8317-8327.

50. Salsali H, Parker W, Sattar S. Impact of concentration, temperature, and pH on inactivation of Salmonella spp. by volatile fatty acids in anaerobic digestion. *CAN J MICROBIOL.* 2006;52(4):279-286.

51. Skrivanova E, Marounek M, Benda V, Brezina P. Susceptibility of Escherichia coli, Salmonella sp. and Clostridium perfringens to organic acids and monolaurin. *VETERINARNI MEDICINA-PRAHA-.* 2006;51(3):81.

52. Kunte D, Yeole T, Chiplonkar S, Ranade D. Inactivation of Salmonella typhi by high levels of volatile fatty acids during anaerobic digestion. *J APPL MICROBIO.* 1998;84(1):138-142.

53. Tenuta M, Conn KL, Lazarovits G. Volatile fatty acids in liquid swine manure can kill microsclerotia of Verticillium dahliae. *PHYTOPHATOLOGY.* 2002;92(5):548-552.

54. Harroff LA, Liotta JL, Bowman DD, Angenent LT. Inactivation of Ascaris Eggs in Human Fecal Material Through In Situ Production of Carboxylic Acids. *ENVIRON SCI TECHNOL* 2017;51(17):9729-9738.

55. Rojas-Oropeza M, Hernández-Uresti AS, Ortega-Charleston LS, Cabirol N. Effect of volatile fatty acids in anaerobic conditions on viability of helminth ova (Ascaris suum) in sanitization of municipal sludge. *ENVIRON TECHNOL.* 2017;38(17):2202-2208.

56. Nakasaki K, Shoda M, Kubota H. Effect of temperature on composting of sewage sludge. *APPL ENVIRON MICROB.* 1985;50(6):1526-1530.

57. Lang NL, Smith SR. Time and temperature inactivation kinetics of enteric bacteria relevant to sewage sludge treatment processes for agricultural use. *WATER RES* 2008;42(8):2229-2241.

58. Ahmed AU, Sorensen DL. Kinetics of pathogen destruction during storage of dewatered biosolids. *WATER ENVIRON RES.* 1995;67(2):143-150.

59. Reimers RS, Bowman DD, Schafer PL, Tata P, Leftwich B, Atique MM. Factors affecting lagoon storage disinfection of biosolids. *PROCED WTR ENVIRON ASSOC.* 2001;2001(1):1218-1235.

60. Farrah S, Bitton G, Hoffmann E, et al. Survival of enteroviruses and coliform bacteria in a sludge lagoon. *APPL ENVIRON MICROB.* 1981;41(2):459-465.

61. O'Connor NA, Surapaneni A, Smith D, Stevens D. Occurrence and fate of Ascaris lumbricoides ova in biosolids in Victoria, Australia: a human health risk assessment of biosolids storage periods. *WATER SCI TECHNOL.* 2017:wst2017222.

62. O'Donnell CJ, Meyer KB, Jones JV, et al. Survival of parasite eggs upon storage in sludge. *APPL ENVIRON MICROB.* 1984;48(3):618-625.

63. Veerannan KM. Some Experimental Evidence on the Viability of Ascaris Lumbricoides Ova *Science* 1977;46(11):386-387.

64. Irwin R, Surapaneni A, Smith D, Schmidt J, Rigby H, Smith S. Verification of an alternative sludge treatment process for pathogen reduction at two wastewater treatment plants in Victoria, Australia. *J WATER HEALTH.* 2017:wh2017316.

65. Pempkowiak J, Obarska-Pempkowiak H. Long-term changes in sewage sludge stored in a reed bed. *SCI TOTAL ENVIRON.* 2002;297(1):59-65.

66. Kinsley C, Kennedy K, Crolla A. A combined reed bed/freezing bed technology for septage treatment and reuse in cold climate regions. *WATER SCI TECHNOL.* 2017:wst2017189.

67. Lai CK, Chen GH, Lo MC. Salinity effect on freeze/thaw conditioning of activated sludge with and without chemical addition. *SEP PURIF TECHNOL.* 2004;34(1-3):155-164.

68. Tao T, Peng XF, Lee DJ. Interaction between ice and floc under freezing. *J CHIN INST CHEM ENG.* 2006;37(3):299-304.

69. Tao T, Peng XF, Lee DJ. Interaction between wastewater-sludge floc and moving ice front. *CHEM ENG SCI.* 2006;61(16):5369-5376.

70. Diak J, Örmeci B. Individual and combined effects of freeze-thaw and ferrate (VI) oxidation for the treatment and dewatering of wastewater sludges. *WATER AIR SOIL POLL.* 2016;227(9):331.

71. Gao W, Smith DW, Li Y. Effects of freezing on the survival of *Escherichia coli* and Bacillus and response to UV and chlorine after freezing. *WAT ENVIRON RES.* 2007;79(5):507-513.

72. Gao W, Leung K, Hawdon N. Freezing Inactivation of *Escherichia coli* and *Enterococcus faecalis* in water: Response of different strains. *WAT ENVIRON RES.* 2009;81(8):824−830.

73. Gao W, Smith DW, Li Y. Natural freezing as a wastewater treatment method: *E. coli* inactivation capacity. *WAT RES.* 2006;40(12):2321−2326.

74. Gunnarsdóttir R, Müller K, Jensen PE, Jenssen PD, Villumsen A. Effect of long-term freezing and freeze-thaw cycles on indigenous and inoculated microorganisms in dewatered blackwater. *ENVIRON SCI TECHNOL.* 2012;46:12408-12416.

75. Torrella F, Lopez JP, Banks CJ. Survival of indicators of bacterial and viral contamination in wastewater subjected to low temperatures and freezing: application to cold climate waste stabilisation ponds. *WATER SCI TECHNOL.* 2003:105-112.

76. Chu CP, Feng WC, Chang B, Chou CH, Lee DJ. Reduction of microbial density level in wastewater activated sludge via freezing and thawing. *WATER RES.* 1999;33(16):3552-3555.

77. Sanin FD, Vesilind PA, Martel CJ. Pathogen reduction capabilities of freeze/thaw sludge conditioning. *WATER RES.* 1994;28(11):2393-2398.

78. Diak J, Ormeci B, Proux C. Freeze-thaw treatment of RBC sludge from a remote mining exploration facility in subarctic Canada. *WATER SCI TECHNOL.* 2011;63(6):1309-1313.

79. Mazur P. Freezing of living cells: Mechanisms and implications. *AM J PHYSIOL.* 1984;16(2):125-142.

80. Mazur P, ed *Physical and chemical basis of injury in single-celled microorganisms subjected to freezing and thawing.* New York: Academic Press; 1966. Meryman HT, ed. Cryobiology.

81. Agency USEP. Method 1684 Total, Fixed, and Volatile Solids in Water, Solids, and Biosolids. In: Technology OoWaSa, ed. Washington, DC2001.

82. Agency USEP. Method 1681: Fecal Coliforms in Sewage Sludge (Biosolids) by Multiple-Tube Fermentation using A-1 medium In: Water Oo, ed. Vol EPA-81-R-06-013. Washington, DC2006.

83. Vitton S, Muszynski M. Strength and Creep Properties of a Frozen Coastal Sand in Saltwater. In: *Mechanical Properties of Frozen Soil.* ASTM International; 2013.

84. Düppenbecker B, Maya C, Kneidl S, et al. Removal of helminth eggs by surface filtration. Paper presented at: 9th International Conference on Water Reuse2013.

85. Wetz K, Zeichhardt H, Willingmann P, Habermehl K-O. Dense particles and slow sedimenting particles produced by ultraviolet irradiation of poliovirus. *J GEN VIROL.* 1983;64(6):1263-1275.

86. Gould J, Rossano M, Lawrence L, Burk S, Ennis R, Lyons E. The effects of windrow composting on the viability of Parascaris equorum eggs. *VETERINARY PARASITOLOGY.* 2013;191(1):73-80.

87. Sidhu J, Toze S. Assessment of pathogen survival potential during managed aquifer recharge with diffusion chambers. *J APPL MICROBIO.* 2012;113(3):693-700.

88. Agency USEP. POTW Sludge Sampling And Analysis Guidance Document. In: Water Oo, ed. Washington, DC1989.

89.   EPA. Method 1684: Total, FIxed, and Volatile Solids in Water, Solids and Biosolids In: U. S. Environmental Protection Agency OoW, ed. Washington, D.C.2001.

90.   EPA. SW-846 Method 9045D: Soil and Waste pH, part of Test Methods for Analyzing Solid Waste, Physical/Chemical Methods. In. Washington, D.C.2004

91.   Anderson G, Yang G. Determination of bicarbonate and total volatile acid concentration in anaerobic digesters using a simple titration. *Water Environment Research.* 1992;64(1):53-59.

92.   Agency USEP. Method 350.1 Determination of Ammonia Nitrogen By Semi-Authomated Colorimetry. In: Development OoRa, ed. Cincinnati, Ohio1993.

93.   EPA. Method 1680: Fecal Coliforms in Sewage Sludge (Biosolids) by Multiple-Tube Fermentation using Lauryl Tryptose Broth (LTB) and EC Medium In. Washington, D.C.2010.

94.   ASTM. Standard Practice for Recovery of Viruses from Wastewater Sludges (ASTM D4994-89). In:2014.

95.   EPA U. Environmental regulations and technology: Control of pathogens and vector attraction in sewage sludge. In: Office of Research and Development Washington, DC; 1992.

96.   Berg G, Safferman RS, Dahling DR, Berman D, Hurst CJ. USEPA manual of methods for virology. In: *USEPA manual of methods for virology.* EPA; 1984.

97.   Bowman DD, Little MD, Reimers RS. Precision and accuracy of an assay for detecting Ascaris eggs in various biosolid matrices. *WATER RES.* 2003;37(9):2063-2072.

98.   EPA. Method 1602: Male-specific (F+) and Somatic Coliphage in Water by Single Agar Layer (SAL) Procedure. In. U.S. Environmental Protection Agency, Office of Water, Washington, D.C2001.

99.   Underground W. Historical Weather. TWC Product and Technology. https://www.wunderground.com/history. Published 2013-2014. Accessed.

100.   Hu K, Jiang J-Q, Zhao Q-L, Lee D-J, Wang K, Qiu W. Conditioning of wastewater sludge using freezing and thawing: role of curing. *WATER RES.* 2011;45(18):5969-5976.

101.   Aanderud ZT, Vert JC, Lennon JT, Magnusson TW, Breakwell DP, Harker AR. Bacterial dormancy is more prevalent in freshwater than hypersaline lakes. *FRONT MICROBIOL.* 2016;7.

102.   Jefferies RL, Walker NA, Edwards KA, Dainty J. Is the decline of soil microbial biomass in late winter coupled to changes in the physical state of cold soils? *SOIL BIO BIOCHEM.* 2010;42(2):129-135.

103.   Deal PH. Freeze-thaw behavior of a moderately halophilic bacterium as a function of salt concentration. *CRYOBIOLOGY* 1970;7(2):107-112.

104.   Lagasse HA, Alexaki A, Simhadri VL, et al. Recent advances in (therapeutic protein) drug development. *F1000RES.* 2017;6:113.

105.   Pohlscheidt M, Kiss R, Gottschalk U. An Introduction to Recent Trends in the Biotechnology Industry: Development and Manufacturing of Recombinant Antibodies and Proteins. *ADV BIOCHEM ENG BIOTECHNOL.* 2018.

106.   Caricati C, Oliveira-Nascimento L, Yoshida J, Stephano M, Caricati A, Raw I. Safety of snake antivenom immunoglobulins: efficacy of viral inactivation in a complete downstream process. *BIOTECHNOL PROG* 2013;29(4):972-979.

107.   Marichal-Gallardo P, Alvarez M. State-of-the-art in downstream processing of monoclonal antibodies: Process trends in design and validation. *BIOTECHNOL PROG* 2012;28(4):899-916.

108.   Johnson SA, Brown MR, Lute SC, Brorson KA. Adapting viral safety assurance strategies to continuous processing of biological products. *BIOTECHNOL BIOENG.* 2017;114(1):21-32.

109.   Morenweiser R. Downstream Processing of Viral Vectors and Vaccines. *Gene Therapy.* 2005:S103-S110.

110.   Nfor BK, Ahamed T, van Dedem GWK, et al. Design strategies for integrated protein purification processes: challenges, progress and outlook. *J CHEM TECHNOL BIOT.* 2008;83(2):124-132.

111.   Zydney AL. Membrane technology for purification of therapeutic proteins. *BIOTECHNOL BIOENG.* 2009;103(2):227-230.

112.   Mattila J, Clark M, Liu S. Retrospective Evaluation of Low-pH Viral Inactivation and Viral Filtration Ddata from a Multiple Company Collabotration *PDA J PHARM SCI TECHNOL* 2016.

113.   Roberts PL. Virus inactivation by solvent/detergent treatment using Triton X-100 in a high purity factor VIII. *BIOLOGICALS* 2008;36(5):330-335.

114.   Huangfu C, Zhang J, Ma Y, et al. Large-scale purification of high purity α1-antitrypsin from Cohn Fraction IV with virus inactivation by solvent/detergent and dry-heat treatment. *BIOTECHNOL APPL BIOC.* 2018;65(3):446-454.

115. Martsev SP, Kravchuk ZI, Vlasov AP, Lyakhnovich GV. Thermodynamic and functional characterization of a stable IgG conformer obtained by renaturation from a partially structured low pH-induced state. *FEBS Lett.* 1995;361(2-3):173-175.

116. Privé GG. Detergents for the stabilization and crystallization of membrane proteins. *METHODS* 2007;41(4):388-397.

117. Song H, Li J, Shi S, Yan L, Zhuang H, Li K. Thermal stability and inactivation of hepatitis C virus grown in cell culture. *VIROLOGY JOURNAL* 2010;7(1):40.

118. Schlegel A, Immelmann A, Kempf C. Virus inactivation of plasma-derived proteins by pasteurization in the presence of guanidine hydrochloride. *TRANSFUSION* 2001;41(3):382-389.

119. Croci L, De Medici D, Di Pasquale S, Toti L. Resistance of hepatitis A virus in mussels subjected to different domestic cookings. *INT J FOOD MICROBIOL.* 2005;105(2):139-144.

120. Russell W, Valentine RC, Pereira H. The effect of heat on the anatomy of the adenovirus. *J GEN VIROL.* 1967;1(4):509-522.

121. Bozkurt H, D'Souza DH, Davidson PM. Thermal Inactivation of Foodborne Enteric Viruses and Their Viral Surrogates in Foods. *J Food Prot.* 2015;78(8):1597-1617.

122. Hirneisen KA, Black EP, Cascarino JL, Fino VR, Hoover DG, Kniel KE. Viral Inactivation in Foods: A Review of Traditional and Novel Food-Processing Technologies. *COMPR REV FOOD SCI F.* 2010;9(1):3-20.

123. Armstrong CT, Mason PE, Anderson JR, Dempsey CE. Arginine side chain interactions and the role of arginine as a gating charge carrier in voltage sensitive ion channels. *Sci Rep.* 2016;6:21759.

124. Hristova K, Wimley WC. A Look at Arginine in Membranes. *J MOL BIOL.* 2011;239(1-2):49-56.

125. Jay A Glasel MPD. *Introduction to Biophysical Methods for Protein and Nucleic Acid Reserach* 1995.

126. Fitch CA, Platzer G, Okon M, Garcia-Moreno BE, McIntosh LP. Arginine: Its pKa value revisited. *Protein Sci.* 2015;24(5):752-761.

127. Arakawa T, Ejima D, Tsumoto K, et al. Suppression of protein interactions by arginine: a proposed mechanism of the arginine effects. *BIOPHYS CHEM.* 2007;127(1-2):1-8.

128. Kheddo P, Golovanov AP, Mellody KT, Uddin S, van der Walle CF, Dearman RJ. The effects of arginine glutamate, a promising excipient for protein formulation, on cell viability: Comparisons with NaCl. *TOXICOL VITRO.* 2016;33:88-98.

129. Arakawa T, Tsumoto K. The effects of arginine on refolding of aggregated proteins: not facilitate refolding, but suppress aggregation. *BIOCHEM BIOPH RES CO.* 2003;304(1):148-152.

130. Allolio C, Magarkar A, Jurkiewicz P, et al. Arginine-rich cell-penetrating peptides induce membrane multilamellarity and subsequently enter via formation of a fusion pore. *PNAS.* 2018;115(47):11923-11928.

131. Li SY, Zheng YD, Xu P, Zhu XX, Zhou CL. L-Lysine and L-arginine inhibit myosin aggregation and interact with acidic amino acid residues of myosin: The role in increasing myosin solubility. *FOOD CHEM* 2018;242:22-28.

132. Maity H, Karkaria C, Davagnino J. Effects of pH and Arginine on the Solubility and Stability of a Therapeutic Protein (Fibroblast Growth Factor 20): Relationship between Solubility and Stability. *CURR PHARM BIOTECHNO.* 2009;10(6):609-625.

133. Yoshizawa S, Arakawa T, Shiraki K. Effect of counter ions of arginine as an additive for the solubilization of protein and aromatic compounds. *INT J BIOL MACROMOL.* 2016;91:471-476.

134. Hirano A, Arakawa T, Kameda T. Effects of arginine on multimodal anion exchange chromatography. *PROTEIN EXPR PURIF.* 2015;116:105-112.

135. Arakawa T, Kita Y. Multi-Faceted Arginine: Mechanism of the Effects of Arginine on Protein. *CURR PROTEIN PEPT SC.* 2014;15(6):608-620.

136. Tsai B. Penetration of nonenveloped viruses into the cytoplasm. *ANNU REV CELL DEV BIOL.* 2007;23:23-43.

137. Lenard J. Virus envelopes and plasma membranes. *ANNU REV BIOPHYS BIO.* 1978;7(1):139-165.

138. Chazal N, Gerlier DJM, reviews mb. Virus entry, assembly, budding, and membrane rafts. *MICROBIOL MOL BIOL REV* 2003;67(2):226-237.

139. Hiller G, Weber K. Golgi-derived membranes that contain an acylated viral polypeptide are used for vaccinia virus envelopment. *J VIROL.* 1985;55(3):651-659.

140. Risco C, Rodríguez JR, López-Iglesias C, Carrascosa JL, Esteban M, Rodríguez DJJov. Endoplasmic reticulum-Golgi intermediate compartment membranes and vimentin filaments participate in vaccinia virus assembly. *J VIROL.* 2002;76(4):1839-1855.

141. Weissenhorn W, Dessen A, Calder L, Harrison S, Skehel J, Wiley D. Structural basis for membrane fusion by enveloped viruses. *MOL MEMBR BIOL.* 1999;16(1):3-9.

142. Kempf C, Stucki M, Boschetti NJB. Pathogen inactivation and removal procedures used in the production of intravenous immunoglobulins. *BIOLOGICALS.* 2007;35(1):35-42.

143. Klamroth R, Gröner A, Simon TLJT. Pathogen inactivation and removal methods for plasma-derived clotting factor concentrates. *TRANSFUSION.* 2014;54(5):1406-1417.

144. Arakawa T, Timasheff SNJB. Stabilization of protein structure by sugars. *BIOCHEMISTRY* 1982;21(25):6536-6544.

145. Cai K, Gierman TM, Hotta J, et al. Ensuring the biologic safety of plasma-derived therapeutic proteins: detection, inactivation, and removal of pathogens. *BIODRUGS* 2005;19(2):79-97.

146. Food U, Administration D. Points to consider in the manufacture and testing of monoclonal antibody products for human use. 1997.

147. Calabrese EJ. Safe Drinking Water Act. In: CRC Press; 1989.

148. Pollard EC. Theory of the physical means of the inactivation of viruses. *ANN NY ACAD SCI.* 1960;83(1):654-660.

149. O'Brien R, Newman J. Structural and compositional changes associated with chlorine inactivation of polioviruses. *APPL ENVIRON MICROB.* 1979;38(6):1034-1039.

150. Brie A, Razafimahefa R, Loutreul J, et al. The Effect of Heat and Free Chlorine Treatments on the Surface Properties of Murine Norovirus. *FOOD ENVIRON VIROL.* 2017;9(2):149-158.

151. Cosmo G. Mackenzie JBM, Paul Beck The Effect of pH on growth, protein synthesis, and lipid-rich particles of cultured mammalian cells. *J BIOPHYS BIOCHEM CYTOLOGY.* 1961:141-156.

152. Kristian Spilling AB, Dagmar Enss, Heiko Rischer The effect of high pH on structural lipids in diatoms. *J APPL PHYCOL.* 2013;25(5):1435-1439.

153.   Misiewicz J, Afonin S, Ulrich AS. Control and role of pH in peptide–lipid interactions in oriented membrane samples. *BBA BIOMEMBRANES.* 2015;1848(3):833-841.

154.   Li R, Wu Z, Wangb Y, Ding L, Wang Y. Role of pH-induced structural change in protein aggregation in foam fractionation of bovine serum albumin. *BIOTECHOL REPORTS.* 2016;9(Supplement C):46-52.

155.   Stegmann T, Booy FP, Wilschut J. Effects of Low PH on Influenza-Virus - Activation and Inactivation of the Membrane Fusion-Capacity of the Hemagglutinin. *J BIOL CHEM.* 1987;262(36):17744-17749.

156.   Waarts BL, Smit JM, Aneke OJ, et al. Reversible acid-induced inactivation of the membrane fusion protein of Semliki Forest virus. *J VIROL.* 2005;79(12):7942-7948.

157.   Weed DJ, Pritchard SM, Gonzalez F, Aguilar HC, Nicola AV. Mildly Acidic pH Triggers an Irreversible Conformational Change in the Fusion Domain of Herpes Simplex Virus 1 Glycoprotein B and Inactivation of Viral Entry. *J VIROL.* 2017;91(5):12.

158.   Miguel L.F. Ruano JP-G. Effect of Acidic pH on the Structure and Lipid Binding Properties of Porcin Sufactant Protein A. *J BIOl CHEM* 1998.

159.   Yang A-S, Honig B. Structural Origins of pH and Ionic Strength Effects on Protein Stability: Acid Denaturation of Sperm Whale Apomyoglobin. *J MOL BIOL* 1994;237(5):602-614.

160.   Jain R, Kumar R, Kumar S, Chhabra R, Agarwal MC, Kumar R. Analysis of the pH-dependent stability and millisecond folding kinetics of horse cytochrome c. *ARCH BIOCHEM BIOPHYS.* 2015;585:52-63.

161.   Dumetz AC, Chockla AM, Kaler EW, Lenhoff AM. Effects of pH on protein-protein interactions and implications for protein phase behavior. *BBA PROTEINS PROTEOMICS.* 2008;1784(4):600-610.

162.   Sahin E, Grillo AO, Perkins MD, Roberts CJ. Comparative Effects of pH and Ionic Strength on Protein-Protein Interactions, Unfolding, and Aggregation for IgG1 Antibodies. *J PHARM SCI.* 2010;99(12):4830-4848.

163.   Eva Y. Chi Sk, Theodore W. Randolph, John F. Carpenter Physical Stability of Proteins in Aqueous Solution: Mechanism and Driving Forces in Nonnative Protein Aggregation. *PHARM RESEARCH.* 2003;20(9):1325-1336.

164. Brorson K, Krejci S, Lee K, et al. Bracketed generic inactivation of rodent retroviruses by low pH treatment for monoclonal antibodies and recombinant proteins. *BIOTECHNOL BIOENG* 2003;82(3):321-329.

165. Tsumoto K, Umetsu M, Kumagai I, Ejima D, Philo JS, Arakawa TJBp. Role of arginine in protein refolding, solubilization, and purification. *BIOTECHNOL PROGR*. 2004;20(5):1301-1308.

166. Kim NA, Hada S, Thapa R, Jeong SH. Arginine as a protein stabilizer and destabilizer in liquid formulations. *INT J PHARM*. 2016;513(1-2):26-37.

167. Miyatake T, Yoshizawa S, Arakawa T, Shiraki K. Charge state of arginine as an additive on heat-induced protein aggregation. *INT J BIOL MACROMOL* 2016;87:563-569.

168. Laine RF, Albecka A, Van De Linde S, Rees EJ, Crump CM, Kaminski CFJNc. Structural analysis of herpes simplex virus by optical super-resolution imaging. *NATURE COMMUNICATIONS*. 2015;6:5980.

169. Bouvier NM, Palese PJV. The biology of influenza viruses. *VACCINE*. 2008;26:D49-D53.

170. Safety SEHa. Herpesvirus Fact Sheet https://ehs.stanford.edu/reference/herpesvirus-fact-sheet. Published 2018. Accessed.

171. Saftey SEHa. Sendai Virus Fact Sheet https://ehs.stanford.edu/reference/sendai-virus-fact-sheet. Published 2018. Accessed.

172. ATCC. ATCC The Essentials of Life Science Reserach https://www.atcc.org/. Published 2018. Accessed.

173. Rein A. Murine leukemia viruses: objects and organisms. *ADVANCES IN VIROLOGY*. 2011;2011.

174. Abolnik C. *Molecular epidemiology of Newcastle disease and avian influenza in South Africa*, University of Pretoria; 2007.

175. Whitley RJ, Roizman BJTl. Herpes simplex virus infections. *THE LANCET*. 2001;357(9267):1513-1518.

176. Chemicalize ChemAxon Ltd. . https://chemicalize.com/. Published 2018. Accessed.

177. Roberts PL, Lloyd DJB. Virus inactivation by protein denaturants used in affinity chromatography. *BIOLOGICALS*. 2007;35(4):343-347.

178. Kelly BJ, Fraefel C, Cunningham AL, Diefenbach RJ. Functional Roles of the Tegument Proteins of Herpes Simplex Virus Type 1. *VIRUS RES.* 2009;145(2):173-186.

179. Agelidis AM, Shukla D. Cell entry mechanisms of HSV: what we have learned in recent years. *FUTURE VIROL* 2015;10(10):1145-1154.

180. Samji T. Influenza A: understanding the viral life cycle. *YALE J BIO MEDICINE.* 2009;82(4):153.

181. Wiley DC, Skehel JJ. The structure and function of the hemagglutinin membrane glycoprotein of influenza virus. *ANNU REV BIOCHEM.* 1987;56(1):365-394.

182. Mair CM, Ludwig K, Herrmann A, Sieben C. Receptor binding and pH stability—how influenza A virus hemagglutinin affects host-specific virus infection. *BIOCHIM BIOPHYS ACTA.* 2014;1838(4):1153-1168.

183. Matrosovich M, Herrler G, Klenk HD. Sialic acid receptors of viruses. In: *SialoGlyco Chemistry and Biology II.* Springer; 2013:1-28.

184. Hsu M-c, Scheid A, Choppin PW. Activation of the Sendai virus fusion protein (f) involves a conformational change with exposure of a new hydrophobic region. *J BIOL CHEM.* 1981;256(7):3557-3563.

185. Murray PR, Rosenthal KS, Pfaller MA. *MED MICROBIOL.* Elsevier Health Sciences; 2015.

186. Nagai Y, Klenk H-D, Rott RJV. Proteolytic cleavage of the viral glycoproteins and its significance for the virulence of Newcastle disease virus. *VIROLOGY.* 1976;72(2):494-508.

187. Dutch RE, Hagglund RN, Nagel MA, Paterson RG, Lamb RAJV. Paramyxovirus fusion (F) protein: a conformational change on cleavage activation. *VIROLOGY* 2001;281(1):138-150.

188. Harris A, Forouhar F, Qiu S, Sha B, Luo M. The crystal structure of the influenza matrix protein M1 at neutral pH: M1-M1 protein interfaces can rotate in the oligomeric structures of M1. Paper presented at: International Congress Series2001.

189. Galloway SE, Liang B, Steinhauer DA. Activation of the Hemagglutinin of Influenza Viruses. In: Böttcher-Friebertshäuser E, Garten W, Klenk HD, eds. *Activation of Viruses by Host Proteases.* Cham: Springer International Publishing; 2018:3-26.

190.   Rice A, Wereszczynski J. Probing the disparate effects of arginine and lysine residues on antimicrobial peptide/bilayer association. *BBA BIOMEMBRANES.* 2017;1859(10):1941-1950.

191.   Shukla D, Trout BL. Interaction of Arginine with Proteins and the Mechanism by Which It Inhibits Aggregation. *J PHYS CHEM B.* 2010;114(42):13426-13438.

192.   Tesei G, Vazdar M, Jensen MR, et al. Self-association of a highly charged arginine-rich cell-penetrating peptide. *P NATL ACAD SCI USA.* 2017;114(43):11428-11433.

193.   Vazdar M, Heyda J, Mason PE, et al. Arginine "Magic": Guanidinium Like-Charge Ion Pairing from Aqueous Salts to Cell Penetrating Peptides. *ACC CHEM RES.* 2018.

194.   Hu Y, Ou SC, Patel S. Free Energetics of Arginine Permeation into Model DMPC Lipid Bilayers: Coupling of Effective Counterion Concentration and Lateral Bilayer Dimensions. *J PHYS CHEM B.* 2013;117(39):11641-11653.

195.   Futaki S. Membrane-permeable arginine-rich peptides and the translocation mechanisms. *ADV DRUG DELIVER REV.* 2005;57(4):547-558.

196.   Futaki S, Suzuki T, Ohashi W, et al. Arginine-rich peptides. An abundant source of membrane-permeable peptides having potential as carriers for intracellular protein delivery. *J BIOL CHEM.* 2001;276(8):5836-5840.

197.   Hu JM, Tian WD, Ma YQ. Computational Investigations of Arginine-Rich Peptides Interacting with Lipid Membranes. *MACROMOL THEOR SIMUL.* 2015;24(4):399-406.

198.   MacCallum JL, Bennett WFD, Tieleman DP. Transfer of Arginine into Lipid Bilayers Is Nonadditive. *BIOPHYS J.* 2011;101(1):110-117.

199.   Das U, Hariprasad G, Ethayathulla AS, et al. Inhibition of protein aggregation: supramolecular assemblies of arginine hold the key. *PLoS One.* 2007;2(11):e1176.

200.   Lin TY, Timasheff, S. N. . On the role of surface tension in the stabilization of globular proteins. *PROTEIN SCI* 1996;5(2):372-381.

201.   Kita Y, Arakawa T, Lin T-Y, Timasheff SN. Contribution of the surface free energy perturbation to protein-solvent interactions. *BIOCHEM* 1994;33(50):15178-15189.

202.   Scholtissek CJAov. Stability of infectious influenza A viruses to treatment at low pH and heating. *Vaccine.* 1985;85(1-2):1-11.

203. Pae J, Säälik P, Liivamägi L, et al. Translocation of cell-penetrating peptides across the plasma membrane is controlled by cholesterol and microenvironment created by membranous proteins. *J CONTROL RELEASE* 2014;192:103-113.

204. Will MA, Clark NA, Swain JE. Biological pH buffers in IVF: help or hindrance to success. *J ASSIST REPROD GEN.* 2011;28(8):711-724.

205. Castelletto V, Barnes RH, Karatzas K-A, et al. Arginine-Containing Surfactant-Like Peptides: Interaction with Lipid Membranes and Antimicrobial Activity. *BIOMACROMOLECULES.* 2018.

206. Lorents A, Säälik P, Langel Ul, Pooga M. Arginine-rich cell-penetrating peptides require nucleolin and cholesterol-poor subdomains for translocation across membranes. *BIOCONJUGATE CHEM* 2018;29(4):1168-1177.

207. Cassai EN, Sarmiento M, Spear PGJJoV. Comparison of the virion proteins specified by herpes simplex virus types 1 and 2. *J VIROL.* 1975;16(5):1327-1331.

208. Möller J, Schroer MA, Erlkamp M, et al. The effect of ionic strength, temperature, and pressure on the interaction potential of dense protein solutions: from nonlinear pressure response to protein crystallization. *BIOPHYS J.* 2012;102(11):2641-2648.

209. Papaneophytou CP, Grigoroudis AI, McInnes C, Kontopidis G. Quantification of the effects of ionic strength, viscosity, and hydrophobicity on protein–ligand binding affinity. *ACS MED CHEM LETT.* 2014;5(8):931-936.

210. Arakawa T, Timasheff SN. Protein stabilization and destabilization by guanidinium salts. *BIOCHEM* 1984;23(25):5924-5929.

211. Shakked Z, Viswamitra M, Kennard O. Interactions of tris buffer with nucleotides: the crystal structure of tris (hydroxymethyl) methylammonium adenosine 5'-diphosphate dihydrate. *BIOCHEMISTRY* 1980;19(12):2567-2571.

212. Gillespie J, McKnight A. Adverse effects of tris hydrochloride, a commonly used buffer in physiological media. *J PHYSIOLOGY.* 1976;259(2):561-573.

213. Mou J, Yang J, Shao Z. Tris (hydroxymethyl) aminomethane (C4H11NO3) induced a ripple phase in supported unilamellar phospholipid bilayers. *BIOCHEM.* 1994;33(15):4439-4443.

214. R.T Irvin TJM, J. W. Costerton Tris (hydroxymethyl) aminomethan Buffer Modifcation of Excherichia Coli Outer Membrane Permeeability. *J BACTERIOL.* 1981;145(3):1397-1403.

215. Piantanida L, Bolt HL, Rozatian N, Cobb SL, Voitchovsky K. Ions Modulate Stress-Induced Nanotexture in Supported Fluid Lipid Bilayers. *BIOPHYS CHEM.* 2017;113(2):426-439.

216. Taha M, Lee MJ. Interactions of TRIS [tris(hydroxymethyl)aminomethane] and related buffers with peptide backbone: thermodynamic characterization. *PHYS CHEM CHEM PHYS.* 2010;12(39):12840-12850.

217. Gupta BS, Taha M, Lee MJ. Interactions of bovine serum albumin with biological buffers, TES, TAPS, and TAPSO in aqueous solutions. *PROCESS BIOCHEM* 2013;48(11):1686-1696.

218. Stellwagen NC, Bossi A, Gelfi C, Righetti PG. DNA and buffers: are there any noninteracting, neutral pH buffers? *ANAL BIOCHEM.* 2000;287(1):167-175.

219. AppliChem. Biological Buffers www.applichem.com Published 2008. Accessed.

220. Pekker M. Interaction between Electrolyte Ions and the Surface of a Cell Lipid Membrane. *J PHYS CHEM B.* 2015;5(2).

221. Rainer A Bockmann AH, Thomas Heimburg, Helmut Grubmuller Effects of Sodium Chloride on a Lipid Bilayer. *BIOPHYS J* 2003;85(3):1647-1655.

222. Vacha R, Berkowitz ML, Jungwirth P. Molecular model of a cell plasma membrane with an asymmetric multicomponent composition: water permeation and ion effects. *BIOPHYS J.* 2009;96(11):4493-4501.

223. Miettinen MS, Gurtovenko AA, Vattulainen I, Karttunen M. Ion Dynamics in Cationic Lipid Bilayer Systems in Saline Solutions. *J Phys Chem B.* 2009;113(27):9226-9234.

224. Redondo-Morata L, Giannotti MI, Sanz F. Structural impact of cations on lipid bilayer models: Nanomechanical properties by AFM-force spectroscopy. *Mol Membr Biol.* 2014;31(1):17-28.

225. Lucas W, Knipe DM. Viral capsids and envelopes: Structure and function. *eLS.* 2010.

226. Mrabet NT, Van den Broeck A, Van den Brande I, et al. Arginine residues as stabilizing elements in proteins. *BIOCHEM* 1992;31(8):2239-2253.

227. Borders Jr C, Broadwater JA, Bekeny PA, et al. A structural role for arginine in proteins: multiple hydrogen bonds to backbone carbonyl oxygens. *PROTEIN SCI.* 1994;3(4):541-548.

228.   Khmelnitsky YL, Belova AB, Levashov AV, Mozhaev VV. Relationship between surface hydrophilicity of a protein and its stability against denaturation by organic solvents. *FEBS Lett.* 1991;284(2):267-269.

229.   Arakawa T, Ejima D, Tsumoto K, et al. Suppression of protein interactions by arginine: a proposed mechanism of the arginine effects. *BIOPHYS CHEM.* 2007;127(1-2):1-8.

230.   Donald JE, Kulp DW, DeGrado WF. Salt bridges: geometrically specific, designable interactions. *PROTEINS* 2011;79(3):898-915.

231.   Lin TY, Timasheff SN. On the role of surface tension in the stabilization of globular proteins. *PROTEIN SCI* 1996;5(2):372-381.

232.   Takeuchi T, Futaki S. Current Understanding of Direct Translocation of Arginine-Rich Cell-Penetrating Peptides and Its Internalization Mechanisms. *CHEM PHARM BULL.* 2016;64(10):1431-1437.

233.   Cutrona KJ, Kaufman BA, Figueroa DM, Elmore DE. Role of arginine and lysine in the antimicrobial mechanism of histone-derived antimicrobial peptides. *FEBS Lett.* 2015;589(24):3915-3920.

234.   Futaki S, Nakase I. Cell-Surface Interactions on Arginine-Rich Cell-Penetrating Peptides Allow for Multiplex Modes of Internalization. *ACC CHEM RES.* 2017;50(10):2449-2456.

235.   Nakase I, Niwa M, Takeuchi T, et al. Cellular Uptake of Arginine-Rich Peptides: Roles for Macropinocytosis and Actin Rearrangement. *MOL THER.* 2004;10(6):1011-1022.

236.   Ter-Avetisyan G, Tuennemann G, Nowak D, et al. Cell Entry of Arginine-rich Peptides Is Independent of Endocytosis. *J BIO CHEM.* 2009;284(6):3370-3378.

237.   Li L, Vorobyov I, Allen T. The different interactions of lysine and arginine side chains with lipid membranes. *J PHYS CHEM B.* 2013;117(40):11906-11920.

238.   Raffy S, Teissie J. Control of lipid membrane stability by cholesterol content. *BIOPHYS J.* 1999;76(4):2072-2080.

239.   Katayama S, Nakase I, Yano Y, et al. Effects of pyrenebutyrate on the translocation of arginine-rich cell-penetrating peptides through artificial membranes: recruiting peptides to the membranes, dissipating liquid-ordered phases, and inducing curvature. *BIOCHIM BIOPHYS ACTA.* 2013;1828(9):2134-2142.

240. Guterstam P, Madani F, Hirose H, et al. Elucidating cell-penetrating peptide mechanisms of action for membrane interaction, cellular uptake, and translocation utilizing the hydrophobic counter-anion pyrenebutyrate. *BIOCHIM BIOPHYS ACTA.* 2009;1788(12):2509-2517.

241. Murayama T, Masuda T, Afonin S, et al. Loosening of lipid packing promotes oligoarginine entry into cells. *ANGEW CHEM INT ED ENGL.* 2017;129(26):7752-7755.

242. Huang K, García Angel E. Free Energy of Translocating an Arginine-Rich Cell-Penetrating Peptide across a Lipid Bilayer Suggests Pore Formation. *BIOPHYS J.* 2013;104(2):412-420.

243. Allolio C, Baxova K, Vazdar M, Jungwirth P. Guanidinium pairing facilitates membrane translocation. *J PHYS CHEM B.* 2015;120(1):143-153.

244. Gaspar LP, Terezan AF, Pinheiro AS, Foguel D, Rebello MA, Silva JL. The metastable state of nucleocapsids of enveloped viruses as probed by high hydrostatic pressure. *J BIOL CHEM.* 2001;276(10):7415-7421.

245. Tumban E, Peabody J, Peabody DS, Chackerian B. A universal virus-like particle-based vaccine for human papillomavirus: longevity of protection and role of endogenous and exogenous adjuvants. *VACCINE.* 2013;31(41):4647-4654.

246. Karni M, Zidon D, Polak P, Zalevsky Z, Shefi O. Thermal degradation of DNA. *DNA CELL BIOL* 2013;32(6):298-301.

247. Sawitzky D, Hampl H, Habermehl K-O. Comparison of heparin-sensitive attachment of pseudorabies virus (PRV) and herpes simplex virus type 1 and identification of heparin-binding PRV glycoproteins. *J GEN VIROL.* 1990;71(5):1221-1225.

248. Marchetti M, Wuite G, Roos W. Atomic force microscopy observation and characterization of single virions and virus-like particles by nano-indentation. *CURR OPIN MICROBIOL.* 2016;18:82-88.

249. Chinniah S, Hinckley P, Connell-Crowley L. Characterization of operating parameters for XMuLV inactivation by low pH treatment. *BIOTECHNOL PROG.* 2016;32(1):89-97.

250. FDA. Guidance for Industry: Q5A Viral Saftey Evaluation of Biotechnology Products Derived From Cell Lines of Human or Animal Origin. In. *U.S. Department of Health and Human Services*1998.

251. Cameron R, Smith K. Virus clearance methods applied in bioprocessing operations: an overview of selected inactivation and removal methods. *Pharmaceutical Biopreocessing.* 2014;2(1):75-83.

252. Nishide M, Tsujimoto K, Uozaki M, et al. Effects of electrolytes on virus inactivation by acidic solutions. *INT J MOL MED.* 2011;27(6):803-809.

253. Blank DE, Corrêa RA, Freitag RA, Cleff MB, de Oliveira Hübner S. Anti-equine arteritis virus activity of ethanolic extract and compounds from Origanum vulgare. *Semina: Ciências Agrárias.* 2017;38(2):759-764.

254. Blaho JA, Morton ER, Yedowitz JC. Herpes simplex virus: propagation, quantification, and storage. *Current protocols in microbiology.* 2005:14E. 11.11-14E. 11.23.

255. Heldt CL, Hernandez R, Mudiganti U, Gurgel PV, Brown DT, Carbonell RG. A colorimetric assay for viral agents that produce cytopathic effects. *J VIRAL METHODS.* 2006;135(1):56-65.

256. Kruger NJ. The Bradford method for protein quantitation. In: *The protein protocols handbook.* Springer; 2009:17-24.

257. Mi X, Lucier EM, Turpeinen DG, Yeo ELL, Kah JCY, Heldt CL. Mannitol-induced gold nanoparticle aggregation for the ligand-free detection of viral particles. *Analyst.* 2019;144(18):5486-5496.

258. Pomeranz LE, Reynolds AE, Hengartner CJ. Molecular biology of pseudorabies virus: impact on neurovirology and veterinary medicine. *MICROBIOL MOL BIOL REV.* 2005;69(3):462-500.

259. Del Piero F. Equine viral arteritis. *VET PATHOLOGY.* 2000;37(4):287-296.

260. Balasuriya UB, Go YY, MacLachlan NJ. Equine arteritis virus. *VET MICROBIOL.* 2013;167(1-2):93-122.

261. Li Y, Wang J, Kanai R, Modis Y. Crystal structure of glycoprotein E2 from bovine viral diarrhea virus. *P NATL A SCI.* 2013;110(17):6805-6810.

262. Neill JD. Molecular biology of bovine viral diarrhea virus. *BIOLOGICALS* 2013;41(1):2-7.

263. Williams P, Pirtle E, Coria M. Isoelectric focusing of infectious particles of porcine pseudorabies virus strains in granulated dextran gels. *CAN J COMPARAT MED.* 1982;46(1):65.

264. Olofsson S. Isoelectric focusing of herpes simplex virus. *ARCH VIROL.* 1975;49(2-3):93-98.

265. Mi X, Bromley E, Joshi PU, Long F, Heldt CL. Virus isoelectric point determination using single-particle chemical force microscopy. *Langmuir.* 2019.

266. Kaplan AS, Vatter A. A comparison of herpes simplex and pseudorabies viruses. *VIROLOGY.* 1959;7(4):394-407.

267. Klupp BG, Baumeister J, Karger A, Visser N, Mettenleiter TC. Identification and characterization of a novel structural glycoprotein in pseudorabies virus, gL. *J VIROL* 1994;68(6):3868-3878.

268. Ren X, Yin J, Li G, Herrler G. Cholesterol dependence of pseudorabies herpesvirus entry. *CURR MICROBIOL.* 2011;62(1):261-266.

269. Favoreel HW, Mettenleiter TC, Nauwynck HJ. Copatching and lipid raft association of different viral glycoproteins expressed on the surfaces of pseudorabies virus-infected cells. *J VIROL* 2004;78(10):5279-5287.

270. Bruckner R, Mansy S, Ricardo A, Mahadevan L, Szostak J. Flip-flop-induced relaxation of bending energy: implications for membrane remodeling. *BIOPHYS J.* 2009;97(12):3113-3122.

271. Mahammad S, Parmryd I. Cholesterol depletion using methyl-β-cyclodextrin. In: *Methods in membrane lipids.* Springer; 2015:91-102.

272. Bajimaya S, Frankl T, Hayashi T, Takimoto T. Cholesterol is required for stability and infectivity of influenza A and respiratory syncytial viruses. *VIROLOGY.* 2017;510:234-241.

273. Takechi-Haraya Y, Nadai R, Kimura H, et al. Enthalpy-driven interactions with sulfated glycosaminoglycans promote cell membrane penetration of arginine peptides. *BIOCHIM BIOPHYS ACTA.* 2016;1858(6):1339-1349.

274. Walter A, Gutknecht J. Permeability of small nonelectrolytes through lipid bilayer membranes. *J MEMBRANE BIOL.* 1986;90(3):207-217.

275. AppliChem. Biological Buffers 2008:1-17.

276. WHO. Guidelines on Viral inactivation and Removal procedures intended to assure the viral saftey of human blood plasma products. *WHO Technical Report.* 2004(924):150-224.

277. WHO. Guidelines on the quality, saftey, and efficacy of biotherapeutic protein products prepared by recombinant DNA technology. *WHO Technical Report Series.* 2013;814.

278. Durno L, Tounekti OJPjops, technology. Viral Inactivation: Low pH and Detergent. *PDA J PHARM SCI TECH* 2015;69(1):163.

279. Gillespie C, Holstein M, Mullin L, et al. Continuous In-Line Virus Inactivation for Next Generation Bioprocessing. *BIOTECHNOL J.* 2019;14(2):1700718.

280. Floyd R, Sharp DG. Viral aggregation: buffer effects in the aggregation of poliovirus and reovirus at low and high pH. *APPL ENVIRON MICROBIOL.* 1979;38(3):395-401.

281. Tafur MF, Vijayaragavan KS, Heldt CL. Reduction of porcine parvovirus infectivity in the presence of protecting osmolytes. *ANTIVIR RES* 2013;99(1):27-33.

282. Hills AG. pH and the Henderson-Hasselbalch equation. *AM J MED.* 1973;55(2):131-133.

283. Zhong H, Li X, Zhao Z, et al. Genome sequences of the novel porcine parvovirus 3, identified in Guangxi province, China. *GENOME ANNOUNC.* 2016;4(2):e00036-00016.

284. Cotmore SF, Agbandje-McKenna M, Chiorini JA, et al. The family parvoviridae. *ARCHIVES OF VIROLOGY.* 2014;159(5):1239-1247.

285. National Center for Biotechnology Information. PubChem Database. Glycine, CID=750. https://pubchem.ncbi.nlm.nih.gov/compound/Glycine. Accessed.

286. National Center for Biotechnology Information. PubChem Database. Acetate, CID=175.

287. Arntfield S, Murray E, Ismond M. Effect of salt on the thermal stability of storage proteins from fababean (Vicia faba). *J FOOD SCI.* 1986;51(2):371-377.

288. Mayr LM, Schmid FX. Stabilization of a protein by guanidinium chloride. *BIOCHEM.* 1993;32(31):7994-7998.

289. Brorson K, Krejci S, Lee K, Hamilton E, Stein K, Xu Y. Bracketed generic inactivation of rodent retroviruses by low pH treatment for monoclonal antibodies and recombinant proteins. *BIOTECHNOL BIOENG.* 2003;82(3):321-329.

290. Mori I, Kimura Y, Naiki H, et al. Reactivation of HSV-1 in the brain of patients with familial Alzheimer's disease. 2004;73(4):605-611.

183

291.	Pouletty P, Chomel J, Thouvenot D, Catalan F, Rabillon V, Kadouche J. Detection of herpes simplex virus in direct specimens by immunofluorescence assay using a monoclonal antibody. *Journal of clinical microbiology.* 1987;25(5):958-959.

A Viral Inactivation Data: Chapter 4

Table A1: Log$_{10}$ reduction values for Figure 4-2. Inactivation of enveloped viruses by arginine. Inactivation at 4°C over 24 hours. Arginine concentration at 1 M. Tris, acetate, and citrate concentration at 20 mM

Virus	Solvents	pH	Time (hours) 1 Average	STDEV	3 Average	STDEV	6 Average	STDEV
HSV-1	Arg	4	3.76	0.24	3.62	0.21	3.70	0.25
		7	0.39	0.61	1.16	0.75	1.41	0.51
	Arg + Tris	4	3.51	0.31	3.72	0.10	3.66	0.37
		7	0.10	0.21	1.36	1.00	1.24	0.49
	Arg + Act	4	3.82	0.37	3.66	0.06	3.76	0.44
		7	0.27	0.46	1.14	0.49	1.22	0.10
	Tris	7	0.11	0.17	0.52	0.73	0.12	0.27
	Act	4	2.56	0.12	2.75	0.54	2.77	0.41
		7	-0.30	0.18	0.26	1.15	0.61	1.24
	Citrate	3.5	4.48	0.04	4.49	0.01	4.49	0.01
SUHV-1	Arg	4	4.05	0.39	4.06	0.40	4.00	0.46
		7	3.39	0.89	4.10	0.41	4.01	0.45
	Arg + Tris	4	3.82	0.13	3.87	0.21	3.85	0.11
		7	3.27	0.90	4.05	0.32	3.97	0.37
	Arg + Act	4	3.99	0.45	4.15	0.46	4.10	0.37
		7	3.16	0.45	4.00	0.33	4.07	0.40
	Tris	7	0.08	0.28	0.29	0.27	0.44	0.32
	Act	4	3.67	0.63	4.00	0.40	3.82	0.49
		7	0.07	0.34	0.35	0.35	0.23	0.25
	Citrate	3.5	4.30	0.10	4.29	0.12	4.30	0.07
EAV	Arg	4	0.21	0.45	1.04	1.20	0.24	0.23
		7	0.13	0.20	0.14	0.23	0.24	0.29
	Arg + Tris	4	-0.07	0.36	0.04	0.14	0.48	0.09
		7	0.12	0.32	-0.04	0.22	0.23	0.64
	Arg + Act	4	0.08	0.81	-0.03	0.43	0.70	0.20
		7	0.17	0.17	0.26	0.21	0.03	0.49
	Tris	7	0.24	0.24	0.18	0.27	0.09	0.44
	Act	4	0.04	0.44	0.48	0.40	0.74	0.20
		7	0.23	0.52	0.24	0.23	0.07	0.27
	Citrate	3.5	0.20	0.69	0.27	0.65	0.38	0.34
BVDV	Arg	4	0.08	0.43	0.28	0.19	0.42	0.47
		7	0.12	0.15	0.14	0.28	0.14	0.33
	Arg + Tris	4	0.44	0.17	0.56	0.47	0.38	0.37
		7	0.25	0.38	-0.05	0.10	0.33	0.47
	Arg + Act	4	0.33	0.24	0.29	0.29	0.38	0.37
		7	0.28	0.36	0.36	0.60	0.11	0.18
	Tris	7	0.41	0.36	0.44	0.40	0.53	0.39
	Act	4	0.52	0.14	0.46	0.22	0.63	0.15
		7	0.14	0.39	0.33	0.19	0.37	0.55
	Citrate	3.5	0.06	0.10	0.20	0.27	0.29	0.30

Table A1 Continued

Virus	Solvents	pH	Time (hours)			
			12		24	
			Average	STDEV	Average	STDEV
HSV-1	Arg	4	3.71	0.17	3.70	0.25
		7	2.13	0.35	2.67	0.93
	Arg + Tris	4	3.71	0.25	3.42	0.55
		7	1.81	0.78	3.46	0.96
	Arg + Act	4	3.77	0.21	3.71	0.15
		7	2.00	0.58	2.62	0.61
	Tris	7	0.59	0.28	0.07	1.20
	Act	4	3.16	0.21	3.35	0.37
		7	0.87	0.77	0.96	0.47
	Citrate	3.5	4.51	0.02	4.54	0.07
SUHV-1	Arg	4	4.07	0.37	3.97	0.40
		7	4.03	0.40	4.03	0.37
	Arg + Tris	4	3.90	0.25	3.79	0.08
		7	3.91	0.40	3.98	0.38
	Arg + Act	4	4.04	0.37	4.03	0.38
		7	4.09	0.36	3.97	0.42
	Tris	7	0.44	0.30	0.75	0.22
	Act	4	3.86	0.46	3.89	0.42
		7	0.45	0.42	0.82	0.56
	Citrate	3.5	4.22	0.13	4.67	0.19
EAV	Arg	4	-0.11	0.39	0.12	0.17
		7	0.17	0.29	-0.21	0.13
	Arg + Tris	4	0.15	0.39	0.10	0.04
		7	0.54	0.77	-0.07	0.03
	Arg + Act	4	0.37	0.48	0.33	0.18
		7	0.22	0.52	0.14	0.30
	Tris	7	-0.04	0.16	0.00	0.19
	Act	4	0.47	0.60	0.50	0.35
		7	0.23	0.55	0.09	0.23
	Citrate	3.5	0.11	0.36	0.61	0.58
BVDV	Arg	4	0.73	0.12	0.99	0.36
		7	0.36	0.27	0.49	0.37
	Arg + Tris	4	0.69	0.37	0.76	0.35
		7	0.35	0.59	0.56	0.16
	Arg + Act	4	0.59	0.44	1.17	0.61
		7	0.39	0.17	0.71	0.53
	Tris	7	0.87	0.55	0.90	0.50
	Act	4	0.87	0.19	1.06	0.43
		7	0.65	0.20	0.97	0.48
	Citrate	3.5	0.51	0.04	0.98	0.47

Table A2: Cholesterol and titer values for Figure 4-3A& B. Effect of cholesterol depletion on the infectivity of HSV-1 and SuHV-1 after 5mM methyl-β-cyclodextrin (MβCD) exposure.

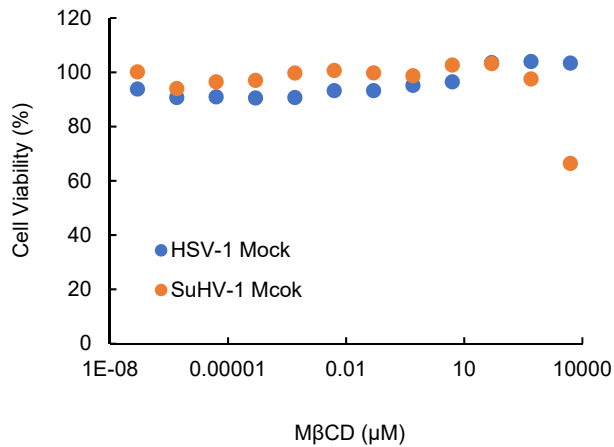| Measurement	Sample	No MβCD		MβCD	
		Average	STDEV	Average	STDEV
Cholesterol (ug/ml)	HSV-1	7.74	0.3	1.07	0.09
	SuHV-1	1.03	0.15	0.36	0.04
	HSV-1 Cells	10.65	2.29	1.13	0.07
	SuHV-1 Cells	1.09	0.37	0.4	0.07
Titer (MTT50/ml)	HSV-1	6.8	0.13	5.4	0.15
	SuHV-1	7.21	0.36	3.27	0.44

Figure A1: Toxicity measurements for Vero cells seeded with HSV-1 and SuHV-1 Mock samples based on MβCD concentration. Mock samples for each virus were tested to give a representative level of cholesterol in solution without added virus. Mock samples were comprised of cells that underwent the same propagation procedure as their respective virus.

Table A3: Log10 reduction values for Figure 4-4B&C. Inactivation of enveloped viruses by agmatine. Inactivation occurred at 4°C over 24 hours. Agmatine concentration at 1 M and acetate concentration at 20 mM.

Virus	Solvents	pH	Time (hours)					
			1		**3**		**6**	
			Average	STDEV	Average	STDEV	Average	STDEV
HSV-1	Agm + Act	4	-0.35	0.24	-0.14	0.29	-0.24	0.24
		7	-0.39	0.31	-0.46	0.10	-0.75	0.49
	Act	4	2.56	0.12	2.75	0.54	2.77	0.41
		7	-0.30	0.18	0.26	1.15	0.61	1.24
SuHV-1	Agm + Act	4	3.03	0.10	3.45	0.00	3.53	0.04
		7	-0.15	0.22	-0.04	0.34	0.04	0.01
	Act	4	3.70	0.60	4.00	0.40	3.80	0.50
		7	0.07	0.34	0.35	0.35	0.23	0.25
EAV	Agm + Act	4	0.03	0.29	0.02	0.18	0.00	0.33
		7	0.04	0.32	-0.08	0.26	0.37	0.16
	Act	4	0.04	0.44	0.48	0.40	0.74	0.20
		7	0.23	0.52	0.24	0.23	0.07	0.27

Virus	Solvents	pH	Time (hours)			
			12		**24**	
			Average	STDEV	Average	STDEV
HSV-1	Agm + Act	4	0.49	0.22	1.89	0.10
		7	0.11	0.20	1.83	0.24
	Act	4	3.16	0.21	3.35	0.37
		7	0.87	0.77	0.96	0.47
SuHV-1	Agm + Act	4	3.37	0.11	3.55	0.01
		7	0.24	0.27	0.69	0.14
	Act	4	3.90	0.50	3.90	0.40
		7	0.45	0.42	0.82	0.56
EAV	Agm + Act	4	0.03	0.05	0.51	0.04
		7	0.02	0.15	0.27	0.11
	Act	4	0.47	0.60	0.50	0.35
		7	0.23	0.55	0.09	0.23

Table A4: Log$_{10}$ reduction values for Figure 4-4D. Comparison of arginine, agmatine, and butyroyl-arginine in the inactivation of HSV-1 after 1 hour at 4°C or on ice. 0.7 M arginine and but-arg represent data reformatted from Katsuyama et al.[10]

Solvent	LRV	STDEV
1M Agm	3.80	0.37
1M Agm	-0.35	0.29
0.7 M Arg	5.00	N/A
0.7 M But-Arg	5.00	N/A

Table A5: Log$_{10}$ reduction values for Figure 4-5. Virus inactivation by arginine peptides. Inactivation occurred after 1 hour at pH 7 in Tris buffered solutions with 10% DMSO. Arginine and CapA6R concentration at 7.6 mM. R8 concentration at 0.95 mM which is equivalent to an arginine concentration of 7.6mM. Tris concentration at 20 mM.

Virus	Solvents	Average	STDEV
HSV-1	CapA6R+ 10% DMSO	1.29	0.35
	R8 + 10% DMSO	0.23	0.07
	10% DMSO	0.19	0.15
	Arg + 10% DMSO	0.06	0.11
	Arg	-0.02	0.07
EAV	CapA6R+ 10% DMSO	1.65	0.63
	R8 + 10% DMSO	0.56	0.07
	10% DMSO	0.27	0.31
	Arg + 10% DMSO	0.05	0.12
	Arg	0.50	0.20

Table A6: Log$_{10}$ reduction values for Figure 4-6. Inactivation of EAV and HSV-1 by arginine with added Pyrenebutyric acid (PYB). Inactivation occurred after 1 hour at 4°C. PYB at 10 mM, arginine at 1 M, and Tris and acetate buffer at 20 mM.
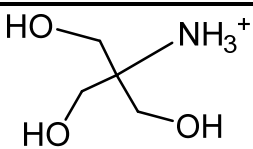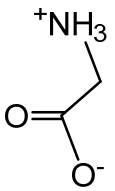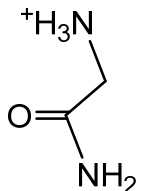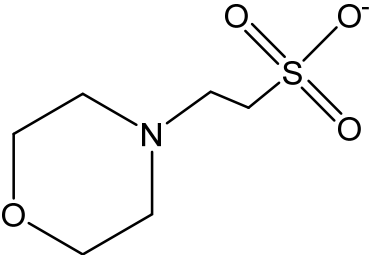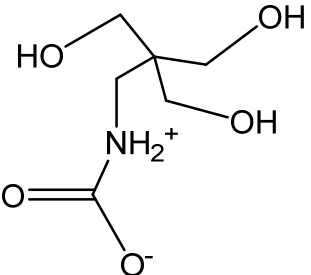
Virus	Solvents	pH	PYB		DMSO	
			Average	STDEV	Average	STDEV
HSV-1	Arg + Tris	7	-0.32	0.22	-0.32	0.22
	Arg + Act	4	3.22	0.13	4.55	0.03
	PBS	7.2	-0.03	0.24	-0.36	0.18
EAV	Arg + Tris	7	1.38	0.38	-0.20	0.32
	Arg + Act	4	0.01	0.47	0.06	0.17
	PBS	7.2	0.37	0.31	0.24	0.26

Table A7: Log$_{10}$ reduction values for Figure 4-7. Inactivation of HSV-1 with Buffer Mimics. Inactivation occurred at 4°C over 24 hours. Arginine concentration at 1 M. Glycine, Glycineamide, MES, and Tricine concentration at 20 mM.

Virus	Solvents	pH	Time (hours)					
			1		**3**		**6**	
			Average	STDEV	Average	STDEV	Average	STDEV
HSV-1	Arg + Glycine	4	4.49	0.29	4.54	0.19	4.63	0.23
		7	0.04	0.37	0.44	0.48	0.84	0.51
	Arg + Glycineamide	4	4.45	0.17	4.46	0.43	4.60	0.21
		7	0.07	0.37	0.57	0.72	0.74	0.58
	Arg + MES	4	4.56	0.21	4.53	0.19	4.50	0.17
		7	-0.07	0.22	0.44	0.84	1.31	0.69
	Arg+ Tricine	4	4.37	0.08	4.52	0.17	4.57	0.15
		7	0.05	0.30	0.22	0.81	0.90	0.15
	Glycine	4	0.33	0.56	0.04	0.79	0.72	0.78
		7	-0.12	0.37	0.18	0.35	0.21	0.82
	Glycineamide	4	-0.07	0.29	-0.02	0.60	-0.22	0.53
		7	-0.12	0.21	-0.09	0.67	-0.01	0.77
	MES	4	0.27	0.78	0.61	0.51	0.72	0.68
		7	-0.19	0.45	-0.18	0.56	0.21	0.66
	Tricine	4	0.26	0.42	-0.16	0.04	0.32	0.43
		7	-0.09	0.25	-0.10	0.26	0.01	0.43

Virus	Solvents	pH	Time (hours)			
			12		**24**	
			Average	STDEV	Average	STDEV
HSV-1	Arg + Glycine	4	4.48	0.17	4.48	0.21
		7	1.39	0.62	2.01	0.67
	Arg + Glycineamide	4	4.43	0.19	4.26	0.09
		7	1.62	0.49	2.41	0.41
	Arg + MES	4	4.42	0.18	4.46	0.14
		7	1.73	0.44	2.41	0.56
	Arg+ Tricine	4	4.54	0.16	4.56	0.24
		7	1.69	0.66	2.15	0.44
	Glycine	4	1.03	0.89	1.51	0.86
		7	0.57	0.37	0.80	0.81
	Glycineamide	4	0.68	0.43	0.09	0.61
		7	0.71	0.62	0.11	0.93
	MES	4	1.23	0.54	1.20	0.60
		7	0.39	0.42	0.32	0.50
	Tricine	4	0.40	0.60	0.78	1.01
		7	0.31	0.65	0.79	0.55

Table A8: Structure at pH 7 and pKa values of the buffer mimics tested in Figure 4-7[176]. Buffer mimics showed similar inactivation to Tris and acetate when used with 1 M arginine at pH 4 and 7.

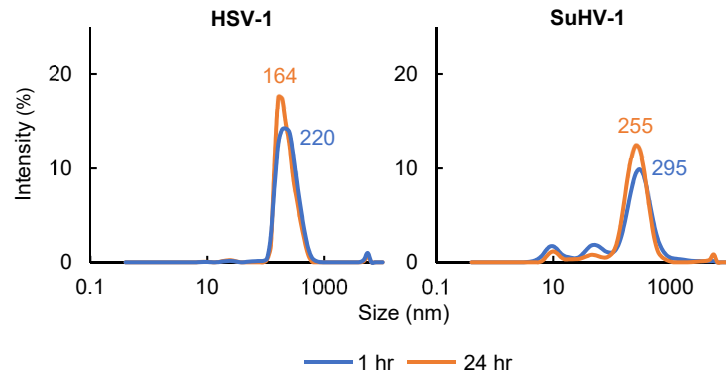| Buffer	Structure at pH 7	pKa Values
Tris		8.95,14.16
Glycine		2.31,9.24
Glycineamide		8.15
MES		-1.52,6.51
Tricine		2.86,7.61

Figure A2: Size changes of control HSV-1 and SuHV-1 in PBS at pH 7.4 measured by DLS after 1 and 24 hours at 4°C. PBS control data over 24 hours for both viruses show minimal changes.
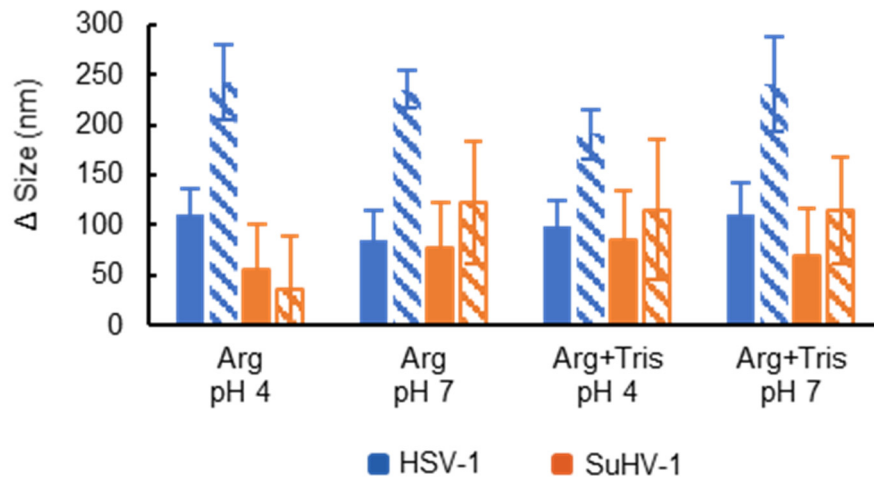

Figure A3. DLS size changes of HSV-1 and SuHV-1 after 1 (solid) and 24 (hashed) hours in comparison to a PBS control. Arginine was at 1 M, Tris was at 20 mM, and PBS was at pH 7.4. Inactivation occurred at 4°C. All DLS measurements showed increasing virus size after arginine exposure. All data points for DLS measurements are in triplicate.

B   Copyright documentation

Please see below for full citation and attribution information.

Chapter 3: Arginine-Enveloped Virus Inactivation and Potential Mechanisms. Licensed Content Publication: Biotechnology Progress. License Number 4799331196331.